MAX-PLANCK-INSTITUT
FÜR METEOROLOGIE

International Max Planck Research School on Earth System Modelling

Impact of Plant Functional Diversity on Climate — A Modelling Study using JeDi-BACH in ICON-ESM

Pin-hsin Hu

Hamburg 2022

Berichte zur Erdsystemforschung
Reports on Earth System Science

256
2022

Hinweis

Die Berichte zur Erdsystemforschung werden vom Max-Planck-Institut für Meteorologie in Hamburg in unregelmäßiger Abfolge herausgegeben.

Sie enthalten wissenschaftliche und technische Beiträge, inklusive Dissertationen.

Die Beiträge geben nicht notwendigerweise die Auffassung des Instituts wieder.

Die "Berichte zur Erdsystemforschung" führen die vorherigen Reihen "Reports" und "Examensarbeiten" weiter.

Anschrift / Address

Max-Planck-Institut für Meteorologie
Bundesstrasse 53
20146 Hamburg
Deutschland

Tel./Phone: +49 (0)40 4 11 73 - 0
Fax: +49 (0)40 4 11 73 - 298

name.surname@mpimet.mpg.de
www.mpimet.mpg.de

Notice

The Reports on Earth System Science are published by the Max Planck Institute for Meteorology in Hamburg. They appear in irregular intervals.

They contain scientific and technical contributions, including PhD theses.

The Reports do not necessarily reflect the opinion of the Institute.

The "Reports on Earth System Science" continue the former "Reports" and "Examensarbeiten" of the Max Planck Institute.

Layout

Bettina Diallo and Norbert P. Noreiks
Communication

Copyright

Impact of plant functional diversity on climate — a modelling study using JeDi-BACH in ICON-ESM

Pin-hsin Hu

Hamburg 2022

Pin-hsin Hu
aus Taoyuan City, Taiwan

Max-Planck-Institut für Meteorologie
The International Max Planck Research School on Earth System Modelling
(IMPRS-ESM)
Bundesstrasse 53
20146 Hamburg

Tag der Disputation: 25. Juli 2022

Folgende Gutachter empfehlen die Annahme der Dissertation:
Prof. Dr. Martin Claußen
Dr. Christian Reick

Vorsitzender des Promotionsausschusses:
Prof. Dr. Hermann Held

Dekan der MIN-Fakultät:
Prof. Dr. Heinrich Graener

Cover image:
Collage by Pin-hsin Hu

Berichte zur Erdsystemforschung / Max-Planck-Institut für Meteorologie 256
Reports on Earth System Science / Max Planck Institute for Meteorology 2022

ISSN 1614-1199 - doi: 10.17617/2.3430193

Pin-hsin Hu

Impact of plant functional diversity on climate — a modelling study using JeDi-BACH in ICON-ESM

ABSTRACT

In ecology, high plant-functional diversity is associated with strong ecosystem resilience and stability. As a high-diversity (HD) ecosystem comprises a large variety of functional traits, some of them contribute redundantly to similar ecosystem functions. This redundancy may determine the resilience of an ecosystem to recover from a disturbance. Growing evidence from field observations has shown that increasing functional diversity enhances ecosystem functioning and resistance. Until now, plant ecology studies have focused on the passive response of global ecosystems to climatic changes while the impacts of plant-functional diversity on climate including its feedback are seldom addressed. Particularly, climate models are often criticized for oversimplifying global vegetation processes. The classic plant functional type (PFT) approach used in the most up-to-date climate models vastly omit the diversity of global plant traits. Thus, one cannot address the impact of plant functional diversity on global climate and ecosystem functioning. This dissertation investigates the plant functional diversity-climate interactions from a new modeling perspective. I have constructed the new model JeDi-BACH into the ICON-Earth System Model. JeDi-BACH is based on the modeling approach first introduced by Kleidon et al. (2009). Instead of prescribing plant types with fixed physiological parameters, global vegetation is mechanistically obtained via ecological trade-off selection. Compared to the PFT-approach, JeDi-BACH achieves a richer representation of plant functional diversity with more ecophysiological realism and fewer diversity constraints in particular by accounting for environmental filtering. JeDi-BACH is the first model using this approach being interactively coupled to an atmosphere model. With this new setup, I investigate two aspects of plant functional diversity: (i) the importance of plant functional diversity on shaping global climate and ecosystems, (ii) the relation between plant functional diversity and resilience under an abrupt warming scenario.

First, I found a "plant functional diversity-climate feedback." The existence of such a feedback has never been recognized before and highlights the role of biodiversity in shaping a robust climate: with increasing diversity, the global vegetation-climate interactions converge and operate towards a state with high water-cycling. As a result, the global climate tends to be cooler and wetter with increasing diversity. This convergence is because HD ecosystems that naturally have more resource-optimal strategies tend to exploit environmental resources (e.g., water or carbon) more effectively. HD ecosystems thus lead by active reg-

ulation to a more robust climate and ecosystem functioning than low diversity (LD) ecosystems. Second, I found that ecosystem adaptability is key to ecosystem resilience and regional climate stability. HD ecosystems are strongly resilient due to their high potential for shuffling composition. However, I found that for particular disturbances also LD ecosystems behave quite resilient, although this is not very likely for general disturbances. Overall, these findings reinforce the biodiversity-resilience relationship and highlight that biodiversity is critical for sustaining a robust climate and ecosystem functioning. Moreover, this thesis demonstrates the potential of JeDi-BACH as a new prototype for investigating the interaction between plant trait diversity and climate especially in non-analogue climates (e.g., paleoclimate where no present-day vegetation existed).

ZUSAMMENFASSUNG

In der Ökologie wird ein Zusammenhang gesehen zwischen einer großen funktionalen Pflanzendiversität in einem Ökosystem und einer hohen Widerstandsfähigkeit und Stabilität des entsprechenden Ökosystems. Da ein Ökosystem mit hoher Diversität (HD) eine große Vielfalt an funktionalen Merkmalen umfasst, gibt es bei mehr Ökosystemfunktionen Redundanz: Mehr funktionale Merkmale erfüllen eine ähnliche Funktion und können einander ersetzen. Diese Redundanz kann bestimmend dafür sein, wie gut sich ein Ökosystem von einer Störung erholt. Wir wissen aus einer wachsenden Fülle an Feldbeobachtungen, dass Ökosysteme besser funktionieren, je höher ihre Diversität ist. Pflanzenökologische Studien haben sich bisher vor allem darauf konzentriert wie globale Ökosysteme auf klimatische Veränderungen (passiv) reagieren, während die umgekehrten Auswirkungen von funktionaler Pflanzendiversität auf das Klima und Kopplungseffekte nur selten untersucht wurden. Vor allem Klimamodelle werden oft dafür kritisiert, dass sie die globalen Vegetationsprozesse zu stark vereinfachen. Der klassische Ansatz der Pflanzenfunktionstypen (PFT), der in den meisten aktuellen Klimamodellen verwendet wird, lässt die Diversität der globalen Pflanzeneigenschaften weitgehend außer Acht. Daher können die Auswirkungen der funktionalen Diversität von Pflanzen auf das globale Klima und die Funktionsweise von Ökosystemen mit diesen Modellen nicht untersucht werden. In dieser Dissertation untersuche ich die Wechselwirkungen zwischen der funktionellen Diversität von Pflanzen und dem Klima aus einer neuen Modellierungsperspektive. Dazu habe ich das neue Modell JeDi-BACH in das ICON-Earth System Model eingebaut. JeDi-BACH basiert auf einem Modellierungsansatz, der erstmals von Kleidon u. a. (2009) vorgestellt wurde. Anstatt Pflanzentypen mit festen physiologischen Parametern vorzuschreiben, wird die globale Vegetation mechanistisch über ökologische Abwägungen ermittelt. Im Vergleich zum PFT-Ansatz erreicht JeDi-BACH eine vielseitigere Darstellung der funktionellen Pflanzendiversität, die unter ökophysiologischen Gesichtspunkten realistischer ist und Diversität weniger einschränkt. Dies wird insbesondere dadurch erreicht, dass die überlebenden Pflanzenarten durch die Umweltbedingungen bestimmt werden. JeDi-BACH ist das erste Modell mit dieser Art Vegetation darzustellen, das interaktiv mit einem Atmosphärenmodell gekoppelt ist. Mit diesem neuen Aufbau untersuche ich zwei Aspekte der funktionellen Diversität von Pflanzen: (i) den Einfluss von funktioneller Diversität von Pflanzen auf das globale Klima und Ökosysteme, (ii) die Beziehung

zwischen der funktionellen Diversität von Pflanzen und der Widerstandsfähigkeit von Ökosystemen bei abrupter Erwärmung.

Bezüglich (i) habe ich eine Rückkopplung zwischen funktioneller Pflanzendiversität und dem globalen Klima gefunden. Die Existenz einer solchen Rückkopplung wurde bisher noch nie gezeigt und unterstreicht die Rolle der Biodiversität für die Entstehung eines robusten Klimas: Mit zunehmender Diversität konvergieren die globalen Wechselwirkungen zwischen Vegetation und Klima und wirken auf einen Zustand mit hoher Wasserzirkulation hin. Infolgedessen wird das globale Klima mit zunehmender Diversität tendenziell kühler und feuchter. Die Konvergenz der Wechselwirkungen ist darauf zurückzuführen, dass HD-Ökosysteme, die von Natur aus über ressourcenoptimale Strategien verfügen, dazu neigen, Umweltressourcen (z. B. Wasser oder Kohlenstoff) effektiver zu auszuschöpfen. HD-Ökosysteme tragen also durch aktive Regulierung zu einem robusteren Klima bei und funktioniere effizienter als Ökosysteme mit geringer Diversität (GD). Bezüglich (ii) habe ich festgestellt, dass die Anpassungsfähigkeit von Ökosystemen der Schlüssel zur Widerstandsfähigkeit von Ökosystemen und zur regionalen Klimastabilität ist. HD-Ökosysteme sind aufgrund ihres hohen Potenzials für eine wechselnde Zusammensetzung der vorkommenden Pflanzenarten sehr widerstandsfähig. Ich habe jedoch festgestellt, dass sich bei bestimmten Störungen auch GD-Ökosysteme recht widerstandsfähig verhalten, obwohl dies bei allgemeinen Störungen nicht sehr wahrscheinlich ist. Insgesamt untermauern diese Ergebnisse, dass es eine Beziehung zwischen Biodiversität und Widerstandsfähigkeit gibt und zeigen, dass die biologische Vielfalt für die Aufrechterhaltung eines robusten Klimas und das Funktionieren von Ökosystemen von entscheidender Bedeutung ist. Darüber hinaus zeigt diese Arbeit das Potenzial von JeDi-BACH als neuen Prototyp für die Untersuchung der Wechselwirkung zwischen der Diversität von Pflanzenmerkmalen und dem Klima, insbesondere in nicht-analogen Klimazonen z. B. Paläoklima, in dem sich die Vegetation entschieden von der heutigen Vegetation unterscheidet.

CONTENTS

LIST OF FIGURES

LIST OF TABLES

1

INTRODUCTION

Forest ecosystems support the greatest biodiversity worldwide, providing hubs for other biological kingdoms. As per a recent estimate (Brummitt, Araújo, and Harris, 2020), there are more than 400,000 known species of terrestrial vegetation. Tropical rainforests are estimated to host 3,000 to 5,000 diverse vascular plant species per ecoregion. Given their major impact on global climate, their biogeographic contributions, and the fact that they harbor an immense amount of biodiversity, terrestrial ecosystems play a dominant role in serving the foundation of most food webs and also provide critical socioeconomic services for human welfare. Biodiversity is generally expected to enhance ecosystem stability (Isbell et al., 2011a). Understanding the changes in their composition, structure, and function are fundamental to many social and economic interests. Since the 1992 United Nations (UN) Earth Summit in Rio de Janeiro, Brazil, a wide range of experimental studies has been conducted to understand the role of biodiversity in shaping ecosystems' dynamics and their functions. Some important questions that these experiments aim to answer are: what forms and regulates biodiversity? what is the connection between diversity and the service it provides? how do losses in diversity influence ecosystems? With the current loss of biodiversity being at an unprecedented rate; the need to answer these questions has become more pressing (Malhi et al., 2008; Bellard et al., 2012; Newbold et al., 2015; Naeem and Li, 1997).

1.1 Plant functional diversity and ecosystem resilience

To what extent biodiversity influences ecosystem processes has always been a heated subject over the years (Loreau et al., 2001). One issue at the center of the debate is that the definition of diversity varies among studies (Huston, 1997). Intuitively, one may think of counting the total number of species in a system as a measure of diversity and then investigate whether a particular process is a function of that number or not. However, considering merely the number of species may include too many ecological processes at the same time and possibly deliver false/vague interpretation in biodiversity experiments. Moreover, the 'hidden treatments' of each experiment lead to contradicting results from one study to another (Huston, 1997).

More recently, ecology communities have started shifting the focus to plant "functional trait" diversity (Reich, 2014; Violle et al., 2007). Functional traits are defined as morpho-physio-phenological traits which control how species perform ecological processes in response to the environment (Díaz et al., 2013). It appears that functional traits are more closely related to how ecosystems function and thus, trait diversity may serve more as a decisive factor in ecosystem processes compared to measures of biodiversity such as the aforementioned number of species (Westoby and Wright, 2006; Díaz et al., 2016). The dissimilarity in plant functions, also called plant functional diversity, is widely believed to enhance ecological resilience and stability (Mccann, 2000; Isbell et al., 2011a; Cadotte, Carscadden, and Mirotchnick, 2011; Biggs et al., 2020; Isbell et al., 2015).

The association between functional traits, diversity, and ecosystem function can be understood as follows. Species differ in their physical structure, ecological functions, and their requirements for abiotic or biotic environmental factors. Species with different functional traits contribute differently to ecosystem processes. An ecosystem process is process that links to the present environment physically, chemically and biologically. For instance, plant species utilize sunlight for photosynthesis and suck up soil water to access essential nutrients. Intuitively, one might imagine that more ecosystem functions appear if more species exist. Yet, the increase in ecosystem function is not always linearly associated with the number of species. Up to a certain point, adding species into an empty ecosystem might increase ecosystem function. However, ecosystem function might not improve any further once additional species contribute functions that are similar to those contributed by existing species in the pool. Cardinale et al. (2006) have found that biodiversity–functioning shows an asymptotic relationship between the number of plant species and three key ecosystem functions (biomass production, nutrient uptake, and litter decomposition). This kind of asymptotic relationship corresponds to the so-called redundancy hypothesis (Walker, 1992). Having many functionally redundant species may appear to be 'worthless' for an ecosystem. The redundancy may in fact play a critical role when an ecosystem is under disturbances. If an ecosystem undergoes persisting changes by environmental or anthropogenic disturbances, the potential to provide replacements for ecological functions by other species is critical to the stability of its community structure (Biggs et al., 2020). In some way, species redundancy determines the resilience of an ecosystem to recover from a disturbance. Therefore, functional diversity acts as an insurance against functional changes (Cardinale et al., 2012) and may as well be vital for shaping global climate under extreme or novel conditions.

1.2 What have paleo records revealed about plant diversity?

Ecosystems with high ecological complexity and diversity have a greater capacity for functional trait evolution as plant assemblies comprise great extents of functional traits. Potential acclimation or replacement by species with traits similar to those of extinct species could adequately fill out the spot. Such a theory is also supported by geological records. During a rapid extreme climate change in End-Triassic, tropics were found to have only a rather small extinction compared to the North American temperate biomes despite global temperatures rising by 5°C within tens of thousands of years (McElwain, 2018). Significant compositional shifts were found in the tropical pollen and spore records, suggesting that tropics underwent a shuffling of the composition of plant communities during global warming (McElwain, 2018). In other words, high diversity regions have a greater likelihood of offering a replacement species in response to global/regional environmental changes so that vegetation could adapt or acclimate to changes. The adaptation of plant traits in the past global climate changes was also evident in paleorecords. During the global warming induced by extreme CO_2 changes in the Triassic-Jurassic transition, Soh et al. (2017) found a shift in vegetation from low to high stress-tolerance taxa in their leaf traits. A similar finding is also evident in a recent global pollen and pore records synergy study (Mottl et al., 2021). They found out that both climate and human effects have primarily driven both regional and global vegetation compositional change over the past tens of thousand of years. From Late Pleistocene to the Early Holocene, vegetation changes were mainly induced by changing climates. These paleoproxies studies suggest that plants are likely to adapt their ecological functioning to cope with climate changes.

1.3 Role of vegetation in the climate systems

Terrestrial ecosystems influence the global exchange of energy, water, momentum, and chemical materials with the atmosphere via biogeochemical and biogeophysical processes (Kabat et al., 2004; Bonan, 2008). By modifying physical characteristics of the surface such as surface albedo or surface roughness, biogeophysical processes regulate energy exchange of latent heat and sensible heat. For instance, changes in albedo over the vegetated surface at high-latitudes can modify net absorption of solar radiation at the surface, e.g., snow-masking effect by forests creates a warmer climate during snow season and earlier snowmelt, Brovkin et al. (2003). Changes in surface roughness influence the turbulent exchange (aerodynamic conductance) at the surface and modify surface heating, e.g., up to 1.3K difference in global mean annual temperature

between a tree and a grass covered world was reported by Brovkin et al. (2009). In addition, changes in water recycling over land is critical to the surface energy balance. Terrestrial evapotranspiration returns about 60 percent of land precipitation to the atmosphere (Oki and Kanae, 2006). Transpiration contributes about 80 to 90 percent of terrestrial evapotranspiration (Jasechko et al., 2013). About half of the total solar energy absorbed by land surface is used in the process (Trenberth, Fasullo, and Kiehl, 2009). Over geological time scales of millions of years, biogeochemical processes significantly influence the process of carbon sequestration from active carbon cycle at Earth surface to being abducted by continental plates. On a shorter time scale, biogeochemical (carbon cycle) processes affect climate via the sources and sinks between the biosphere, atmosphere, ocean, and geosphere over periods of years to centuries and to many millennia. On such time scales, both terrestrial and aquatic plant life play a major role in removing atmospheric CO_2 into organic forms. Terrestrial ecosystems remove carbon via photosynthesis, sequestrate carbon in plant tissues and soils, and release carbon via respiration. The net ecosystem exchange, a measure of the carbon exchange between ecosystems and the atmosphere, influences atmospheric CO_2 and thereby modifies the global climate. The outcome of these physical, chemical and biological processes jointly influences global climate.

1.4 Current treatment of plant diversity in models

Earth system models (ESMs) are one of the most widely used tools to understand how vegetation may be altered by climatic changes and, reciprocally, how changes in vegetation influence climate. Though being state-of-the-art tools, the fundamental approach used for representing terrestrial vegetation in ESMs has been criticized for many issues (Harrison et al., 2021; Fisher et al., 2014).

In models, the wealth of global vegetation is commonly categorized into only a finite set of plant functional types (PFTs). Plant species that show similar morpho-physiological, phenotypic features and bioclimatic limitation conditions are grouped into the same plant functional type. Each PFT is assigned to a set of fixed parameters to account for the biochemical and biophysical influence. The parameter values are often crudely chosen to represent the broad feature for each PFT, and the values are well-tuned for different ESMs in order to optimize model performance. Growing evidence has shown that PFTs are insufficient for representing the full diversity of plant traits; the field ecology community has pointed out that there is a greater trait variation within a PFT than between PFTs for many plant traits (Kattge et al., 2009; Pappas, Fatichi, and Burlando, 2014; Kattge et al., 2020). The divergence between field measurements and parameterized PFTs may lead to inaccurate estimations of terrestrial

ecosystems' responses to changes in the environments under different climate regimes (Alton, 2011; Verheijen et al., 2013).

Moreover, the parameter values of PFTs are often static and do not change in their functional behavior. Such practice with only static parameters implies that the current plant traits will remain the same despite any climate change. As a result, ESMs do not account for potential plant adaptation for future scenario projections. How to reasonably parameterize vegetation processes is therefore critical for modeling communities. A modeling study (Groner et al., 2018) has shown that the timing and the region for desertification in the Sahel region around the mid-Holocene are highly sensitive to the initial selection of PFTs. This suggests that model simulations are prone to subjective decisions hidden behind model-tuning. Drawing conclusions in the aspect of climate-vegetation interaction from model simulations that are based on PFTs is therefore challenging. It is necessary to seek a different approach, robust to parameterization, to address vegetation and climate interaction.

1.5 Previous attempt on trait variation in an Earth system model

One conceptual study has attempted to investigate the impact of trait variation on climate using the Max Planck Institute Earth System Model (MPI-ESM). Verheijen et al. (2013) included a simple trait variation method where three trait parameters of PFTs (specific leaf area and two photosynthetic parameters) change depending on the local climate conditions. They found that including plant-trait variation led to robust changes in global productivity and the hydrological cycle. They thereby raised the attention of the importance of potential plant plasticity for climate change studies. However, some corresponding trait trade-offs (negative correlation between two or more traits) were not accounted for by the modified trait parameters in their model simulations. For instance, the specific leaf area (SLA) – a trait parameter describing the area of leaves a unit of leaf dry mass grows – is not linked to leaf phenology (which determines the total intercepted sunlight by leaves) in the model. Hence, varying SLA does not influence plant productivity nor reflects any consequence for building thick or thin leaf tissues. Such limitation led to unrealistic combinations of traits and plant responses in their study. Given that many fundamental ecological processes are missing, such as decoupling of leaf phenology and SLA or that growing additional plant tissue has no functional benefit/cost, it is difficult to justify or interpret the causality if trait-variation has no reasonable trade-offs considered in their study.

1.6 Next-generation vegetation models: trait-based approach

Realistic biological-process representation is ergo vital to studying plastic plant-responses to environmental changes. Several global-scale plant economics spectra have emerged from mega-data analyses using the global plant trait database (Wright et al., 2004; Chave et al., 2009; Reich, 2014; Díaz et al., 2016). The economics spectra provide some general correlations for some key plant traits and trade-offs on a global scale. In the past decade, new generations of global vegetation models were developed based on economics spectra and other plant functional traits, such as aDGVM (Scheiter, Langan, and Higgins, 2013), LPJmL-FIT (Sakschewski et al., 2015), and JeDi-DGVM (Pavlick et al., 2013). As more explicit physiological representations are being considered, these models have helped advance the understanding of ecosystem functioning from a more process-based aspect than the PFT approach. However, these models are only forced by a prescribed climate (so-called offline models). To be precise, studies using these models have only focused on how vegetation emerges/varies under certain climate scenarios but entirely ignores vegetation's feedback on climate and hence leads to over-prediction. For instance, ignoring potential feedback from vegetation changes while predicting climate change overestimates the frequency and severity of drought in offline land surface models (Swann, 2018; Berg and Sheffield, 2018; Greve, Roderick, and Seneviratne, 2016).

Given that PFT-based ESMs ignore potential adaptation on plant traits and offline land surface models neglect vegetation feedback on climate, I implemented the new trait-based plant functioning trade-off model JeDi-BACH (Jena Diversity Biosphere-Atmosphere Coupled model in Hamburg) into the ICON-Earth System Model. This is the first trait-based functional trade-off vegetation model that has an interactive atmospheric component. Such a setup allows for investigation of the effect of plant trait diversity on the coupled vegetation-climate system. The traditional PFT-based approach is replaced by the so-called JeDi approach (Pavlick et al., 2013; Kleidon and Mooney, 2000). The essential difference of JeDi to the PFT approach is not to simulate global vegetation by a predefined set of PFTs but to obtain suitable plant strategies as a result of environmental filtering. The difference can be summarized in three aspects.

1. The representation theory of the JeDi approach is built on several well-observed plant functioning trade-offs that link the plant functions to environmental factors.

2. Each plant species' functional ability is determined by a set of plant trait parameters randomly 'born (sampled)' to each species. Each parameter set realizes a plant growth strategy with different plant functional abilities.

3. The selection of suitable plant species at different climate regions is chosen by the environment, following a widely used biogeography hypothesis of "Everything is everywhere; but environment selects."

In this way, a richer set of growth strategies are generated via several mechanistic trade-off selections by the environment. JeDi-BACH allows for more ecological investigations based on plant traits. It is possible to assess trait combinations that are so far underappreciated by ESMs (the case of SLA in MPI-ESM mentioned before). JeDi-BACH is the first plant functional trade-off based DGVM to explore the importance of plant-trait diversity for shaping the climate-vegetation in an interactive setup, i.e., a setup where the feedback between vegetation and climate are part of the model simulations.

1.7 Research objectives

To address the importance of plant functional diversity on global climate, I first introduce the new plant functional diversity model JeDi-BACH. In Chapter 2, I provide insights into the modeling concept of JeDi and the development of JeDi-BACH. Though the method is largely based on the model from Pavlick et al. (2013), several necessary modifications (of the methods) and new ecological features are added into JeDi-BACH to suitably adapt the functional trade-off scheme into an existing land surface model JSBACH. I particularly focus on some critical modifications that give a more plausible realization of ecological processes in JeDi-BACH. I consider the following guiding question throughout the chapter:

- **How to build a model that explicitly accounts for adaptive vegetation interaction with climate and that is sufficiently flexible for use in climate simulations?**

Chapter 3 is partitioned into two studies: In the fist study, I investigate the importance of plant functional diversity for shaping global climate and ecosystems. The offline model JeDi-DGVM has pointed out that global productivity enhances with increasing diversity (Pavlick et al., 2013). How does plant functional diversity influence global climate? To address this question, I perform a series of simulations with different levels of diversity using JeDi-BACH in a coupling setup with an interactive atmosphere. I ask the following research question:

1a What is the role of plant functional diversity in shaping the global climate-vegetation systems?

In the second study, I assess the sensitivity of model results. The goal of using JeDi-BACH is to generate adaptive vegetation via environmental filtering so that empirical decisions that may cause model biases can be avoided. However, during the development of JeDi-BACH, I identified some ambiguity in four trait parameters of which the values were not fully justified. Therefore, I investigate whether global climate are sensitive to these trait parameters. I pose the question:

1b How does global climate depend on the treatment in some plant trait representations that are yet justified?

In Chapter 4, I carry out a case study to investigate the role of plant functional diversity in shaping vegetation and climate interaction in an abrupt warming scenario. I investigate whether the hypothesis of diversity-resilience relationship plays a role in shaping global climate. Studies have predicted that future climate change will lead to non-analog vegetation in their functioning traits (Reu et al., 2014; Williams and Jackson, 2007; Pfeiffer et al., 2020). As a result of climate change, plants may alter their functional trait to adapt to a new climate. High functional diversity is thought to be a fundamental factor affecting the stability and resilience of an ecosystem to perturbation (Isbell et al., 2011a). So, an ecosystem with high functional diversity may be more capable of adjusting the functional traits to cope with environmental changes. With JeDi-BACH coupled to the atmospheric model of ICON-ESM, it is now possible to investigate how plant trait diversity may respond and shape global climate under climate change. A question of particular interest is whether a system with high plant functional diversity that consistently adjusts with climate will be more resilient to climate change. To answer this, I design a pair of experiments using JeDi-BACH, where one has high plant functional diversity and the other has low plant diversity. I consider the following question:

2 How does a different level of plant diversity influence the resilience to drastic climate change?

2

THE NEW TRAIT-BASED PLANT DIVERSITY MODEL: JEDI-BACH

2.1 Background

The JeDi-approach to model global vegetation is built on a trait-based plant functional trade-off scheme originally developed by Kleidon and Mooney (2000). Kleidon and Mooney established three fundamental concepts for their modeling approach: 1) they introduce a basic set of plant trait functions that are linked with several trade-offs to represent a "hypothetical plant species" in the model, 2) they generate these plant species' ability by random sampling, 3) they mimic the concept of "environmental filtering" for species selection. This novel approach provides a more ecological/biospheric framework for imitating the life form (or strategy to survive). With this framework one can simulate plant physiologic features with more flexibility. Using prescribed climate information, Kleidon and Mooney (2000) were able to model a general geographic distribution of vascular plant diversity which is similar to an observation estimate (Barthlott, Lauer, and Placke, 1996). Based on the original work of Kleidon and Mooney (2000), Pavlick et al. (2013) extended the method from simulating individual plant species to account for the community-level (assemblage) characteristics and built the model Jena Diversity Dynamic Global Vegetation Model (JeDi-DGVM). JeDi-DGVM is able to reproduce the large-scale global hydrological and carbon processes of vegetation better than the PFT-based approach in many aspects (Pavlick et al., 2013). Hereafter, the term "JeDi" is used to refer to the general modeling concept from these studies (Kleidon and Mooney, 2000; Pavlick et al., 2013). Considering that the previous studies using JeDi only focused on how changes in climate may shape global vegetation (Reu et al., 2014; Warszawski et al., 2013), this dissertation aims to investigate the reciprocal influence between vegetation and climate. I introduce the new plant diversity model (also a land surface model) JeDi-BACH, which employs the JeDi modeling concept and includes an atmospheric model interacting with the land surface, is introduced to explore the importance of plant trait diversity in shaping regional

climate.

The following part of the chapter is separated into two. In the first part, the general modeling concept of JeDi is presented. The explanation starts from the definition of the general structure of a plant species and of plant functions used in JeDi and then how the environment comes into play for the success of plant species. In the second part, a complete model description of JeDi-BACH is presented. Despite that JeDi-BACH is constructed based on Pavlick et al. (2013), many modeling aspects are modified. Because some of the original plant formulations implemented in JeDi-DGVM violate the modelling concept of JeDi and give beneficial conditions for certain plant species to outcompete others easily. In addition, I introduced new features such as a structural difference between trees and grasses and different biochemical pathways for photosynthesis that are known to be important outcomes of nature's history in JeDi-BACH.

2.2 General JeDi modeling concept

2.2.1 The universal plant

One essential idea of the JeDi modeling concept is that JeDi assumes that all plant species are located on a "universal plant" spectrum. Each plant species in JeDi is a distinct point on this spectrum. This universal plant has three primary features: 1) The universal plant has a fixed set of functional organs which all individual species inherit. Each organ has a respective plant function and corresponding trade-offs. 2) The universal plant has 15 plant traits. Each individual species is determined by a set of values for each of these 15 plant trait parameters that determine its life history strategy and growth-related features depending on environmental conditions. 3) Each plant's ultimate goal is to optimize growth, reproduction, and survival.

In JeDi, the set of functional organs comprises: the storage pool, leaves, stem, coarse root, fine root, and seed. Each organ has an essential function that contributes to at least one of the plant's goals.

1 The storage pool behaves like a "bank." It stores resources and distributes "savings" to the other organs. The state of the storage pool indicates survival: positive storage suggests that the species is alive and thriving, whereas negative or no storage means it cannot maintain itself and is thus dead.

2 Among the above-ground tissues, leaves are the essential organs that harvest sunlight for photosynthesis and produce energy (carbon assimilation)

for the whole plant. Leaves are the interface to the atmosphere and control the water and CO_2 exchange.

3 Stems are woody tissues that connect leaves with roots and support the vertical growth of the canopy for reaching more sunlight.

4 Beneath the soil, coarse roots and fine roots anchor plants in the ground and serve as pipes to suck up soil water for photosynthesis. Coarse roots are woody tissues, which can penetrate into deeper soil layers.

5 Fine roots are hairy tissues that grow into the pores between soil particles to suck up water.

6 Last, the function of the seed pool is to represent two stages of life: reproduction and germination. When seeds sprout and start to develop, a life cycle begins. The other stage is that plants generate embryos (seeds) to assure the species' survival.

These six organs operate together to maintain the life of a plant species. The functional capability and the life history strategy of a specific plant in JeDi are defined by its plant trait parameters. A "plant growth strategy (PGS)" is a specification of the universal plant by a set of trait parameters that quantify the behaviour of a species (see next section for more illustration for a PGS and a set of plant trait parameters). This universal plant structure allows JeDi to sample a spectrum of different PGSs with marginally different functional capabilities. In other words, as long as the trade-offs considered by the universal plant are sufficiently complex, the universal plant spectrum shall cover a wide range of growth strategies in the model.

It is vital to highlight one advantage of the universal plant structure: It can represent grasses and trees. In the original JeDi, grasses were barely (or rarely) simulated in the model, which contradicts the observed abundance of grasses in reality. Grasses and trees are two different structural strategies. Trees are long-lived, slow-growing, and grow tall with time. Grasses are short-lived, fast-growing, and, compared to full-grown trees, short. Each of the two plant categories has distinct advantages for their survivals. To include grasses, two universal plants are implemented in JeDi-BACH. One universal plant contains woody pools such as coarse roots and stem to represent trees. The other one has no woody pools to represent grasses. The definition of a plant growth strategy and trade-offs is illustrated in the next section.

2.2.2 Plant growth strategy

For survival, each plant species has its own strategy to cope with the surrounding environmental conditions. For instance, vegetation growing in arid regions develops drought-tolerance to cope with the lack of water; trees in tropical rainforests competing with other species form deep canopies to have greater access to light; deciduous trees in temperate climate regions have thin, and fast-growing leaves to efficiently utilize the warm but short summers and they shed these low-cost leaves to survive cold winters by saving the energy otherwise used on maintaining unproductive leaves. Although these plant growth strategies found in different climate regions are very different, their essential goal is to grow, maintain living costs, and reproduce to survive. To achieve this, resource allocation is critical. According to the optimal allocation theory (Bloom, Chapin III, and Mooney, 1985), plants allocate resources to those plant parts that limit plant growth most. Plants tend to optimize growth as resources are limited, and any ineffective investment could be at the cost of the plants' life.

The way how plants optimize their restricted resources is based on various trade-offs. A trade-off refers to a negative correlation between two factors, suggesting that each investment has a corresponding cost-benefit relationship. I illustrate this using two different allocation strategies:

> When a tree preferentially invests carbon into the growth of leaves to harvest more sunlight, it has less of the available carbon left to grow deep roots. Consequently, this tree has less access to water from the deep soil. Likewise, when a tree favors growing deep and complex roots to improve its soil water and nutrient access, it has less carbon left to develop a high canopy and has less access to sunlight.

Hence, there is a strong link between plant growth strategies and trade-offs, and the idea of JeDi is to obtain the former from the latter.

2.2.3 Plant functional traits and trade-offs

Before explaining each specific trade-off of JeDi, I present some definitions used throughout the entire thesis. In JeDi, a plant species is defined as a "plant growth strategy (PGS)." Hereafter, the terms "strategy," "species," or "PGS" all refer to a plant growth strategy. Each PGS is represented by a set of 15 plant trait parameters. Each trait defines either a conceptual parameter or a parameter representing an actual plant trait. For simplicity, I refer to "trait" as a "plant trait parameter" throughout this dissertation. Table 1 summarizes each trait used in JeDi, and illustrates the advantages and risks for one example strategy.

A set of 15 parameters describes three general aspects: how plants respond to environmental changes, their life history strategy, and whether they have a fast or slow growth strategy.

- To mimic how plant growth responds to its environment, three aspects (5 traits, t_1 to t_5) control the timing for growth: the length of the growing season, how fast a plant responds to environmental fluctuation and how fast a plant responds to mortality. A similar environment-dependent control for germination is also introduced (4 traits, t_1 to t_3 and t_6).
- To determine their life history strategies, a trade-off among growth, reproduction, and survival is introduced. Allocation traits, the relative aboveground/below-ground growth, and the relative allocation between woody and fine tissues are key (4 traits, t_6 to t_9).
- Whether the growth strategy is fast or slow is determined by the turnover time for woody and fine tissues (2 traits, t_{13} and t_{14}). Associate to this, a trade-off between a high assimilation rate due to a high leaf nitrogen concentration and the resulting high respiratory costs for maintaining such high nitrogen concentrations is introduced (1 trait, t_{15}).

Note that a trait does not always correspond to a single trade-off. As processes (growth, decay, reproduction, and mortality) are interdependent and indirectly and non-linearly influence each other via trade-offs, it is possible that similar plant growth strategies can be realized by different sets of trait values in different environments. Examples of potential advantages/risks are listed in the table 1. More complex trade-offs are hidden behind the combination of multiple traits. More detailed explanations for each trait will be given in the next chapter.

	Trait description	Example illustrating the trade-off of a large t_i to a small t_i	
		Advantage	Risk
t_1	Response time of a species to growth during favourable soil condition.	Smaller risk of extinction due to short-term wet event	Insufficient time for growth.
t_2	Response time of a species to growth when weather is warm.	Smaller risk of extinction due to warm fluctuation.	Insufficient time for growth.
t_3	Critical temperature to trigger growth. Determine if it is warm- or cold-adapted species.	Assure growth in warm seasons or in warm regions.	Not able to survive in cold condition or shorter growing season.
t_4	Critical temperature to terminate growth.	Early termination of growing season and start to store carbon.	Shorter growing season.
t_5	Response time to mortality.	Resist to short-term tough periods.	Extra maintenance expenditure and risk of extinction if short of storage.
t_6	The portion of seeds that germinates from the seed bank.	More small or few strong offspring enters growing stage.	Considerable loss once reproduction failed.
t_7	The portion of carbon allocated for reproduction.	More chances to preserve species	Less C for growth.
t_8	The portion of carbon allocated to aboveground growth.	Access to more sunlight and have more production.	Less soil water accessibility or less storage or less seeds.
t_9	The portion of C allocated to belowground growth.	Secure more soil water accessibility.	Less C for seeds, storage, or less access to sunlight.
t_{10}	The portion of C kept for storage.	Can survive sudden or longer bad spell (continuous negative NPP).	Less C for reproduction and growth.
t_{11}	The relative portion of aboveground growth for woody tissues.	Having stronger stem to survive windthrow and has less respiration cost.	Less leaves for photosynthesis
t_{12}	The relative portion of belowground growth for woody tissues.	Coarse root can penetrate to deeper soil and have larger maximal potential soil water available.	Less fine root and potentially larger water stress.
t_{13}	Turnover time for woody tissue pools.	Require less C to regrowth once reaching static static and is often spatially extend.	Require longer time to reach static state and have a higher maintenance cost.
t_{14}	Turnover time for fine tissue pools.	Require less C to regrowth once reaching static static.	Require longer time to reach static state and have higher maintenance cost.
t_{15}	Nitrogen content for leaf photosynthetic trait.	Higher photosynthetic capacity.	Higher maintenance cost on fine tissues.

Table 1: Description of the 15 trait parameters. These parameters were first introduced by Kleidon and Mooney (2000). An illustration of each trait parameter is given as an example of a growth strategy with a large corresponding trait value compared to a species with a small trait value. t_1 to t_5 specify a plant's response time to environmental fluctuation and mortality. t_6 to t_{12} specify a plant's life history strategy. t_{13} to t_{15} define whether it is a fast or slow growth strategy. C is short for carbon.

2.2.4 Environmental filtering

The hypothesis of *"Everything is everywhere; but the environment selects"*, brought up by Becking (1934), has been widely used to link the biogeographic distribution to the environmental attributes. In other words, this "environmental filtering" hypothesizes that the environmental conditions will select a few surviving species from many: whichever species adapts to the local environment can survive. This hypothesis has been widely discussed in environmental microbiology (De Wit and Bouvier, 2006; O'Malley, 2007) and has been also adapted by other scientific communities to investigate biogeography.

To illustrate this concept, I use the two different allocation strategies given in Section 2.2.2. Two trees (one prefers to grow leaves; one prefers to grow roots) are growing in the same rainforest where it is warm year-round with plenty of rainfall. The tree with a more extensive canopy can grow faster than the tree with deep roots, as the former harvests more sunlight. Because there is plenty of soil water available, having only shallow roots is sufficient to survive. However, if a long-lasting drought occurs, the high-canopy tree cannot survive beyond a certain aridity threshold while the deep-root tree might be able to persist. Therefore, if all plant strategies are assumed to be able to potentially grow everywhere, the survivors are determined by the environment. Note that no plant can survive in all climatic conditions, so no species will thrive globally. Environmental filtering will result in a gradient of species richness: the more variable the environment is, i.e., the harsher the environment is, the fewer species can survive. In the rainforest, both the trees with shallow and with deep roots can survive, though one might thrive faster. But under a variable environment with periods of droughts, the deep-rooted tree can more likely survive.

The philosophy of JeDi is clear now. JeDi aims to generate plant species in the model as a result of environmental filtering. To achieve this, JeDi applies a two-step approach:

1. "Trait generation": Numerous growth strategies are randomly generated from the 15-dimensional trait space so that all PGSs have a different functional capability.

2. "Environmental filtering": All species are allowed to grow everywhere over land, but only those, which are capable of maintaining themselves in the given environment using their inherent functional capabilities can survive.

To sum up, in JeDi, all PGSs have the same structure, either with 6 (for trees) or 4 (for grasses) tissue pools and the same number of trait parameters representing functional trade-offs. But each PGS has a different functioning "capability" depending on the value of its plant trait parameters. By randomly sampling

species across wide ranges of functional "capability" in the 15-dimensional trait space, JeDi creates a spectrum of plant growth strategies. Moreover, species can not survive in all kinds of environments due to trade-offs. Via environmental filtering, JeDi obtains a richer set of plant functional diversity with more ecophysiological realism and fewer diversity constraints compared to the PFT approach.

2.3 Generation of hypothetical traits

As explained earlier, JeDi creates a spectrum of PGSs via random sampling in the 15-dimensional trait space. However, it is challenging to sufficiently explore such a high-dimensional space. If only two values in each dimension are sampled, for instance, the minimal and the maximal value, more than 32,000 combinations are needed to simulate all possible strategies. This amount of strategies is not feasible concerning the computational resources needed. JeDi uses the Latin-hypercube sampling (LHS) method to explore the multi-dimensional space effectively(Stein, 1987). Two steps summarize the procedure for random sample in trait space:

1. "Latin hypercube sampling": numerous species are evenly sampled in the 15-dimensional space by LHS. The value of each dimension ranges from 0 to 1.

2. "Scaling to trait space": the values (from 0 to 1) are next scaled to the range of the respective trait parameter (see trait description in table1; values of each trait are described in different sections of Chapter 2.5).

As mentioned, grasses are barely sampled in JeDi-DGVM. Since grasses are plants without woody tissue, the traits determining the inclination of a species to form woody tissue need to be zero ($t_{11} = t_{12} = 0$ in table1). It is improbable to randomly sample a PSG where the two relevant traits are both zero. Plants without the woody pools are sampled separately in Jedi-BACH during trait generation to resolve this issues. Roughly 60% of the total sampling species is with woody tissue in JeDi-BACH to avoid undersampling of trees because trees are much harder to survive compared to grasses.

2.4 Aggregation to ecosystem-scale

The last concept of JeDi that needs to be explored is the aggregation from individual strategy to the ecosystem level. To estimate how the individual plant

strategy's contributes to the ecosystem level, Pavlick et al. (2013) assumes that the aggregation of both the terrestrial fluxes and functional properties (from individual species) to the ecosystem scale follow the so-called "biomass-ratio theory" (Grime, 1998). The review of Grime (1998) synthesises experimental evidence that the dominant species is usually taller, more expansive in morphology and has large biomass proportion but is fewer in number than the subordinates species. These large-extent dominant species make a large total contribution to the community. Based on this evidence, Grime hypothesized that the relative importance (or contribution) of individual species to the community is likely to be closely proportional to the relative contribution of that species to the total plant biomass of the community. Namely, an ecosystem can be characterized as the sum of the functional traits of all the species in the community, weighted by the abundance of individual species. This theory is also supported by other studies as a reasonable approximation for measuring functional diversity in a plant community (Laliberté and Legendre, 2010; Dıaz and Cabido, 2001). Thus, JeDi scales the contribution of a species using to the total biomass of the species relative to the total vegetation biomass in a community (see section 2.4 for more details).

It is worth noting that the biomass scaling also serves as a broad realism for measuring the competition between tree/grass-type species. In natural environment, trees benefit from their high canopy to intercept light at a higher level compared to grasses. Trees also have higher resistance to natural disturbance (such as fire or windthrow) due to their woody structure. Therefore, biomass-scaling gives trees potentially more weights or dominance compared to grasses. Nevertheless, trees do not always have advantage over grasses. In the early stage of succession, trees have a disadvantage over grasses because trees grow slow and need to spend a considerable portion of energy on constructing and maintaining woody tissues. Hence, grasses can outcompete trees when a bare land appears. The biomass ratio thus ambiguously accounts for the structural advantage of trees and also some aspects of ecological succession.

2.5 Model description of JeDi-BACH

JeDi-BACH is the first trait-based dynamic vegetation model embedded in the ICON-Earth System Model (ICON-ESM). As mentioned, JeDi-BACH is based on the JeDi modeling approach developed by Kleidon and Mooney (2000) and Pavlick et al. (2013). I implemented it in the land component model JSBACH of the ICON-ESM (Reick et al., 2021). JeDi-BACH inherits the land physics from JSBACH, but the JeDi modeling approach replaces many plant-relevant processes.

JSBACH is the land surface model developed jointly by the Max-Planck Institute for Meteorology and the Max Planck Institute for Biogeochemistry (Reick et al., 2021). The latest model version JSBACH4 is developed aiming for the new generation Earth System Model of ICON-ESM. JSBACH provides the surface boundary conditions such as land physics and biosphere-related physical/chemical processes for the atmospheric component of ICON-ESM. In JSBACH, the surface energy balance, soil heat transport, and soil hydrology are computed over different land cover types. Merging JSBACH and JeDi, I carefully modified and replaced the calculation of carbon allocation, phenology, autotrophic respiration, and the surface characteristics (e.g., albedo and the surface roughness) (see table2).

The main goal of this chapter is to explain each component of JeDi-BACH as well as the adjustments to the base model JSBACH4 necessary to couple JeDi-BACH with the atmosphere model. The following sections will start with an overview of a "universal plant's" tissue structure and its dynamics. Explanations for acronyms and symbols used in the following sections are given in table3. A section with a title including the symbol "Box" indicates that some novel developments which deviate from the original JeDi are implemented in that process. A summary of these changes to JeDi is be presented in two yellow boxes, Box1 and Box2.

2.5.1 Six plant functional organs and the dynamics

In JeDi-BACH, a PGS comprises six organs (living biomass pools): the storage, seed, leaves, stem, coarse root, and fine root. Fig. 1 illustrates the carbon pool structure.

A PGS is alive only if it can maintain a positive carbon storage. If a strategy has a negative carbon flow, it would eventually go extinct as it runs out of

		JeDi-DGVM	JSBACH	JeDi-BACH Brief remarks
Plant productivity and carbon fluxes	Carbon allocation	✓		Each plant consists of six organ pools: leaves, stem, coarse root, fine root, seed, and storage. Allocation fraction for each pool is determined by allometry traits.
	Carbon assimilation		✓(**P**)	Photosynthetic model for C_3 plants: the Farquhar model (Farquhar, Caemmerer, and Berry, 1980); for C_4 plants: the Collatz model (Collatz, Ribas-Carbo, and Berry, 1992).
	Autotrophic respiration	✓		A simple biomass-based method for autotrophic respiration (Ryan, 1991).
Phenology	Leaf phenology	✓		Leaf area index depends on the amount of leaf biomass and specific leaf area (SLA).
	Growing season	✓((**M**)		Species' growing season depends on temperature and soil wetness according to their abiotic traits.
Belowground physiological properties	Water stress		✓((**M**)	Water stress limiting productivity is regulated by soil moisture in the root-zone, root-shoot ratio, and potential evapotraspiration.
	Rooting depth	✓(**P**)		Rooting depth is a function of coarse-root biomass.
Aboveground biophysical properties	Canopy albedo	✓		Canopy albedo is a function of prescribed leaf nitrogen content (Hollinger et al., 2010).
	Roughness length		✓(**P**)	Surface roughness length is dependent on growth form (tree, grass).
	Canopy radiation		✓	Canopy radiation model computes the amount of radiation absorbed in the canopy.
Land physics	Surface energy balance and soil heat budget		✓	Determine the exchange of energy between land surface and atmosphere.
	Water budget		✓	Aboveground water budget and soil hydrology.
	Lakes/River runoff/Glaciers		✓	Land water fluxes to the ocean.

Table 2: Different components of JeDi-BACH and the corresponding original processes in JeDi-DGVM and JSBACH. A check-mark in the column "JeDi-DGVM" indicates that the respective process is newly implemented and replaces a corresponding process description of JSBACH. Instead, a check-mark in the column "JSBACH" indicates that the process implementation of JSBACH is taken over into JeDi-BACH. (**P**) indicates some parameters are modified for JeDi-BACH. (**M**) indicates that the processes are substantially modified for JeDi-BACH. A brief remark of the process adapted in JeDi-BACH is presented in the last column.

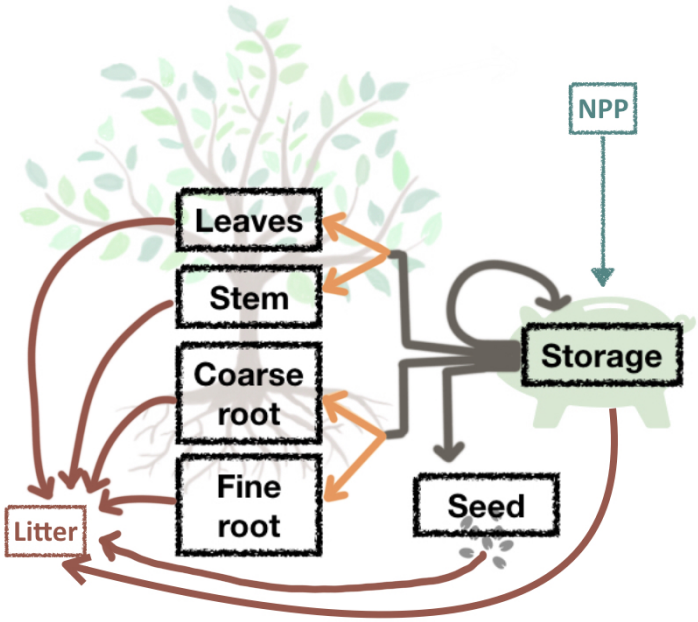

Figure 1: Structure of the six carbon pools. Arrows indicate the carbon fluxes between the pools.

storage carbon which it needs to keep functioning. The dynamics of the whole plant growth and the resource distribution among the six pools are critical for determining the functional capabilities of a PGS. The dynamics of the six pools are described in eq.(1) - eq.(6). The biomass of a specific organ is denoted by C_{organ} , A_{organ} represents the allometric fraction, $k_{RES,organ}$ is the construction constant (that determines the portion of energy for building up tissue), τ_{organ} is the turnover time. GPP is the gross primary productivity, R_m is the maintenance respiration, and GERM is the carbon flux from seed germination. For more detailed parameter descriptions and for the units of the variables used in the JeDi-BACH please refer to table 3. The equations below describe the carbon fluxes in and out of each organ and have a common structure: on the left-hand side, it shows the net carbon flux in or out of the organ (time derivative of the carbon allocated in the organ). The right-hand side comprises incoming fluxes (carbon gain from allocation or germination) and the outgoing fluxes (energy used for construction cost or deterioration of biomass).

$$\frac{dC_{storage}}{dt} = (GPP - R_m) + GERM - \frac{C_{storage}}{\tau_{storage}} - C_{storage} \sum A_{organ}(1 - k_{RES,organ}) \tag{1}$$

$$\frac{dC_{seed}}{dt} = C_{storage} A_{seed} (1 - k_{RES,seed}) - GERM - \frac{C_{seed}}{\tau_{seed}} \tag{2}$$

$$\frac{dC_{leaves}}{dt} = C_{storage} A_{leaves} (1 - k_{RES,leaves}) - \frac{C_{leaves}}{\tau_{leaves}} \tag{3}$$

$$\frac{dC_{stem}}{dt} = C_{storage} A_{stem} (1 - k_{RES,stem}) - \frac{C_{stem}}{\tau_{stem}} \tag{4}$$

$$\frac{dC_{csroot}}{dt} = C_{storage} A_{csroot} (1 - k_{RES,csroot}) - \frac{C_{csroot}}{\tau_{csroot}} \tag{5}$$

$$\frac{dC_{fnroot}}{dt} = C_{storage} A_{fnroot} (1 - k_{RES,fnroot}) - \frac{C_{fnroot}}{\tau_{fnroot}} \tag{6}$$

The daily net growth of a plant is determined by the balance of two main fluxes with opposing sign. The plant loses carbon due to respiration and deterioration of existing carbon pools and gains carbon through photosynthesis. The total carbon fixed is called gross primary productivity (GPP). Most of this carbon is immediately spend on maintaining existing tissue (maintenance respiration, R_m) without being added to any pool. The left-over carbon remains in the storage pool, part of which deteriorates naturally at a rate determined by the turnover time ($\tau_{storage}$) as shown in eq.(1).

When seeds germinate, a PGS moves a portion of seed carbon (GERM) to the storage pool for growth. Additionally, the storage pool receives the remaining carbon from it's productivity $(GPP - R_m)$. Then, plants distribute carbon from the storage pool for growth of different organs. The allometric fraction (A_{pool}) determines the ratio between growth and storage for each biomass pool. The amount of carbon kept in the storage pool is mathematically chosen as one minus the sum of the non-storage allometric fractions to assure carbon conservation. This means that the storage pool keeps all the remaining carbon. A PGS with a large storage pool (relative to other organs) has a conservative strategy as it prefers storage over growth/reproduction. Likewise, a small storage pool represents a liberal strategy with an preference for investing over savings.

The dynamics of the leaves, stem, coarse root and fine root pool have an analogous dynamic. The development of these biomass pools is balanced between

growth and natural deterioration (see eq. (2) - eq.(6)). The amount of carbon allocated to growth is controlled by the respective allometric fraction (A_{pool}) and the carbon content of the storage pool. A fixed ratio of the carbon available for growth is lost due to construction costs ($k_{RES,pool}$), labeled growth respiration. The natural deterioration of tissue is determined by the respective turnover time for each organ pool (τ_{pool}) .

The dynamics of the seed pool is controlled by reproduction, germination, and deterioration of seeds (eq. (2)). The allocation trait for seed (A_{seed}) and the carbon content of the storage pool determine the amount of seed reproduction. If a strategy reproduces a large amount at once, this can be interpreted as reproduction by either a few large (biomass) seeds or by many tiny seeds. After seeds germinate, the germinated carbon flows to the storage pool (this flux is denoted as GERM). The deterioration of seeds is determined by the seed turnover time (τ_{seed}) and is assumed the same value for all PGSs.

2.5.2 Plant allometry

How is carbon distributed among the individual plant organs? Optimal partitioning theory (Bloom, Chapin III, and Mooney, 1985) suggests that plants allocate more resources to the organ that is ultimately limiting the overall plant growth. As resources are limited, plants need balance their growth in each organ to optimize resources. The growth of each plant organ relative to the whole plant is thus critical for determining their fitness and survival. In JeDi-BACH, the allometric fraction A_{organ} determines the distribution of carbon among different carbon pools (one pool per organ) which is defined as follows for each organ:

$$\begin{aligned}
A_{seed} &= F_{grow} F_{seed} \frac{t_7}{t_{total}} \\
A_{stem} &= F_{grow} \frac{t_8}{t_{total}} \cdot t_{11} \\
A_{leaves} &= F_{grow} \frac{t_8}{t_{total}} \cdot (1 - t_{11}) \\
A_{csroot} &= F_{grow} \frac{t_9}{t_{total}} \cdot t_{12} \\
A_{fnroot} &= F_{grow} \frac{t_9}{t_{total}} \cdot (1 - t_{12})
\end{aligned} \tag{7}$$

F_{grow} and F_{seed} are "on-off" functions that determine the timing for plant growth and reproduction (eq. (13) and eq. (14) for definition). As mentioned,

the preference of a PSG to store carbon in specific organs is a key characteristic of this PSG. t_{7-12} are the traits of the universal plant which determine the allometry (Table 1). These traits fall into two categories. t_{7-10} divide the carbon between seed, above- and below-ground growth, and storage, respectively. t_{total} denotes the sum of these four allometric traits.

$$t_{total} = t_7 + t_8 + t_9 + t_{10} \tag{8}$$

To assure carbon conservation the sum of the allometric fractions t_i/t_{total} in eq. (7) equals one:

$$\sum_{i=7}^{10} \frac{t_i}{t_{total}} = 1, \tag{9}$$

Both the above- and below-ground growth are sub-divided into woody (stem and coarse-root) and non-woody (leaves and fine-root) growth by the relative woody allometric traits (t_{11} and t_{12}), which constitute the second category of allometric traits. These two traits are critical to determine whether a plant has a tree-type or a grass-type strategy: grass-type strategies have no woody tissue ($t_{11} = t_{12} = 0$). If a species does not invest in growing new tissues (no plant growth, $F_{grow} = 0$), the storage pool keeps the non-allocated carbon to ensure carbon conservation.

2.5.3 Timing of plant growth and mortality

It is known from observations that the timing of several key plant biological events is tightly linked to the surrounding environment, such as the local climatic conditions, or water and resource availability (Lieth, 1974). For instance, leaf buds develop during spring when the weather gets warmer. When the weather gets colder during autumn, deciduous trees shed their leaves to reduce energy loss from maintenance respiration and to survive winter. The timing of these ecological events varies substantially across different vegetation types and climate regions. These differences are linked to a trade-off related to response time: an early start of growth gives early access to resources but puts species at risk because weather is not always stably favorable to growth in early spring. The environment is more stable later in the year, reducing the risk for the plant due to changing weather. But a late start of growth comes with the disadvantage of a shorter growing season. In JeDi-BACH, the timing for the start and end of the growing season, for the seed germination, and and for stressed-induced mortality are driven by two environmental attributes: the near-surface temperature and the relative soil moisture.

Under natural conditions, environmental conditions fluctuate on various timescales. Plants don't react immediately to short-term weather improvements in early spring but often wait until the weather is moderate enough to avoid false carbon investment. To simulate this behavior of plants, I applied a technique to compute abiotic "pseudo" variables that contain information of the recent weather while smoothing out hourly and daily variations.

2.5.3.1 Pseudo variables[Box1]

To simulate how plants store information on past environmental conditions, I defined "pseudo" variables to calculate the time-weighted value of a period over the recent past. This technique is adapted from Reick et al. (2021). The pseudo-variable $\overline{X}^n$ at time n is calculated as

$$\begin{aligned} \overline{X}^n &= \frac{1}{N} \sum_{n'=-\infty}^{n} X^n e^{-(n-n')\frac{\Delta t}{\tau}} \\ N &= \sum_{n'=-\infty}^{n} e^{-(n-n')\frac{\Delta t}{\tau}} \end{aligned} \tag{10}$$

X^n is the environmental state variable at time n that one aims to smooth. τ characterizes the time length of memory of $\overline{X}^n$, and Δt is the length of the time step. A pseudo-variable stores the time-averaged behavior of the corresponding state variable. In each time step, the most recent past has biggest weight. The older the information, the less it is taken into account.

Numerically, eq.(10) is implemented as

$$\begin{aligned} \overline{X}(n+1) &= \frac{X(n)}{N} + \overline{X}(n)\, e^{-\frac{\Delta t}{\tau}} \\ N &= \frac{1}{1 - e^{\left(-\frac{\Delta t}{\tau}\right)}} \end{aligned} \tag{11}$$

A PGS with a small value of τ (short memory) characterizes a responsive species that stores only recent environmental information. It reacts quickly once the environment is favorable. Likewise, a large value of τ (long memory) characterizes a conservative species that stores information of the recent past for a long time. It responds slowly to changes in the environment. In the following sections, only the numeric form of the pseudo-variables is presented (e.g., (**??**)).

2.5.3.2 Timing of plant growth [Box1]

In JeDi-BACH, the timing of plant growth depends on ambient temperatures and the relative soil wetness. There are three pseudo variables used for determining the timing of growth, based on the three following environmental

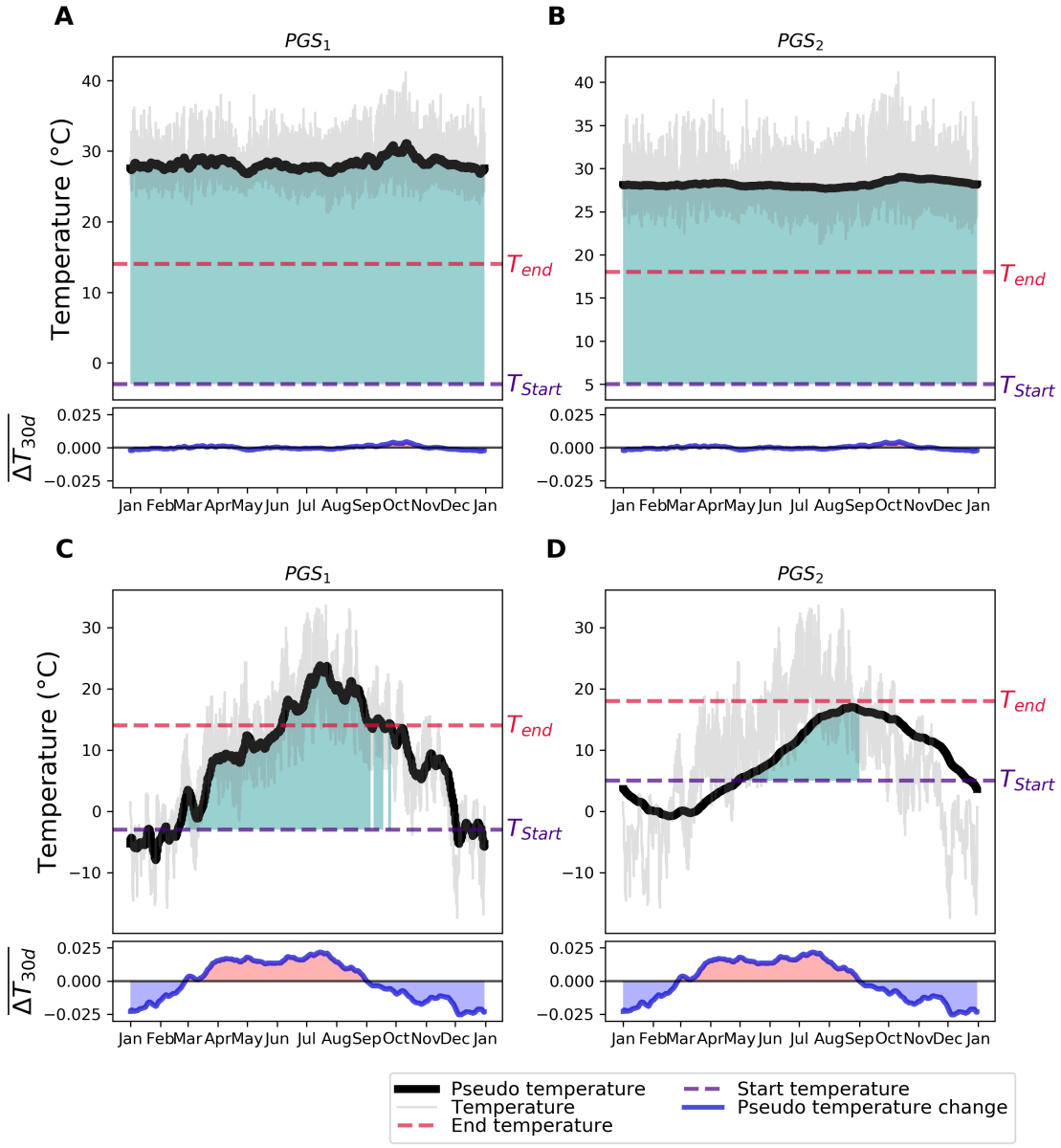

Figure 2: Examples of two PGSs' response to temperature changes in two climate zones. Upper panels: central Amazon (60W,3.7S); bottom panels: central Europe (13E,52N). The left panels (**A**, **C**) show the response of reactive PGS_1 with $T_{start} = -3°C$, $T_{end} = 10°C$, and memory characteristic $\tau_T = 7$ days. The right panels (**B**, **D**) show the response of conservative PGS_2 with $T_{start} = 5°C$, $T_{end} = 18°C$, and memory characteristic $\tau = 30$ days. 4 hourly atmospheric temperatures are shown as the grey line. Black thick solid line shows the pseudo temperature ($\overline{T}_{grow}$). Purple and red dash lines indicate the threshold temperatures for the beginning (T_{start}) and termination (T_{end}) of growing seasons for the respective PGS. Turquoise shaded areas mark the time window for growing seasons. The pseudo temperature changes ($\overline{\Delta T_{30d}}$) are shown in the sub-figures (at the bottom of each figure). Red shaded areas indicate a warming trend and blue shared area indicates a cooling trend.

variables. T is the near-surface air temperature, W is the relative soil moisture within the root zone, and ΔT is the difference between daily mean temperature and yesterday's mean.

$$\begin{aligned}
\overline{T}_{grow}^{n+1} &= T^n \left(1 - e^{-\frac{\Delta t}{\tau_T}}\right) + \overline{T}_{grow}^{n} \cdot e^{-\frac{\Delta t}{\tau_T}}; \;\; \tau_T = 10^{1.1t_2+0.9} \\
\overline{W}_{grow}^{n+1} &= W^n \left(1 - e^{-\frac{\Delta t}{\tau_W}}\right) + \overline{W}_{grow}^{n} \cdot e^{-\frac{\Delta t}{\tau_W}}; \;\; \tau_W = 10^{1.1t_1+0.9} \\
\overline{\Delta T_{30d}}^{n+1} &= \Delta T^n \left(1 - e^{-\frac{\Delta t}{\tau_T}}\right) + \overline{\Delta T_{30d}}^{n} \cdot e^{-\frac{\Delta t}{\tau}}; \;\; \tau = 30 \;\; days
\end{aligned} \tag{12}$$

$\overline{T}_{grow}$, $\overline{W}_{grow}$, and $\overline{\Delta T_{30d}}$ are the pseudo surface air temperature, pseudo soil wetness, and pseudo daily temperature change[*2] (over the past 30 days). JeDi-BACH features a new implementation of $\overline{\Delta T_{30d}}$ compared to JeDi. This pseudo variable indicates the termination of a growing season, especially in mid-to high-latitude ecoregions. The trait values t_1 and t_2 (eq. (12)) characterize the response time to changes in T and W for each PGS. The memory characteristics of surface temperature (τ_T) and of the soil moisture within the root zone (τ_W) are sampled from weeks to a few months in the calculation of the respective pseudo-variables (eq. (11)). The timing of growth is calculated as follows:

$$F_T = \begin{cases} 1, \overline{T}_{grow} > T_{start} \text{ and } \overline{\Delta T_{30d}} \geqslant 0 \\ 0, \overline{T}_{grow} < T_{end} \text{ and } \overline{\Delta T_{30d}} < 0 \end{cases} \tag{13}$$

$$F_{grow} = \begin{cases} 1, \overline{W}_{grow} \geqslant 0.5 \text{ and } F_T = 1 \\ 0, \overline{W}_{grow} < 0.5 \;\; \text{or} \;\; F_T \neq 1 \end{cases} \tag{14}$$

F_T is an "on-off" switch that indicates whether the environment is withing a species's thermal adaptation range. F_{grow} is also an "on-off" switch that specifies the timing of growth start and end. T_{start} and T_{end} specify the the temperature range that a PGS favors to grow. These two temperatures determine the beginning and the end of a growing season. T_{start} is scaled from the trait t_3 (with value ranging from 0-1) to -5 °C and 15 °C. Similarly, T_{end} is scaled from the trait t_4 (with value ranging from 0-1) to 10 °C and 15 °C. $\overline{\Delta T_{30d}}$ indicates a cooling or warming trend. A positive value signals a warming conditions and negative value signals cooling conditions (see eq.(13)). A growing season starts ($F_{grow} = 1$) when the pseudo relative soil wetness is greater than 50 % and the ambient temperature is within the thermal adaptation range (see eq. (14)). A growing season ends ($F_{grow} = 0$) when either $\overline{W}_{grow}$ is less than 50 % or both $\overline{T}_{grow}$ is below T_{end} and $\overline{\Delta T_{30d}}$ is negative.

To illustrate how pseudo-variables control the timing of growth, Fig. 2 shows the response of two PGSs to temperature in two different climates (one tropical rainforest and one temperate climate).

- PGS_1 is characterized by $T_{start} = -3°C$, $T_{end} = 10°C$, and a memory characteristic $\tau_T = 7$ days.
- PGS_2 is characterized by $T_{start} = 5°C$, $T_{end} = 18°C$, and a memory characteristic $\tau_T = 60$ days.

In central Amazon (panel **A** and **B** in fig. 2) with prevailing high temperatures throughout the year, both PGSs have a year-round growing season. However, in the temperate climate zone (panel **C** and **D** in fig. 2), PGS_1 has a longer growing season than PGS_2 as PGS_1 is a rather cold adaptation strategy than PGS_2. PGS_1 is fast and responsive to temperature variations (short τ_T). It swings between 'to grow' and 'to stop' when temperatures fluctuate near T_{end} towards mid-autumn. PGS_2 stops allocating carbon to growth a month earlier then PGS_2, so it might have more time to fill up the storage pool before winter. On the other hand, PGS_1 might deplete it's storage pool during winter. This interpretation only give a general comparison between the two strategies considering only two trade-offs, a fast vs. a slow response strategy and a cold adaptation vs. a warm adaptation strategy. As there are more complex trade-offs involving other traits, one cannot conclude which of the two strategies is more successful from the growth strategies discussed here alone.

2.5.3.3 Timing for germination and for seedlings

The dynamics of the seed pool C_{seed} are determined by two time-dependant fluxes, germination GERM (see eq.(2)) and seedlings. The timing for seed germination GERM is controlled by an "on-off" switch F_{seed}. F_{seed} is dependant on the pseudo surface temperature (see eq.(13)) and the pseudo topsoil moisture. Pseudo topsoil moisture is calculated as

$$\overline{W_{5cm}}^{n+1} = W_{5cm}\left(1 - e^{-\frac{\Delta t}{\tau_W}}\right) + \overline{W_{5cm}}^{n} \cdot e^{-\frac{\Delta t}{\tau_W}} \tag{15}$$

W_{5cm} denotes the relative soil moisture in the top 5 cm of the soil and $\overline{W_{5cm}}$ is corresponding pseudo variable. τ_W is the characteristic memory for pseudo soil moisture (see eq.(12)). The timing F_{germ} and the carbon flux GERM of germination are calculated as follows:

$$F_{germ} = \begin{cases} 0, \overline{W_{5cm}} < 0.5 \text{ or } F_T \neq 1 \\ 1, \overline{W_{5cm}} \geqslant 0.5 \text{ and } F_T = 1 \end{cases} \tag{16}$$

$$GERM = F_{germ}\gamma_{germ}C_{seed};\ \ \gamma_{germ} = 10^{3t_6-3} \tag{17}$$

F_{germ} is an "on-off" switch that controls the timing for germination. Germination occurs when both temperature and the topsoil moisture are favorable. In addition, when seeds germinate, a portion of seed carbon is moved from the seed pool to the storage pool (see eq. (2)). How much carbon is moved to storage is controlled by a trait called the 'germination fraction' γ_{germ}, ranging from 0 to 1. A small value of γ_{germ} defines a conservative PGS that germinates only a small amount of it's seeds; a large value of γ_{germ} characterizes a PGS which invests heavily into reproduction.

The timing for the development of seedlings (denoted as F_{seed}) depends on productivity:

$$F_{seed} = \begin{cases} 0, NPP \leqslant 0 \\ 1, NPP > 0 \end{cases} \tag{18}$$

Seedlings develop only during a period with a carbon gain (see eq.(2) and eq.(7)). In other words, plants only produce seeds when net primary production is positive.

2.5.3.4 Timing of stress-induced mortality

When weather strongly deviates from it's average state such as during persisting droughts or extreme cold events, plant productivity is considerably reduced. Carbon storage in starch or sugars may be quickly depleted due to maintenance costs. When maintenance costs are higher than the photosynthetic production, the net carbon flow of the plant is negative. If photosynthetic production is constrained over a prolonged period, this negative carbon flow (negative NPP) may eventually lead to the death of the plant. To survive these harsh periods, plants may abandon some of their tissues to reduce the cost of maintaining tissues which are not useful at the moment. In JeDi-BACH, this effect is introduced by shortening the turnover time of fine tissues, namely the leaves and fine-root pools. In JeDi-BACH, leaves and fine root pool are assigned with the same turnover rate. In other word, deterioration of easily disposable carbon is sped up under life-threatening stress. I call this deterioration 'stress-induced mortality'. The natural turnover rate of fine tissue $\tau_{leaves,0}$ is:

$$\tau_{leaves,0} = \frac{365}{12}10^{2t_{14}} \tag{19}$$

The timing of mortality F_{stress} depends on the sign of the net primary productivity NPP, which represents the net carbon flux of the plant:

$$F_{stress} = \begin{cases} 0, \overline{NPP} \geqslant 0 \text{ or } NPP \geqslant 0 \\ 1, \overline{NPP} < 0 \text{ and } NPP < 0 \end{cases} \tag{20}$$

with the pseudo variable for the net primary productivity $\overline{NPP}$

$$\overline{NPP}^{n+1} = NPP^{n} \left(1 - e^{-\frac{\Delta t}{\tau_{NPP}}}\right) + \overline{NPP}^{n} \cdot e^{-\frac{\Delta t}{\tau_{NPP}}}; \tag{21}$$

$$\tau_{NPP} = 10^{1.1 t_5 + 0.9} \tag{22}$$

τ_{NPP} is the characteristic memory time of $\overline{NPP}$ with values ranging from weeks to months. Mortality is triggered when both persisting negative productivity $\overline{NPP}$ and negative NPP occur simultaneously.

In JeDi-BACH, stress-induced mortality has only effects on fine tissues because they are rich in nitrogen that commonly requires lots of maintenance. Once mortality is triggered, the turnover rate for both leaves and fine-roots increases considerably driven by the senescence constant κ_{SEN}.

$$\tau_{fnroot} = \tau_{leaves} = \left(\frac{1}{\tau_{leaves,0}} + F_{stress} \cdot \frac{1}{\kappa_{SEN}}\right)^{-1} \tag{23}$$

The expensive tissues deteriorate and shed substantially faster than the natural turnover rate in case of stress. In this way, plants reduce their maintenance costs to avoid a persisting negative carbon flux and increase their chance for survival. The woody tissues (stem and coarse-root) are sturdy and last longer. In JeDi-BACH, the woody tissues are assumed to have the same turnover rate:

$$\tau_{stem} = \tau_{csroot} = 365\,(79 t_{13} + 1) \tag{24}$$

τ_{stem} and τ_{csroot} denotes the turnover rate of the stem and the coarse-root pools, respectively, and is given values between one to eighty years. t_{13} is the trait modulating the turnover time of woody tissues.

Box 1:Remarks on section 2.5.3: Timing of plant growth and mortality

Overall, three modifications are first introduced in JeDi-BACH:

1 A new mathematical expression to perform the time averaging for pseudo-variables $\overline{X}$ is introduced.

Previously, JeDi-DGVM simulates with a resolution of one time step per day. The original formula for time averaging a variable is designed for this daily time step. JeDi-BACH has a much higher temporal resolution (commonly 15-20 minutes or less) due to the coupling with the atmospheric model. Besides, JeDi-BACH can flexibly run on different modeling time steps depending on the user's interest. To account for the a higher and a flexible temporal resolution, I introduced the pseudo-variables for time averaging. Notably, the model time step is now automatically taken into account when computing the pseudo variable (see Δt in eq. (10)).

2 The termination of plant growth is modified.

JeDi-BACH features an improved computation of the length of the growing season. In Pavlick et al. (2013), the same threshold temperature is used to bound the start and the end of a growing season ($T_{start} = T_{end}$) — this choice results in rather a late termination of the growing season in mid to high latitudes. Plants still grow new tissues that are likely to be useless as productivity is reduced when days become shorter in late summer. This carbon which was needlessly allocated to plant growth is missing in the storage pool, which plants store in the summer to survive the winder. To remedy this, I introduced a separate threshold temperature for termination of the growing season in JeDi-BACH. This new threshold is combined with a new variable for detecting the warming/cooling trend ($\overline{\Delta T_{30d}}$). With these two changes, the growing season ends when the weather gradually becomes colder and plant growth ends earlier than in JeDi-DGVM.

3 The relative deterioration between fine tissues is removed.

In JeDi-DGVM, strategies comprise a trait that determines the relative deterioration between fine roots and leaves if mortality occurs. This trait is removed in JeDi-BACH because it breaks the fixed root-shoot ratio concept associated with the soil water accessibility of a species (see section 2.5.4.2 for more details).

2.5.4 Rooting strategy and water constraint

Roots serve several critical functions related to the survival of plants. Roots anchor plants in the ground. They transport soil water and nutrients into the plant which are essential for photosynthesis. Roots function like pipes connecting the water from soil levels with the atmosphere. Soil water diffuses into roots, following the gradient of the hydrological potential, and moves through the xylem to the canopy. There it is transpired to the atmosphere via stomata at the leaf surfaces. This soil-plant-atmosphere continuum is critical for determining plant productivity and the water exchange between soils and the atmosphere. Besides roots, the ambient atmospheric condition also influences plant productivity. When the ambient atmosphere is saturated, the water vapor gradient between the leaf surfaces and the atmosphere vanishes. This suppresses transpiration and creates stress for the plants, which need the flow of water to get access to the nutrients from the soil. In JeDi-BACH, water stress affects productivity jointly by soil-water availability and the ambient atmospheric water vapor. This is described in the following by first introducing the relevant definitions for roots and then explaining the calculations for the water stress case.

2.5.4.1 Pipe model

The root system is partitioned into two functional carbon pools: the coarse roots C_{csroot} and the fine roots C_{fnroot}. Coarse roots are woody tissues that can penetrate deep soil layers determining the root depth and supporting the network of fine roots. Fine roots are hairy fine tissues that grow into tiny soil pores to suck up soil water. Fine-root tissues provide plant's with the actual ability to access soil water while the root depth is a key factor determining the total amount of soil water accessible to plants.

Inspired by the work of Shinozaki et al. (1964), JeDi-BACH treats the whole leaves-stems-coarse roots-fine roots system as an assemblage of pipes connecting soils and the atmosphere. The upper end are the leaf stomata, and the lower ends are the fine roots. In between, stem and coarse roots form the "pipes." I determine the depths of lower end, the root depth, depending on the size of the coarse roots carbon pool C_{csroot}. A schematic diagram of root pipes growing over a cross-section of soil is shown in fig. 3 for illustration. Let us consider a soil column of cross-sectional area A interspersed with a number of root pipes (each black line indicates a pipe in the fig. 3). JeDi assumes that fine roots are distributed homogeneously in the whole soil column. The density of "pipe ends" ρ ("pipe ends" are shown as solid dots in fig. 3) is constant within the

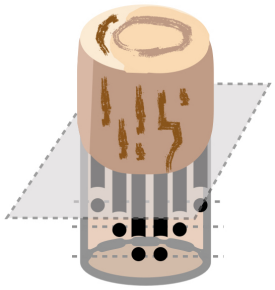

Figure 3: Sketch of the root pipes in a soil column. The black lines indicate the root "pipes," and the black dots indicate the "pipe ends."

soil column. Thereby, more "pipes" are closer to the surface, with a maximum number of pipes at the surface. The number of root pipes N_{pipe} at depth z is:

$$N_{pipe}(z) = \int_z^{l_r} \rho A \, dz = \rho A (l_r - z), \tag{25}$$

where l_r indicates the root depth. Assuming that all coarse-root carbon is used to construct pipes and letting c_{spl} denote the specific pipe length, i.e. the length of pipe grown per unit coarse-root carbon, the total length L_{pipe} of all pipes in the considered soil column is

$$L_{pipe}(l_r) = c_{spl} \cdot C_{csroot} \cdot A \tag{26}$$

The total length of root pipes in the soil column down to depth d is

$$L_{pipe}(d) = \int_0^d N_{pipe}(z)\, dz = \rho A \left(l_r \, z - \frac{1}{2} z^2 \right) \Big|_0^d = \rho A \left(l_r \, d - \frac{1}{2} d^2 \right) \tag{27}$$

Equating the two equations for $L(d)$, eq. 26 and eq. 27 gives at root depth $d = l_r$

$$L_{pipe}(l_r) = \rho A \left(l_r^2 - \frac{1}{2} l_r^2 \right) = \frac{1}{2} \, l_r^2 \, \rho \, A = c_{spl} \, C_{csroot} \, A \tag{28}$$

Finally, the rooting depth is

$$l_r = \sqrt{\frac{2 \, c_{spl} \, C_{csroot}}{\rho}} \tag{29}$$

A conversion coefficient κ_{rd} is introduced to relate C_{csroot} to the root depth ($\kappa_{rd} = 2 \, c_{spl} \, C_{csroot} / \rho$). Then the rooting depth is

$$l_r = \max \left[l_0, \sqrt{\kappa_{rd} C_{csroot}} \right] \tag{30}$$

l_0 is the minimal rooting depth. The relative soil wetness withing the root zone is is defined as the fraction of the actual water content to the maximal water holding capacity within the root zone:

$$W = \frac{W_{root}(l_r)}{W_{max}}; \quad W_{root}(l_r) = \int_0^{l_r} V(z)\,dz \tag{31}$$

W, $W_{root}(l_r)$, and W_{max} denote the total water, the total maximal water holding capacity, and the relative soil wetness in the root zone, respectively. $V(z)$ indicates the volumetric soil water content at soil depth z. The global distribution of the maximal soil water holding capacity is prescribed by the soil properties from FAO data (Hagemann, 2002).

2.5.4.2 Water constraint on plant productivity[Box2]

The calculation of photosynthetic productivity follows the routine of JSBACH (Reick et al., 2021). Therein, the photosynthetic productivity is computed in a two-step approach, which separates the potential carbon gain from the potential water loss (stomatal conductance) during photosynthesis. In the first step, the potential productivity is computed without any soil-water constraint (the so-called "unstressed" productivity). Next, the potential water loss is computed based on the potential productivity. In the second step, the "unstressed" productivity is scaled by the water-stress factor to account for the water limitation (resulting in the "stressed" productivity). Last, the actual water loss is computed based on the stressed productivity. The water-stress factor is represented by the factor α. In JSBACH, relative soil wetness is used to constrain productivity. All different PFTs experience the same water-stress simultaneously because all PFTs share the same root depth in JSBACH. When there is no water stress, the stressed productivity is equal to unstressed productivity ($\alpha = 1$.

The water-stress factor is computed differently in JeDi-BACH than in JSBACH. To account for varying degrees of water stress arising from individual rooting strategies in reaction to the prevailing atmospheric and soil conditions, I link the water-stress factor α with (i) the ability of a plant to access soil water, (ii) the relative soil wetness in the root zone, and (iii) the near-surface atmospheric condition for evaporation (see eq. (33) below).

A parameter for the root-shoot ratio (γ) is used to quantify a plant's accessibility to soil water. γ is defined as the ratio between the surface area of fine-roots and of leaves. Harris (1992) found out that the water-transport ability in a soil-plant system is related to the biomass ratio between roots and leaves. To further explain, a tree with proportionately more leaf growth than root growth

favors carbon investments to enhance access to light for photosynthesis. On the opposite, a strategy with proportionately more root than leaf growth favors moisture absorption to enhance productivity by reducing water stress. A recent study analyzing the root traits of vegetation on the global scale reports that regions with higher water scarcity feature vegetation with a higher root-shoot ratio (Qi et al., 2019). In JeDi-BACH, the ability of a plant to transport soil water is related to it's root-shoot ratio as

$$x(\gamma) = 1 - \exp\left(\frac{-4.6 * \gamma}{\gamma_{opt}}\right), \tag{32}$$

where $x(\gamma)$ is the normalized ability of a PGS to transport soil water, with a value ranging from 0 to 1. γ_{opt} is the optimal root-shoot ratio. The water stress factor is

$$\alpha = \min\left[1, \frac{E_{pot}}{k_\varepsilon}\left(1 - \exp\left(-\frac{k_\varepsilon \cdot W \cdot x(\gamma)}{E_{pot}}\right)\right)\right] \tag{33}$$

Here W is the relative soil wetness in the root zone calculated by eq. (31), ranging from dry soil condition (at a value of ~ 0) to wet soil condition (at a value of ~ 1). k_ε denotes the maximal total transpiration rate of leaves. The potential atmospheric demand for transpiration is E_{pot} (see calculation in Reick et al. (2021)).

In a situation when the near surface relative humidity is not saturated, plants can transpire freely. A PGS with proportionately more root to shoot growth ($x(\gamma) \sim 1$) can access soil water in the root zone so that $\alpha \approx W$. Likewise, a PGS with less root to shoot growth ($x(\gamma) \sim 0$) cannot access soil water well so that $\alpha \approx 0$. However, if the surface air is nearly saturated with water vapor ($E_{pot} \sim 0$), the vapor pressure gradient from the leaf surface to the atmosphere is low (such as in the case of dew formation). Then, plants cannot transpire water, and this limits productivity independently of the root shoot ratio of a PSG.

Box2: General remarks on section 2.5.4: Rooting strategy and water constraint

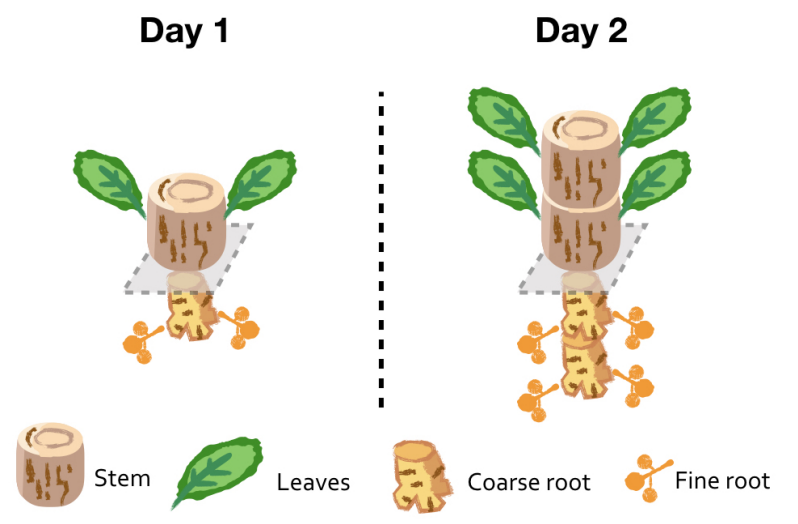

Figure 4: Development of an example growth strategy. Each icon represents a unit of respective tissue growth.

A new formulation that associates the fine roots carbon pool to the accessibility of soil water is introduced in JeDi-BACH due to shortcomings in the original JeDi. In JeDi, all strategies' allocation fraction to each biomass pool is fixed for their entire life, i.e. the relative amount of growth between different biomass pools remains fixed. To better explain this static allocation concept, a sketch describing the growth of an example strategy is presented in Fig. 4. On day 1, the strategy grows two (units of) leaves, one stem, one coarse root, and two fine roots. On day 2, the strategy has four (units of) leaves, two stem, two coarse roots, and four fine roots. Due to static allocation fraction, the biomass ratio between leaves and fine roots does not change over time and so the ability for fine roots supporting photosynthesis per unit leaf remains the same. In other words, the plant's soil water accessibility is independent of the fine-roots pool size. However, JeDi-DGVM violates this static allocation concept in the formulation of quantifying a strategy's water accessibility. There, the estimate of the potential supply rate for transpiration is linearly related to the amount of fine roots pool, meaning that water stress may disappear once the fine roots pool is large. This treatment gives some strategies an advantage by eliminating their water stress. In JeDi-BACH, a plant strategy's ability to access soil water is associated to its root-shoot ratio (RSR). A strategy with a large RSR (more fine roots per leaves) accesses soil water better. As the root-shoot ratio is fixed for each species, the ability to access soil water remains unchanged throughout their life.

2.5.5 Leaf properties: Photosynthesis, Nitrogen, and Lifespan

The essential function of leaves is to photosynthesize and synthesize carbon (food) for plants. The ability of plants to photosynthesize depends not only on their leaf traits but also on the ambient atmospheric conditions. To simulate different phenological dynamics, several key trade-offs are identified and incorporated in JeDi-BACH. To explain how leaf functions are modeled in JeDi-BACH, three topics are presented in this section: (i) the photosynthesis-nitrogen relationship, (ii) photosynthesis models, (iii) what are the leaf traits used in JeDi-BACH?

2.5.5.1 The photosynthesis-nitrogen relationship

Plants develop a competitive advantage (strategy) to cope with limitations in different regions, and nitrogen is one of the mineral nutrients most limiting to plant growth (Vitousek and Howarth, 1991). Through a cross-continent analysis on various plant traits, Wright et al. (2004) found that some of the leaf traits fall along a spectrum of correlations. The authors described these correlations as the leaf economics spectrum. For instance, leaf longevity is correlated to leaf thickness across different climate regions Wright et al. (2004). Leaves with shorter lifespans tend to be thinner and, thus, are cheaper in terms of construction costs. Thick leaves are constructional expensive, so they are often long-lived and more robust to unfavorable environmental conditions (Reich, Walters, and Ellsworth, 1997). In addition, because the enzyme that synthesizes carbon in leaves (called Rubisco) is rather rich in nitrogen, there is an observed strong relationship between nitrogen content and the photosynthetic capacity of a leaf (Field and Mooney, 1986; Reich et al., 2008). Leaves with higher nitrogen content per leaf area tend to have higher photosynthetic capacities, leading to higher maintenance costs. These observed correlations are used to construct leaf traits and trade-offs in JeDi.

2.5.5.2 Photosynthetic model

JeDi-BACH employs the photosynthetic model of Farquhar, Caemmerer, and Berry (1980) for the C3 photosynthetic pathway and of Collatz, Ribas-Carbo, and Berry (1992) for the C4 photosynthetic pathway. These models were already implemented in JSBACH (Knorr, 1997; Reick et al., 2021). In general, both the Farquhar model and the Collatz model calculate the photosynthetic product of C3 and C4 leaves, respectively, using the intercepted sunlight, CO_2 availability, the temperature-dependent kinetics of the enzyme, and some species depen-

dent parameters.

In the Farquhar model, the carboxylation capacity parameter V_{max}^{25} at the reference temperature 25°C is a key parameter in determining the plant photosynthesis rate per unit area of leaf. Originally, JSBACH assigns a specific V_{max}^{25} for each plant functional type based on Knorr (1997). However, the carboxylation capacity parameter is known to be linearly related to leaf nitrogen content (Kattge et al., 2007). To construct a spectrum of leaf functions following the photosynthesis-nitrogen relationship, the next section explains how the related plant traits were constructed for JeDi-BACH.

2.5.5.3 Leaf traits and parameters

Three leaf traits are used in JeDi-BACH: leaf longevity, specific leaf area, and leaf nitrogen content. Leaf longevity τ_{leaves_0} is sampled among the range of one to a hundred months (see eq. (19)). Based on the correlation of leaf longevity with specific leaf area (SLA), defined as the ratio of leaf area to leaf dry mass (or leaf thickness) reported in Wright et al. (2004) and in Reich, Walters, and Ellsworth (1997), the relation between SLA and $\tau_{leaves,0}$ is described as:

$$SLA = 0.323 \left(\frac{365}{\tau_{leaves_0}} \right)^{0.46} \tag{34}$$

The leaf nitrogen content per unit area [N] follows an empirical relationship proposed in Ollinger et al. (2008):

$$[N] = 0.0457 + 0.211 * t_{15} \tag{35}$$

As mentioned previously, photosynthetic capacity correlates strongly with leaf nitrogen. In JeDi-BACH, the carboxylation capacity parameter V_{max}^{25}, which is used in the Farghuar model, is linearly associated with [N]. This relation is chosen based on the eq. (1) from Kattge et al. (2009):

$$V_{max}^{25} = i_v + s_v * [N] \tag{36}$$

The values for slope (s_v) and intersection (i_v) are randomly sampled within the the values published in table 2 from Kattge et al. (2009). The photosynthetic parameters for C_4 vegetation are inherited from the original JSBACH.

2.5.6 Leaf phenology

The carbon dynamics of leaves C_{leaves} (see eq. (3)) affects several plant functions that are key to plant survival. The growth of leaves can result in more

interception of light for photosynthesis, and, in turn, plants obtain more carbon. On the other hand, losing leaves can reduce the high maintenance costs of leaf tissue. Thus, it might be beneficial for a plant to shed it's leaves when the photosynthetic rate decreases. Such changes (either seasonal, inter-annual, or intra-annual) of leaves are described in the model by the Leaf Area Index (LAI). The LAI is defined as the projected one-sided green leaf area per unit ground area. LAI is calculated as the product of leaf biomass and SLA,

$$LAI = SLA \cdot C_{leaves} \tag{37}$$

LAI is used to scale up the total amount of GPP from over m^2leaf to the total leaf area of a plant. LAI is associated with the total intercepted light in the canopy (see Section 5.2 in Reick et al. (2021)). Besides productivity, LAI is also used to determine the physical properties such as albedo and transpiration rate over a vegetated surface.

In JeDi-BACH, a light limitation parameter $fapar$ is newly introduced in the model code to prevent unrealistic growth of leaves. The previous JeDi-models simulate an unrealistic leaf area index up to 30-50 ($m^2leaf/m^2ground$). The new $fapar$ parameter ($fapar = 0.9$) serves to prevent overinvestment in plant growth. $fapar$ operates like a brake that slows down plant growth to avoid overinvestment when light interception by a strategy gets too high. For instance, a growth strategy will reduce investing in growing new tissues when the total light interception at the canopies approaches 90%.

2.5.7 Autotrophic respiration

Many carbonhydrates stored by plants are later on used for plant respiration: to supply energy for growth and repair existing tissues. Both of these applications are aggregated under the term 'autotrophic respiration. However, in JeDi-BACH, each purpuse is computed separately (Thornley, 1970; Thornley and Cannell, 2000). A fixed fraction of the carbon added to a biomass pool, to grow further tissue in this pool, is attributed to growth respiration R_g (measured in carbon units). R_g is calculated as the total construction cost from all tissue pools.

$$R_g = C_{storage} \sum \left(A_{organ} k_{R_g,organ} \right) \tag{38}$$

$k_{R_g,organ}$ is a constant that determines the fraction for R_g. The maintenance respiration R_m is computed based on the nitrogen concentration, the tissue's biomass, and as a function of temperature (Ryan, 1991):

$$R_m = k_m Q_{10}^{\frac{T-20}{10}} \left[[N_{mass}] \cdot (C_{leaves} + C_{fnroot}) + k_{sapwood} (C_{stem} + C_{csroot}) \right] \tag{39}$$

where κ_m is the maintenance respiration coefficient. Q_{10} is the temperature sensitivity of autotrophic respiration. $[N_{mass}]$ is the nitrogen content per unit biomass converted from [N] by SLA. In JeDi, the fine root pool and the leaves pool are treated as fine tissues, and the stem pool and the coarse root pool are treated as woody tissues. Fine tissues contain higher nitrogen content (proteins) leading to higher maintenance cost than woody tissues. Several studies (Thornley and Cannell, 2000; Thornley, 1970) have evidenced the association of leaf R_m with leaf nitrogen content so that R_m can be estimated quantitatively. However, whether (or to what extent) nitrogen in fine tissue can be used for calculating fine-root R_m and the mechanism for accounting fine root R_m is still unclear. JeDi-BACH inherited the respective implementation from JeDi-DGVM. R_m of fine roots pool is assumed to have the same magnitude as R_m of leaves. Hence, the nitrogen content of fine roots and leaves is assumed to be equal. The ratio of sapwood to woody carbon and the nitrogen content for woody tissue is also assumed to be equal and are specified by the constant $k_{sapwood}$.

2.5.8 Coupling to the atmosphere

The exchange of the energy and mass fluxes influences the microclimate near the land surface. JeDi-BACH interactively provides land-surface information to the lowest atmosphere. For coupling purpose, two of the land-surface characteristics are associated with two above-ground traits of JeDi-BACH. These are the canopy albedo and the roughness length over a vegetated surface.

Canopy albedo

The albedo of vegetated surface α_{veg} is computed as a function of the nitrogen content of the canopy following the empirical relationship found by Hollinger et al. (2010). According to their findings (see fig. 4 in Hollinger et al. (2010)), the canopy nitrogen concentration ranges from 3%N to 0.89%N (% means 1 gram of N to 100 grams of dry leaf matter^{-1}) and the minimal and maximal albedo values are given as 0.08 and 0.221, respectively. I include this information in the following way.

$$\alpha_{veg} = \begin{cases} 0.08, [N_{mass}] < 0.89\% \\ 3.216\,[N_{mass}] + 0.02, 0.89\% \leqslant [N_{mass}] \leqslant 3\% \\ 0.221, [N_{mass}] > 3\% \end{cases} \tag{40}$$

Roughness length

The small-scale land-surface topography influences the exchange of momentum and fluxes between the land surface and the atmosphere. This interaction is parameterized through the roughness length, a measure of flat the surface is. In JeDi-BACH, the roughness length over a vegetated surface is combined from the roughness of the grass-covered and tree-covered surface fractions. The parameter values are adapted from JSBACH(Reick et al., 2021).

$$l_{rough} = \begin{cases} 0.05, & Gass \\ 1 - 1.4, & tree \end{cases} \tag{41}$$

2.5.8.1 Scaling from individual plant strategy to ecosystem-scale

Climate models discretize the earth's surface into coarse fragmented pieces (grid boxes). Depending on the model's resolution, the size of the individual boxes ranges from a few to a few hundred square kilometers. At a resolution of a few hundred kilometers, a land surface box accommodates a mixture of various land surfaces and vegetation types. One needs some technique to estimate the energy fluxes from different land surfaces (the sub-grid scale heterogeneity) to the atmosphere, JeDi-BACH inherits the mosaic 'tiling' approach from JSBACH (Reick et al., 2021). A model grid box over land is sub-divided into various cover tiles such as glacier, lake, vegetated (represented by PFTs), and desert. Each tile has a corresponding cover fraction with respect to the grid box area. All relevant processes are calculated in each tile, and aggregated for each grid-box as the sum of all individual tiles multiplied by their respective cover fraction.

How to address the individual species' contribution relative to others in the same grid box? JeDi-BACH computes the community fluxes assuming biomass-ratio theory (Grime, 1998) (see section 2.4). The contribution of each species to the ecosystem functions is scaled by its total biomass relative to the community's total biomass. In other words, JeDi-BACH computes each growth strategy's "cover fraction" r_i as their biomass divided by the total community's biomass:

$$r_i = \frac{\overline{M_i}}{\sum_{i=1}^{N} \overline{M_i}} \tag{42}$$

$$\overline{M_i}^{n+1} = M^n \left(1 - e^{-\frac{\Delta t}{\tau_M}}\right) + \overline{M_i}^{n} \cdot e^{-\frac{\Delta t}{\tau_M}}; \quad \tau_M = 10 \ \ year \tag{43}$$

where i denotes the number of the PGS, N is the total number of non-dead PGSs in a grid cell, M_i is the total biomass carbon from the leaves, stem, coarse root and fine root pool of PGS_i. $\overline{M_i}$ is a pseudo-variable that is introduced to account for time-averaging the "cover fraction" change of PGS_i. The characteristic memory τ_M is set to 10 years. The timescale of composition change in an ecosystem is still an open topic among vegetation modeling communities. The contribution of species at different levels (e.g., direct physiological responses at tissue level or changes in the growth pattern of a whole plant or ecological feedback at the ecosystem level) very much depends on the interest of individual models. JeDi-BACH chooses a decade-long memory for smoothing out unrealistic rapid changes, particularly between grass/tree types. The aggregated community fluxes are calculated as

$$\langle f \rangle = \sum_{i=1}^{N} f_i \cdot r_i \tag{44}$$

where $\langle f \rangle$ represents the aggregated value of a certain flux, summing through all individual flux f_i times their corresponding 'cover fraction'.

Table 3: Variables and parameters used in JeDi-BACH. Column 1 presents the symbol used in equations. Column 2 gives a brief description of the symbol and column 3 gives the possible range of the value or the units.

Symbol	Description	Units/Value
	Living biomass carbon pools	
$C_{storage}$	Storage carbon pool	$mol(C)/m^2$
C_{seed}	Seed carbon pool	$mol(C)/m^2$
C_{leaves}	Leaves carbon pool	$mol(C)/m^2$
C_{stem}	Stem carbon pool	$mol(C)/m^2$
C_{csroot}	Coarse roots carbon pool	$mol(C)/m^2$
C_{fnroot}	Fine roots carbon pool	$mol(C)/m^2$
	Allocation and germination	
$A_{storage}$	Allocation fraction for storage	$[0-1]$
A_{seed}	Allocation fraction for seed bank	$[0-1]$
A_{leaves}	Allocation fraction for leaves	$[0-1]$
A_{csroot}	Allocation fraction for coarse roots	$[0-1]$
A_{fnroot}	Allocation fraction to fine roots	$[0-1]$
γ_{GERM}	Allocation fraction to fine roots	$[0-1]$
	Carbon dynamics fluxes	
GPP	Gross primary productivity	$mol(C)/m^2/s$
NPP	Net primary productivity	$mol(C)/m^2/s$
R_m	Maintenance respiration	$mol(C)/m^2/s$
R_g	Growth respiration	$mol(C)/m^2/s$
GERM	Germination flux	$mol(C)/m^2/s$
Q_{10}	Temperature coefficient for autotropic respiration	1.6
$\kappa_{sapwood}$	Fraction of sapwood carbon to woody carbon	0.05
	Growing conditions and state variables	
$\overline{T_{grow}}$	Pseudo surface temperature	$\circ C$

Continued

Symbol	Description	Units/Value
$\overline{W_{grow}}$	Pseudo relative soil moisture	$[0-1]$
$\overline{W_{5cm}}$	Pseudo relative soil moisture at top 5cm	$[0-1]$
$\overline{\Delta T_{30d}}$	Pseudo daily temperature variation over one month	$\circ C$
F_{grow}	Condition for growth	$[0,1]$
F_T	Condition for growth depending on temperature	$[0,1]$
F_{germ}	Condition for germination	$[0,1]$
F_{seed}	Condition for reproduction	$[0,1]$
T_{start}	Critical temperature to start growing seson	$\circ C$
T_{end}	Critical temperature to terminate growing season	$\circ C$
τ_T	Memory characteristics of surface temperature	$[days-weeks]$
τ_W	Memory characteristics of surface temperature	$[days-weeks]$
	Tissue turnover and senescence	
$\overline{NPP}$	Pseudo net primary productivity	$mol(C)/m^2/s$
τ_{NPP}	Memory characteristics of net primary productivity	$[days-weeks]$
κ_{sen}	Memory characteristics of net primary productivity	$[days-weeks]$
F_{stress}	Condition for senescence	$[0,1]$
τ_{leaves}	Turnover time for leaves	$[days-weeks]$
τ_{fnroot}	Turnover time for fine roots	$[days-weeks]$
τ_{stem}	Turnover time for stem	$[weeks-months]$
τ_{csroot}	Turnover time for coarse root	$[weeks-months]$
	Aboveground traits and state variables	
SLA	Specific leaf area	$m^2(leaf)/mol(C)$
LAI	Leaf area index	m^2/m^2
$[N]$	Nitrogen content measured on area based	$mol(N)/m^2(leaf)$
$[N_{mass}]$	Nitrogen content measured by biomass	$mol(N)/mol(C)$

Continued

Symbol	Description	Units/Value
α_{veg}	Canopy albedo	—
	Belowground traits and state variables	
l_r	Root depth	m
l_0	Minimal root depth	$0.05m$
κ_{rd}	Coefficient for root carbon to root depth	$m/mol(C)$
W	Relative soil wetness within root zone	$[0-1]$
W_{root}	Total soil water with root zone	m
W_{max}	Maximum plant available soil water within root zone	m
γ	Root-shoot ratio	$mol(C)/mol(C)$
γ_{opt}	Optimal root-shoot ratio	$mol(C)/mol(C)$
$x(\gamma)$	Water transport ability	$[0-1]$
α	Water stress factor	$[0-1]$
E_{pot}	Potential evaporation rate in atmosphere	$kgH_2O/m^2/s$
κ_ϵ	Maximal specific stomatal conductance	$2.69 \times 10^{-5} kgH_2O/m^2(leaf)/s$ (Larcher, 1996)
	Coupling to the atmosphere	
l_{rough}	Roughness length	m
$\overline{M_i}$	Pseudo total biomass carbon	$mol(C)/m^2$
τ_M	Memory characteristics of composition change	10 year

3

ASSESSMENT OF JEDI-BACH AND THE EFFECT OF BIODIVERSITY IN SHAPING A ROBUST CLIMATE

3.1 Background

Over the past few decades, Dynamic Global Vegetation Models (DGVMs) have extensively progressed in many geoscientific areas. With a growing number of sophisticated processes, the ultimate goal is to resemble a reasonable analogy to the Earth's terrestrial ecosystems. The so-called plant functional types (PFTs) approach is a classic method for representing global vegetation. The immense diverse forms of plants are crudely parameterized into only a handful of discrete sets of PFTs. Though parametrization captures the mean geographic terrestrial features such as plant physiology and biogeochemistry, the PFT approach is criticized for overgeneralizing the complex role of ecosystem functions and neglecting the role of inter- and intra-specific plant trait variability (Wullschleger et al., 2014; Kattge et al., 2020; Pappas, Fatichi, and Burlando, 2014).

A drawback from such an issue is that Earth System Models (ESMs), which often include DGVMs for their terrestrial processes, may not be adequate for understanding the impact of plant functional diversity on climate, in particular for situations in non-analog climates. For instance, Amazon forests were predicted to substantially dieback towards the end of the century in a future warming scenario (Betts et al., 2004; Cox et al., 2004). This prediction was made based on an early generation DGVM, where vegetation types and ecosystem processes were largely under-represented. To some degree, missing pieces in ecosystem processes resulted in drastic predictions in the Amazon. A follow-up study reported reduced dieback of the Amazon as more sophisticated dynamic vegetation processes are included in the model (Huntingford et al., 2008), em-

phasizing the needs to resolve emergent processes that are critical to vegetation dynamics. Both complex modeling and conceptual studies have reported that plant diversity tends to dampen out the instability of the interaction between climate and vegetation with the introduction of more sophisticated ecosystem processes (e.g., increased in PFTs in models) (Claussen et al., 2013; Huntingford et al., 2008). Therefore, if one aims at predicting or understanding how ecosystems and climates change in novel/future climate scenarios, it is necessary to seek a different modeling approach, that better relates plant diversity and key ecological processes in DGVMs. In this spirit, plant functional trait and trade-off-based approaches have emerged.

In line with the direction of research in the previous chapter, an alternative modeling approach called JeDi is introduced when setting up the new plant diversity model JeDi-BACH. The advantage of the JeDi-approach can be best summarized by:

> *"In such a (JeDi) model, the diversity of prevailing plant trait combinations is an emergent property of the DGVM, rather than a prescribed input."*
>
> —- S. Zaehle (Chapter 22.3, Schulze et al. (2019))

Instead of prescribing plant types with fixed physiological parameters, JeDi simulates a group of hypothetical plant species, that are generated with random combinations of plant traits. Each hypothetical species is essentially a unique plant growth strategy. JeDi predicts the diverse outcome of strategies based on plant functional trade-offs through environmental (trait) filtering. In this way, the composition of the surviving species is more "tailored" to regional environments. On top of that, JeDi-BACH is the first JeDi-series model that includes an interactive atmosphere. A coupled land-atmosphere setup with JeDi-BACH is of particular interest for non-analog climate applications. Hereafter, the term "coupled" is used to indicate "coupled land-atmosphere setup."

The predecessor model JeDi-DGVM (Pavlick et al., 2013) demonstrated relatively good performance in several biogeographic aspects against observations compared to PFT-based land surface models. To some degree, it is an expected outcome as one makes a present-day prediction of the terrestrial vegetation distribution under prescribed climate. One investigates the passive response of vegetation to the environment and assumes that climate works as the only decisive factor determining the vegetation's biogeographic distribution. Though JeDi-DGVM predicts a good first principle global biogeography, the same issues appear like for any other non-coupled (offline) DGVMs: missing atmospheric components can lead to the under/over-estimation of changes in vegetation/-climate. Edward Lorenz's "butterfly effect" theory articulates — tiny changes in initial condition in a non-linear system can lead to large differences in the later state. The response in a terrestrial ecosystem due to climate change may

further contribute to greater uncertainties in novel climates. The dynamics between vegetation and climate are more complex and non-linear than in a solely offline setup. For instance, offline models overestimate the frequency and severity of drought due to the missing role of plants in mediating water availability – the soil-plant-atmosphere coupling (Berg and Sheffield, 2018). The water budget between precipitation, surface evaporation, transpiration, drainage, run-off, and the control of plant roots on soil water over land all play an important role in droughts. Missing land-atmosphere feedback may give a false perception of how droughts may develop under a changing climate (Greve, Roderick, and Seneviratne, 2016). Indeed, regional-scale climate change is found to be highly sensitive to the described surface characteristics in coupled climate modeling studies (Claussen, Brovkin, and Ganopolski, 2001; Bonan, 2008; Seneviratne et al., 2013; Groner et al., 2018; Swann, 2018).

3.2 Aims of the chapter

The impact of variation in ecosystem function, such as changes in dominant traits on the coupled vegetation-climate system, is still largely unexplored. Little is known about the relative magnitude or the impact of functional diversity on climate (Verheijen et al., 2013). This chapter is partitioned into two studies to investigate the role of plant functional diversity using JeDi-BACH coupled with an interactive atmosphere.

Here, I first define what diversity means in JeDi-BACH. In the JeDi modeling approach, there are two types of plant diversity, the "potential diversity" and the "actual diversity". Potential diversity refers to the initial set of randomly sampled growth strategies used in a model experiment. Actual diversity refers to the final state of the ecosystem. A high potential diversity means that a system (or a world) composes of many random sampled plant growth strategies. A high actual diversity implies that many growth strategies managed to survive in a model experiment. The probability of the survival of a growth strategy depends primarily on environmental filtering. The connection between these two types of diversity is intuitive: a high potential diversity world, in theory, provides more (in total number) survivors worldwide than a low potential diversity world as more dissimilar growth strategies are allowed to survive somewhere on Earth.

For this thesis, understanding to what extent one can investigate the importance of plant functional diversity using JeDi-BACH is a primary task. The model uncertainty of JeDi-BACH with an interactive atmosphere is yet unknown. Ecosystem functions are ecological processes that control the fluxes

of energy, nutrients and organic matter through an environment. Inherently, a high actual diversity system provides various ecosystem functions. However, what does a high potential diversity system or a high actual diversity system represent in a coupled setup? It is essential to explore how model results depend on the number of sampled strategies. To tackle these questions, I conducted a series of sensitivity simulations spanning from low potential diversity to high potential diversity in the first part of this chapter. I focus on how climate or ecosystem functioning change with increased diversity. I ask the question:

- **2a What is the role of plant functional diversity in shaping the global climate-vegetation system ?**

The biodiversity and ecosystem functioning (BEF) relationship shows that an increase in functional diversity is positively (not necessarily linearly) associated with ecosystem functions until an asymptotic level (Cardinale et al., 2012). I suspect that global climate may stabilize with increased diversity in model simulations.

Besides the sensitivity of the level of diversity, another aspect of JeDi-BACH has not yet been tested. One highlight of the JeDi-approach is to allow the environment to select survivors in different climate regions so that one can, to some extent, move away from the traditional static trait parametrization approach (the PFT-approach). It is necessary to evaluate whether the climate is sensitive to some parameters used in JeDi-BACH. For this purpose, in the second part of this chapter, I conduct a series of sensitivity experiments to see how model results depend on the values of the chosen parameters. Four parameters that control the dependence of plant respiration on temperature, the depth of root, the effect of light limitation on leaf growth, and the timing for entering/terminating a growing season are selected because their values are not adequately justified by observations and are identified to be critical for model simulation. The goal of these tests is not to determine what parameter value is better than the others, but to give an overview of the potential climate variation that may result from the subjective choice of parameters. I then ask the question:

- **2b To what extent is the global climate dependent on the treatments in some plant trait representations that are yet justified ?**

In addition, these sensitivity tests provide insights about the potential for tuning in future model development. Climate model tuning is an essential aspect of numerical modeling in order to reproduce the solution as a whole, in line with aspects of the observed climate (Hourdin et al., 2017). However, some technical challenges are rather invincible when performing JeDi-BACH coupled with atmospheric model ICON-A. Ideally, JeDi-BACH would simulate thousands of plant species to obtain sufficient coverage of potential trait diversity. But, an

increased number of sampled species in the model quickly makes a coupled simulation burdensome. A few adjustments to the model configuration were needed to reduce the workload and optimize the total simulation time intended for this chapter. The following section (Section 3.3) discusses the most dominant technical difficulties while using JeDi-BACH in ICON-ESM. Sections 3.4 and **??** give an overview of the configurations, some technical aspects of JeDi-BACH, and discusses the procedure for conducting a spin-up simulation.

3.3 Computational constraints

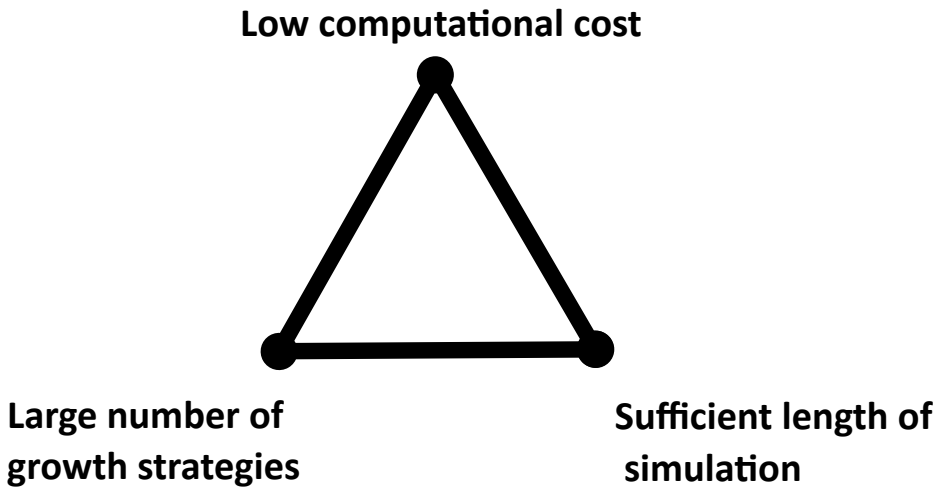

Figure 5: One can achieve only two of the three desirable targets.

Ideally, three targets have to be achieved when using JeDi-BACH in a coupled setup: (i) to simulate a sufficient amount of plant growth strategies (PGSs), (ii) to perform a sufficiently long simulation for carbon to reach an equilibrium state, (iii) to minimize the cost for computational resources for each simulation. However, three challenges come along with this.

The first challenge is to simulate a "sufficient amount" of strategies from a multi-dimensional trait space. The word "sufficient" has two meanings here: a sufficiently large number of strategies and a sufficient sampling in the trait space. These two requirements are crucial for the JeDi modeling approach. A "sufficient amount" of growth strategies that are "sufficiently diverse" is needed to obtain a spectrum of adaptive species via global environmental filtering. Since every point in the trait space represents a PGS with definite functional capability, the more species are sampled, the more species with marginal functional properties can grow.

Nevertheless, it is unfeasible to simulate the PGS of every point in the multi-dimensional trait space. One needs a technique to explore as much of the trait space as possible. The Latin-hypercube sampling method is applied to sample each multi-dimensional trait space to conquer this issue (see Chapter 2.3).

The second challenge concerns the constraints posed by having only limited computational resources. As mentioned in the first challenge, sufficiently

many species are necessary to obtain robust results. While the most up-to-date ICON-ESM simulates mainly only a few to a dozen PFTs in each model grid box, JeDi-BACH must simulate hundreds of growth strategies at every model grid point. An increase by several orders of magnitude in the number of simulated species makes the computational-intensive ICON-ESM furthermore burdensome. Moreover, another obstacle is the time needed for global forest ecosystems to develop. Carbon cycle processes require a long spin-up time for the biomass carbon pools to achieve an equilibrium. It often requires weeks to a few months to perform a complete spin-up simulation and costs thousands of CPU hours. This challenge hinders model testing during the development process in general and limits the total number of simulations that can be conducted (in a feasible time frame) for this chapter.

The final challenge is an issue combining the first two challenges: deciding on a robust number of simulated species for a coupled setup simulation while keeping a reasonable speed for model simulation. Such a decision involves a trilemma composed of three desirable targets: "low computational cost," "a large number of growth strategies," and "a large number of simulated years." An increased number of species with a sufficient simulation length inevitably leads to substantial computational costs. Fulfilling any of the two targets leads to an unwilling concession of the third target. Therefore, a well-planned simulation strategy is needed to achieve sufficiently robust results compromising of these targets. The next section discusses the simulation strategy and the model configuration.

3.4 Model configuration

The ICON-ESM (ICOsahedral Nonhydrostatic Earth System Model) is the latest ESM developed at the Max Planck Institute for Meteorology (MPIM). ICON-ESM consists of three model components: the ocean dynamics model ICON-O (Jungclaus et al., 2022), the atmosphere model ICON-A (Giorgetta et al., 2018), and the land surface model JSBACH4 (Reick et al., 2021). The new plant trait diversity model JeDi-BACH is built on top of JSBACH4, where the representation theory of JeDi (Kleidon and Mooney, 2000; Pavlick et al., 2013) replaces all PFT-related processes. JeDi-BACH inherits most of the land surface physical processes from JSBACH4 so that it is possible to operate with ICON-A for a land-atmosphere coupling simulation. JeDi-BACH can also be conducted in a stand-alone setup with prescribed meteorological fields. Out of many inherited features, the parallel infrastructure is a critical requirement for JeDi-BACH as handling I/O (input/output) in the model is the most consuming issue for CPU time. A crucial factor that needs to be considered here is that, as mentioned earlier, a trilemma occurs when conducting simulations with JeDi-BACH. A few adjustments to the model configuration were necessary to minimize the total simulation time needed for this chapter.

Only a coarse model resolution, denoted as the R2B3 ICON-ESM configuration, is feasible to obtain an operational experiment strategy. R2B3 is configured with an approximately isotropic horizontal grid mesh of around 320 km over the ocean and land surface and comprises 47 vertical atmospheric levels. It is important to note that the climate of ICON-A in the R2B3 resolution has never been tuned nor investigated by the development team at the MPIM. By default, R2B3 inherits the atmospheric parameter values from a higher resolution (R2B4). The R2B3 configuration leads to an unrealistic climate in some regions that differs substantially from the observed present-day climate. For instance, an underestimate in precipitation and a seasonality of precipitation shifted by several months in Eurasian areas is observed in the ICON-ESM simulation (Jungclaus et al., 2022). Substantial precipitation reduction in Eurasian regions leads to profound dying out of vegetation (Fig. 12 in Schneck et al. (2022, submitted)). Unavoidably, coupled simulations with JeDi-BACH inherit from R2B4 configuration a similar model performance (Appendix A.1). The atmospheric parameters used in a fully coupled experiment SWITCH (Jungclaus et al., 2022) are adapted in this study. Nevertheless, simulation results of JeDi-BACH in the R2B3 configuration still adequately capture general global precipitation and near-surface temperatures.

All coupled simulations conducted in this chapter follow an AMIP-type simulation set up according to the standard configurations used for CMIP6 (Eyring et al., 2016). The ocean dynamics model is switched off to isolate the effects from the land-atmosphere interaction by prescribing the observed sea surface temperatures (SSTs) and the sea ice concentration (SIC). Land-use change, soil, and litter decomposition are excluded in JeDi-BACH. All simulations conducted in this chapter focus only on the interaction between the atmosphere and the natural vegetation without natural (fire and windbreak) and anthropogenic (land use and land cover change) disturbances.

3.4.1 Spin-up procedure

To investigate the effect of plant trait diversity on the coupled vegetation-climate system before performing experimental simulations, a pre-condition is required: global climate must be stationary. This means that, in particular, the following three requirements need to be achieved:

1. The selection of species by environmental filtering has largely come to halt.
2. Terrestrial/global climate is in quasi-equilibrium.
3. Biomass carbon pools reach a quasi-equilibrium.

As mentioned in the previous section, computational constraints substantially limit the number and the total length of simulation conducted with JeDi-BACH. Two alternative procedures are developed to perform a complete spin-up. The first is to conduct the spin-up entirely in a coupled setup. The second one is to perform it in a hybrid format, starting from an offline setup and then continuing in a coupled setup. The second option is developed to reduce total computational time to boost the model development process.

For the coupled setup, SSTs and SICs, anthropogenic aerosol optical properties, ozone, greenhouse gases, and the solar irradiance forcing are prescribed as AMIP forcing[1] (Gates et al., 1999). Data from the years 1945 to 1974 is cyclically applied during the spin-up simulation for about 1000 years. Ideally, one wishes to perform the whole spin-up procedure in a coupled setup to account for vegetation-atmosphere interactions properly. But, it is not always feasible to perform several coupled spin-up simulations: for instance, a 1000-year coupled simulation with 400 species using 32 nodes (equal to 768 CPUs of the supercomputer MISTRAL of German Climate Computing Centre (Deutsche Klimarechenzentrum, DKRZ)) needs at least 50 days to complete. This quickly adds up to a

1 https://www.wcrp-climate.org/modelling-wgcm-mip-catalogue/modelling-wgcm-mips-2/240-modelling-wgcm-catalogue-amip

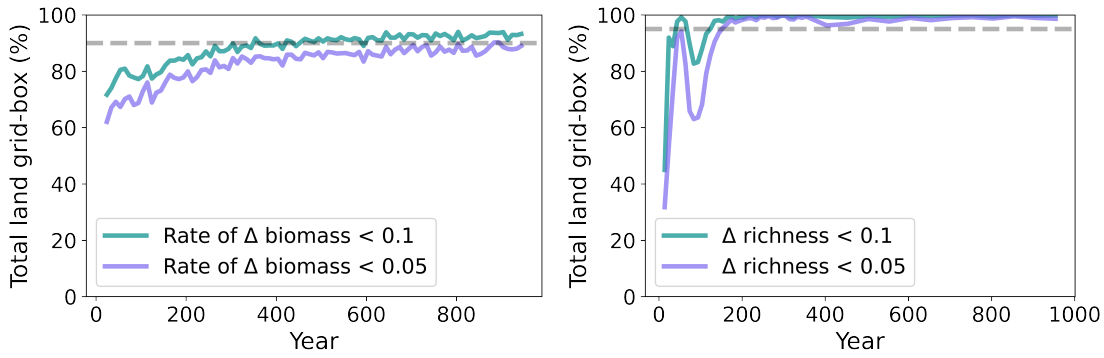

(a) (b)

Figure 6: Percentage of land where during spin-up the relative decadal change in total plant biomass and the relative change in total number of survival strategies are less than 0.1 and 0.05. Grey dash lines mark the 90 % threshold.

few months if the administrative time (i.e., queuing time until actual execution) is also considered. Fig. 6 demonstrates the situation by an example of a coupled spin-up with 400 growth strategies. The left panel shows the percentage of the land grid-boxes for which the rate of the relative total plant biomass change over a decade is lower than 5% and 10% per century. The relative total biomass change is calculated as the difference between consecutive decades divided by the biomass of the last decade, namely the relative biomass change compared to the previous decade.

Similarly, the right panel displays, for the same spin-up simulation, the development of the percentage of land where the relative change in richness (calculated as the total number of survival strategies) is less than 5% and 10%. The selection of strategies slows down substantially already after 200 years of simulation. The equilibrium of biomass carbon (after around 500 years of simulation) appears later than the selection of strategies because the woody biomass takes much longer to spin-up.

This lengthy process considerably challenges the feasible number of testing simulations during model development of JeDi-BACH. Therefore, an alternative hybrid spin-up procedure was developed to speed up the whole process. JeDi-BACH can be conducted in a stand-alone configuration where global climate is prescribed. Because the calculation for atmospheric circulation is left out, an offline setup performs much faster than a coupled one. The hybrid procedure is first to conduct an offline spin-up until both global biomass carbon and species selection reach a quasi-equilibrium (to fulfill the second and third

requirements for a successful spin-up). Next, the spin-up is continued in a coupled setup. Duration for spinning-up global climate is reduced since species and biomass pool selection are already in equilibrium when the coupled simulation starts. It is important to note that the prescribed climate forcing used for an offline spin-up is critical for the transition from an offline to a coupled setup because the variability of the atmospheric variables is much larger in a coupled setup. Climate forcing data is generated from the output data of an existing coupled simulation to avoid inconsistency between an offline and a coupled setup. Here, it is important to keep the climate variability generated from a coupled setup. The offline spin-up is driven by daily minimal and maximal near-surface temperature, surface wind speed, longwave and shortwave radiation, near-surface air specific humidity, and precipitation that are generated from a coupled simulation. Also, the data is de-trended before use as forcing to remove any potential underlying drift in climate. The de-trended climate data, which by construction has a similar climate variability as the coupled setup, is then prescribed for the JeDi-BACH offline setup. In brief, a 30-year climate forcing is obtained from a coupled AMIP-type simulation to perform a spin-up procedure in an offline setup for 600 years of simulation. After global biomass pools reach a quasi-equilibrium in the offline setup, the state of all carbon and state-dependant variables at last simulation time-step is taken as initial state for the coupled setup and run for another 200 years to assure no further drift in global climate. At this point, the whole spin-up procedure is finally complete. A hybrid spin-up procedure using 32 nodes takes about 25 days to complete.

Once a spin-up procedure from either of the options is completed, experimental simulations can proceed from the results of the last spin-up time-step.

3.5 Exploration of the role of plant functional diversity on ecosystem function and climate

3.5.1 Experiment setup

To assess the role of plant functional diversity, simulations at seven levels of potential diversity were conducted in a coupled setup, namely with 10, 20, 40, 100, 200, 400, and 600 sampled plant growth strategies (PGSs). Each individual level comprises three ensemble members that were initiated with a different set of growth strategies. Their trait parameters are generated by the Latin-hypercube sampling approach (see Chapter 2.3 for more details). All experiments were configured with the same AMIP-type forcing used in the coupled spin-up (see description in Section 3.4.1). A total of about 350 simulation years was conducted for all ensemble members beginning from a "desert world" (meaning that all terrestrial grid cells grow species from scratch during spin-up). Due to limited computational resources, the maximum number of potential diversity was set to 600.

3.5.2 Concept to analysis the model results

Here, I explain the concept for the analysis presented in the next section. Each ensemble member's last 60 years of simulation results are used for analysis. To smooth out climate variability, all results presented in this chapter are averaged over the last 60 years of simulation results. For ease of discussion, "diversity" is referred to as "potential diversity" in this section.

3.5.2.1 Ensemble mean and ensemble spread

I analyze the ensemble mean and ensemble spread for understanding how robust climate/ecosystem function may change with diversity. The ensemble mean is calculated at each grid cell as the average of the three ensemble members at each respective potential diversity. The ensemble mean characterizes the general geographic pattern at a given diversity level. The ensemble spread is calculated as the standard deviation over the three ensemble members at each grid cell. The ensemble spread is a measure of the robustness of model results and depends on the diversity level. A small spread implies that the ensemble members have, at the considered diversity level, similar model results. This indicates that model results converge among ensemble members.

3.5.2.2 Functional richness

"Functional richness" is a term commonly used in ecology to refer to the number of species within a community. It represents the survivor fraction in model results to avoid confusion with other terms associated with diversity. Functional richness is defined as the total number of PGSs that survive in a grid cell. Here, functional richness is equivalent to the term "actual diversity" as defined previously. The "relative richness" is the normalized richness calculated as the total number of surviving PGSs in a grid-cell divided by the total number of sampled strategies. In this way, the relative number of surviving species allows for comparison across different levels of potential diversity. Apart from treating every strategy equally, trees and grasses, the two most distinguishable growth strategies, are also estimated separately. The "relative tree richness" is defined as the total number of surviving tree-like PGSs over the total number of surviving PGSs.

3.5.2.3 Dominance of strategies

In JeDi-BACH, the contribution of individual PGSs to the variables at the community level (grid-cell level in the model) follows the "biomass-ratio theory" proposed by Grime (1998) (see Chapter 2.5.8.1 for details). Principally, it is assumed that the contribution of a PGS to an ecosystem-wide variable is proportional to its relative abundance. In JeDi-BACH, a PGS's relative abundance is calculated as its total biomass relative to the total biomass of all surviving PGSs within a grid cell. In a way, the relative abundance can be interpreted as how a PGS dominates the ecosystem function in an ecosystem: the greater the relative abundance a PGS has, the more it dominates at the community level. Similar to the relative abundance, the dominance of trees in a grid cell is estimated by the ratio of the total tree biomass to the total biomass of all surviving species.

3.5.2.4 Community-weighted mean traits

The functional traits determine how a plant strategy responds to the environment. The community-weighted mean (CWM) traits are used to measure the average trait of survivors at each grid cell. The relative abundance of each PGS is its total biomass relative to the total biomass of all PGSs in a grid cell. CWM trait parameters are the sum of all PGS' trait parameters weighted by the abundance of each PGS. In this way, the 'average' functional traits at each grid cell can be obtained.

3.5.3 Results

3.5.3.1 Terrestrial climate

In the conducted AMIP-simulations, the state of the ocean broadly defines the global mean surface temperature as two-thirds of the Earth's surface, i.e., the ocean surface temperatures are prescribed. Rather than the global means, I focus on the terrestrial averages. Antarctica and Greenland are excluded from the analysis.

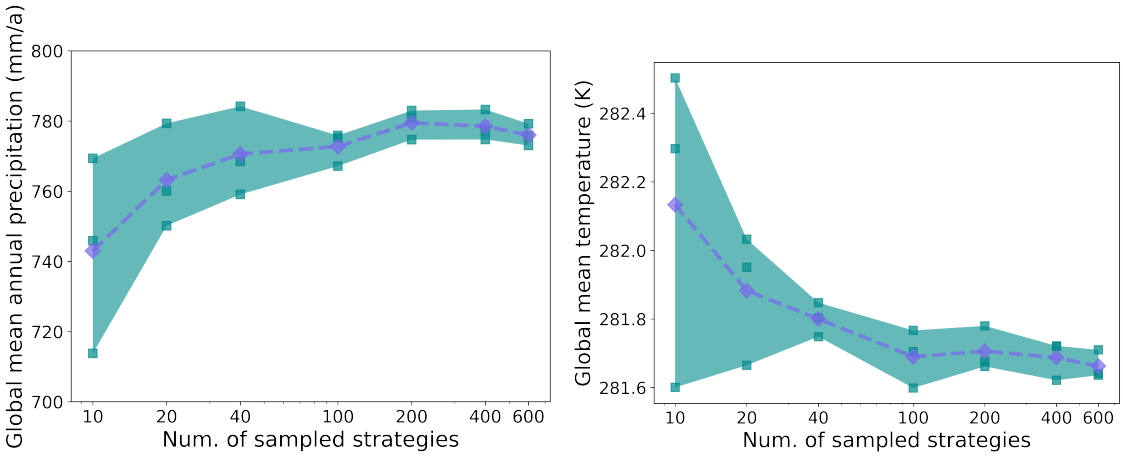

(a) (b)

Figure 7: (a) Terrestrial mean annual precipitation. (b) Terrestrial mean annual surface temperature. Purple diamond dash-line shows the ensemble mean and Cyan squares show each ensemble members.

The ensemble mean precipitation (Fig. 7(a)) increases with increasing diversity. The annual mean precipitation steadily increases from 740 mm/year in a low diversity world to roughly 780 mm/year in a high diversity world. The maximal values of annual terrestrial precipitation at the respective diversity levels, seemingly, reveal an upper bound at around 780 mm/year. The ensemble mean near-surface air temperature steadily decreases from 282.1 K to 281.7 K with increasing diversity (Fig. 7(b)). The minimal temperature across diversity levels appears to outline the minimum temperature boundary at around 281.7K. These results imply that terrestrial climate is becoming wetter and cooler with increasing diversity.

Apart from the ensemble means, the global mean climate converges substantially when more than 100 sampled strategies are simulated. The ensemble spread in precipitation (shown as shaded area) decreases with increasing di-

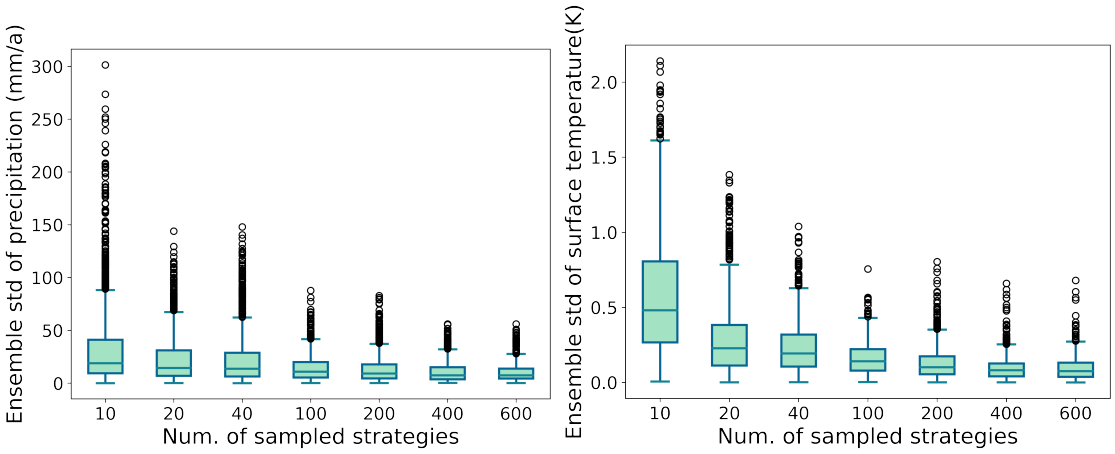

Figure 8: Box plots showing the geographic variation of (a) the ensemble standard deviation (std) of terrestrial precipitation (mm/a) and (b) the ensemble standard deviation of terrestrial surface temperature (K).

versity. The ensemble spread in the low diversity worlds (N=10) is roughly 60 mm/year and the spread decreases to about 10 mm/year in the high diversity worlds (N=600). Similarly, the ensemble spread in temperature decreases with increasing diversity. The spread is roughly 1K at the low diversity level (N=10) and decreases to 0.1K at the high diversity level (N=600). The large spreads in the climate variables suggest that the terrestrial mean climate differs considerably in a low diversity world when only 10 or 20 sampled strategies are sampled. The differences in the low diversity worlds can be as much as a 1K in annual mean temperature and 60 mm/year in annual mean precipitation. In contrast, the ensemble spread decreases with increasing diversity, implying that the terrestrial mean climate converges with increasing diversity.

Besides the global mean, the regional climate also shows convergence with increasing diversity. In Fig. 8, the box-whisker plots show the spatial distribution of the ensemble spread at different diversity levels. For both precipitation (Fig. 8 (a)) and temperature (Fig. 8 (b)), the ensemble spread, the inter-quantile ranges and the median values decrease with increasing diversity. The worldwide reduction in ensemble spread of regional climate implies that regional climate is becoming pretty similar among ensemble members towards a high diversity world. This implies that a similar degree of vegetation-climate interaction appears with increasing diversity. Additionally, global climate seems to be approaching a high water-cycling state. This state is explained in the next

section.

3.5.3.2 Root depth and evapotranspiration

One key factor that influences the terrestrial hydrology in the coupled simulation is the variation of root depth, which is a prognostic variable in JeDi-BACH. Fig. 9 shows the ensemble mean global root depth of (a) 10 sampled strategies and (b) 600 strategies. A worldwide deepening of root depth occurs with increased diversity (results of other diversity levels not shown). Root depth determines the total amount of soil water accessible for plants and is also associated with the amount of water that can be transported via the plants to the atmosphere (transpiration). Essentially, at a larger scale, root depth determines the "active" amount of soil water that can be cycled over land. Ideally, the deeper the roots grow, the higher the total soil water is available for plants to use. Evapotranspiration therefore increases with a deepening of roots.

The ensemble terrestrial annual mean evapotranspiration (ET) shows a consistent trend as speculated. As shown in Fig. 10, the ensemble mean ET increases from roughly 485 mm/year to 530 mm/year with increasing diversity. The ensemble spread is larger in the low diversity world The spread of ET among the three simulations with 10 sampled strategies is around 90 mm/year. The spread considerably converges to 530mm/year with above 200 sampled strategies. The increase in terrestrial precipitation observed in the previous section is associated with the deepening of root depth because more ET leads to more precipitation. Combined with the results of terrestrial precipitation, terrestrial hydrological fluxes enhance with increasing diversity. Terrestrial mean precipitation approaches roughly 780 mm/year and the maximal ET values at each diversity level seem to converge to an upper boundary of around 530 mm/year. The temperature decreases to about 281.7 K at high diversity levels. These results point out that global and regional climates not only converge with increasing diversity, but they are also converging towards a high water-cycling state with increasing diversity: a wet and cool climate.

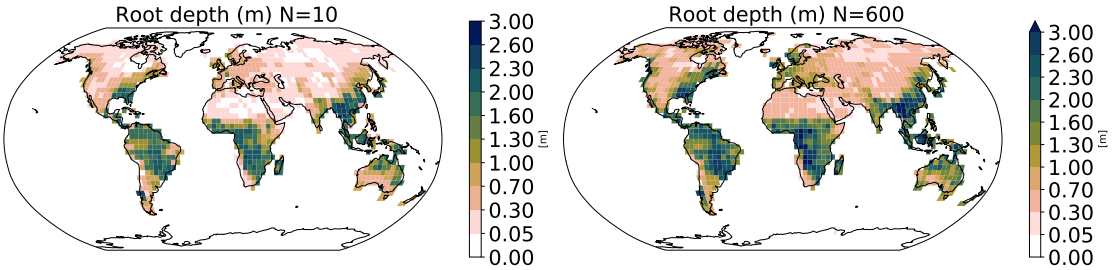

(a) (b)

Figure 9: Ensemble mean global distribution of root depth (a) with 10 sampled strategies and (b) with 600 sampled strategies.

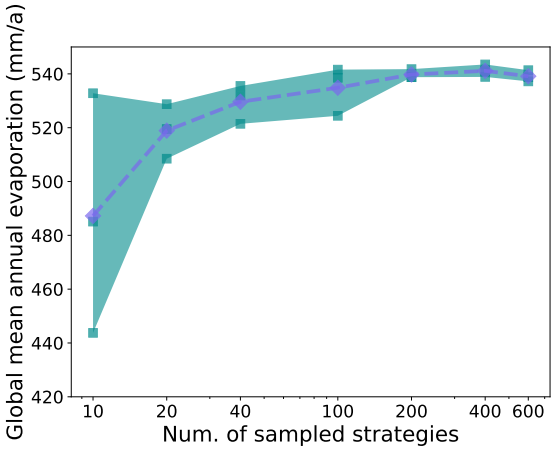

Figure 10: Ensemble mean annual mean evapotranspiration.

3.5.3.3 Relative richness and tree richness

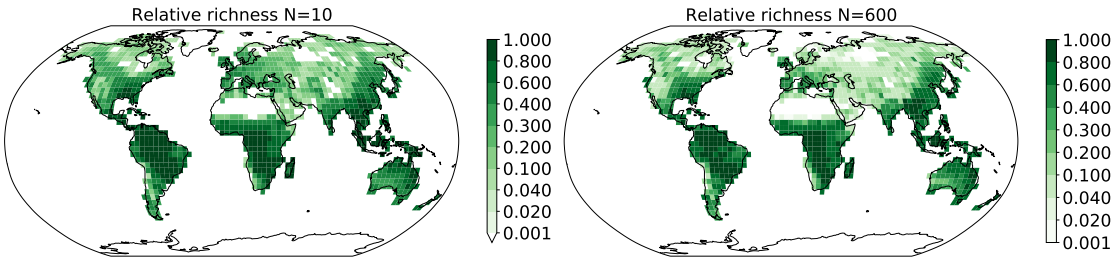

(a) (b)

Figure 11: Global richness(a) with 10 sampled strategies and (b) with 600 sampled strategies.

In line with the widely recognized biodiversity patterns in ecology, the global distribution of relative richness shows a gradual reduction with increasing latitude (Fig. 11). In Fig. 12 (a), the box plots show that the distribution of the ensemble mean's relative richness varies with particular diversity. There is a decrease in the median values from 10 to 40 sampled strategies. The relative richness is fairly stable above 40 sampled strategies and the median and the interquartile range are robust with increased diversity. Fig. 12 (b) shows the geographic variation of ensemble spread of the relative richness. A substantial decrease in ensemble spread occurs with increased diversity, meaning that the survivor rate converges worldwide (at almost every grid-cell) in high diversity ensembles. This implies that the geographic variation of the relative richness stabilizes with increased diversity and the geographic pattern of richness is becoming more robust with an increased number of sampled strategies.

However, the relative richness between trees and grasses differs. The survival fraction of grass strategies is much higher than tree strategies (Fig. 13). In the box-whisker plots, the median values decrease from 10 to 40 sampled strategies and stabilize above 40 sampled strategies. The interquartile values of the relative tree (grass) richness fall within 18 - 30 % (65-80 %) and the median values fall at around 30 % (70 %). The low relative richness of trees suggests that trees are less able to survive worldwide than grasses.

Because trees are less able to grow than grasses, the number of tree survivors likely varies more at low diversity levels. Therefore, the ensemble spread of the relative tree richness is greater at the low diversity levels. This is observed in the global distribution of the ensemble spread of the relative tree richness (Fig. 14). The white regions shown in the figures indicate that no species survive in any of the three ensemble members. The total white area is much more prominent in 10 than 600 sampled strategies, implying that regions without any tree sur-

vivors in mid-to-high latitudes are more probable at low diversity levels. This is the first hint of higher resilience at larger diversity levels.

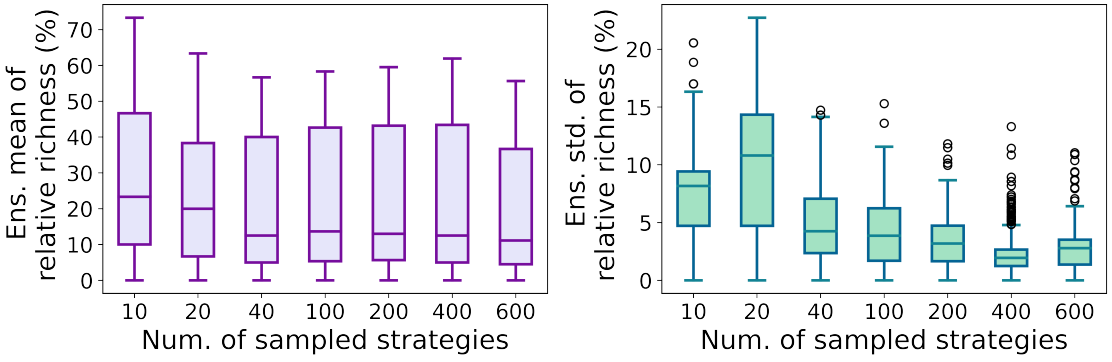

(a) (b)

Figure 12: Box plots showing how the distribution of worldwide values of (a) the ensemble mean relative richness and (b) the ensemble standard deviation of the relative richness depends on potential diversity.

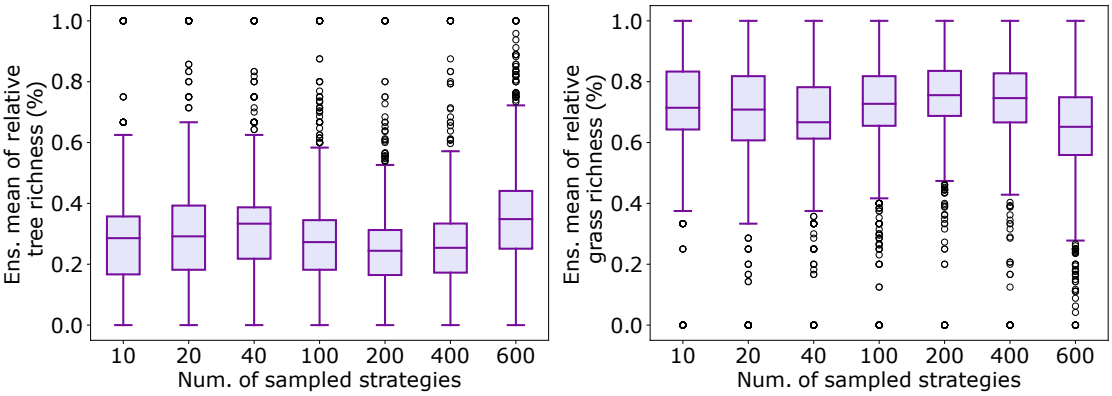

(a) (b)

Figure 13: Box plots showing how the distribution of worldwide values of (a) the ensemble mean relative tree richness and (b) the ensemble mean relative grass richness depends on potential diversity.

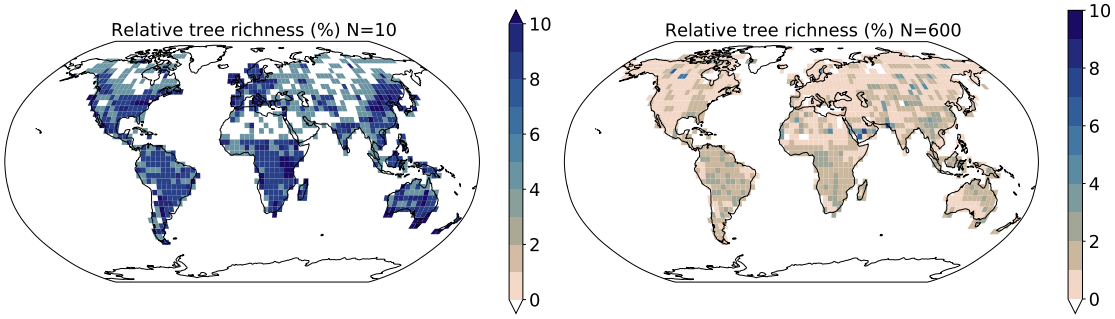

(a) (b)

Figure 14: Global distribution of the ensemble spread of the relative tree richness (a) with 10 sampled strategies and (b) with 600 sampled strategies. The white areas over land imply no tree strategies.

3.5.3.4 Tree dominance

To investigate whether the dominance of trees is associated with the observed climate difference across diversity, the dominance of trees (relative to grasses) is analyzed (the meaning of dominance is explained in Chapter 3.5.2.3). Based on the results of the relative tree richness shown in the previous section, the survival of trees is more affected by unstable climate conditions than grasses and therefore more easily become extinct. The relative tree richness has a larger spread if a few growth strategies are sampled (as in the case of 10 sampled strategies). With increasing diversity, the number of tree survivors stabilizes. In JeDi-BACH, only tree strategies have woody tissues and so, the presence of trees therefore make a substantial difference in the biomass composition of an ecosystem. Having more tree strategies in an ecosystem therefore leads to higher tree dominance (simply because trees are larger in their total biomass). A substantial increase in tree dominance already occurs at low diversity levels (Fig. 15 (a)). The median values increase from roughly 50 to 85 % along with an increased number of sampled strategies from 10 to 40. Above 100 sampled strategies, the increase is small and gradual. In Fig. 15 (b), the interquartile of the ensemble spread decreases substantially at low diversity levels and slows down with high diversity.

In Fig. 16, the ensemble mean global distribution of tree dominance with (a) 10 and (b) 600 sampled strategies is presented. The tree dominance shows a worldwide expansion at high diversity levels that progressively develops between the two diversity levels (not shown). The large ensemble spread at low diversity is mainly caused by the large variance in the relative tree richness. These results suggest that tree dominance increases with increased diversity and converges among ensemble members with increased diversity. Although the global relative tree richness is relatively stable across the different diversity levels (Fig. 13 (a)), the tree's dominance increases with diversity (see comparison with Fig. 15(a)).

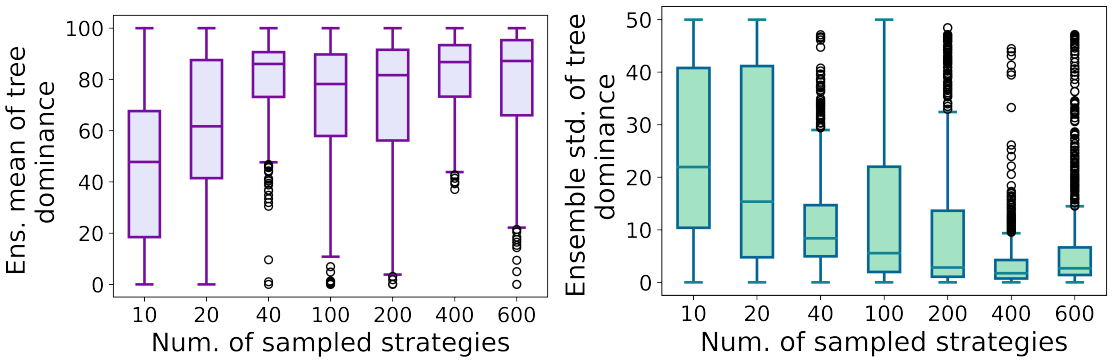

(a) (b)

Figure 15: Box plots showing how the distribution of worldwide values of (a) the ensemble mean of tree dominance and (b) the ensemble standard deviation of tree dominance depends on potential diversity.

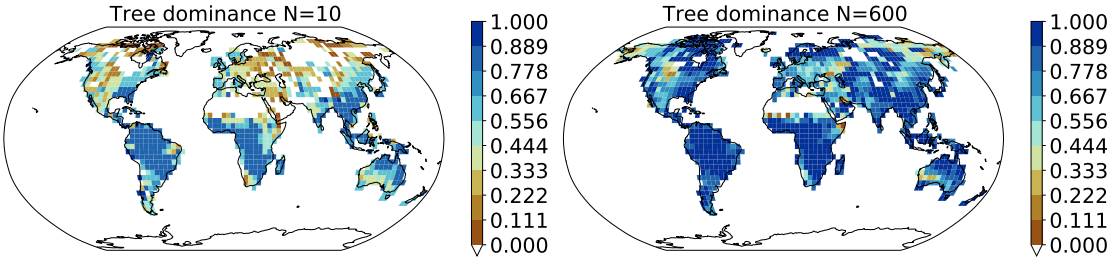

(a) (b)

Figure 16: Ensemble mean global distribution of tree dominance (a) with 10 sampled strategies and (b) with 600 sampled strategies.

3.5.3.5 Community weighted mean traits

In JeDi-BACH, 15 trait parameters are used to determine the functional capability of a PGS. To provide an insight of how a trait parameter varies across different ensemble members, the community weighted mean of a trait $CMT(trait)$ at different diversity levels is used. Here, one example of the trait parameter "T_{start}" is presented (see details in Section 2.5.3.2) as the other traits show similar outcomes to T_{start} (not shown). T_{start} is a trait parameter that determines the threshold temperature for the start of a growing season, namely T_{start} determines the thermal adaptation range of a growth strategy. Fig. 17 shows the distribution of $CWM(T_{start})$ of all terrestrial grid-cells for only trees. The peaks (the most frequent value) and the shapes vary substantially at low diversity ensembles. With only ten sampled strategies, there are possibly only a few tree strategies surviving worldwide so that the distribution of T_{start} is concentrated at only one or two values. The possible combinations of $CWM(T_{start})$ diversify with increased diversity. With increased diversity, the distribution of $CWM(T_{start})$ is becoming more similar among ensemble members at the same diversity level. The distribution seems to merge to a similar shape with diversity. Similar behavior is also found in the other trait parameters (not shown). Fig. 18 shows box plots of the distribution of worldwide values of the ensemble spread of all traits $CWM(traits)$ pooled into a single distribution for (a) tree strategies and (b) grass strategies. The distributions show a robust worldwide decrease in the ensemble spread with increasing diversity for both trees and grasses. These results hint that the cluster space realized by the survivors in the trait space is becoming identical with increasing diversity. Namely, ecosystems composed of similar combinations of strategies having much the same functional traits appear with increasing diversity. These results support the speculation that a similar degree of vegetation-climate feedback emerges at a high diversity level proposed in the previous section.

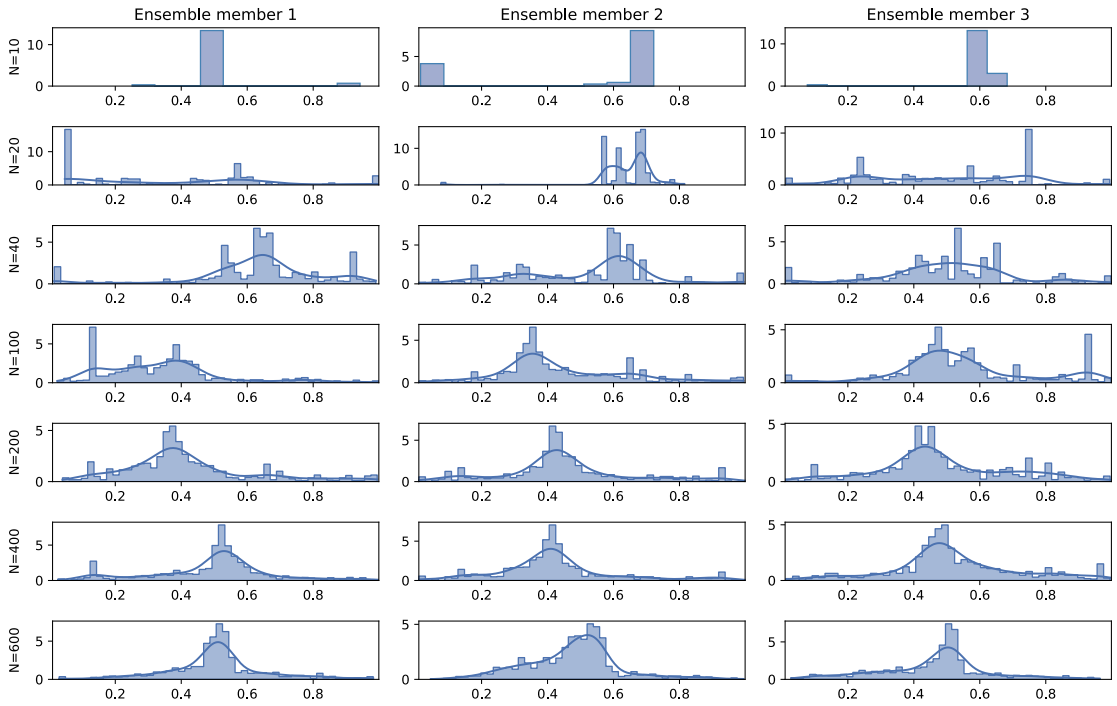

Figure 17: Probability distribution of the global community-weighted mean of the "un-scaled" trait parameter T_{start}. T_{start} is a trait parameter that defines the threshold temperature of a growth strategy to enter a growing season. The "un-scaled" values are the original values obtained from the Latin hypercube sampling, ranging from 0 to 1. These "un-scaled" values are then "scaled" to the actual trait values in JeDi-BACH. For instance, these "un-scaled" values are "scaled" to -5 to 15°C. Three ensemble members of a respective diversity level (N) are presented in the same row. The x-axis shows the "un-scaled" value of T_{start}.

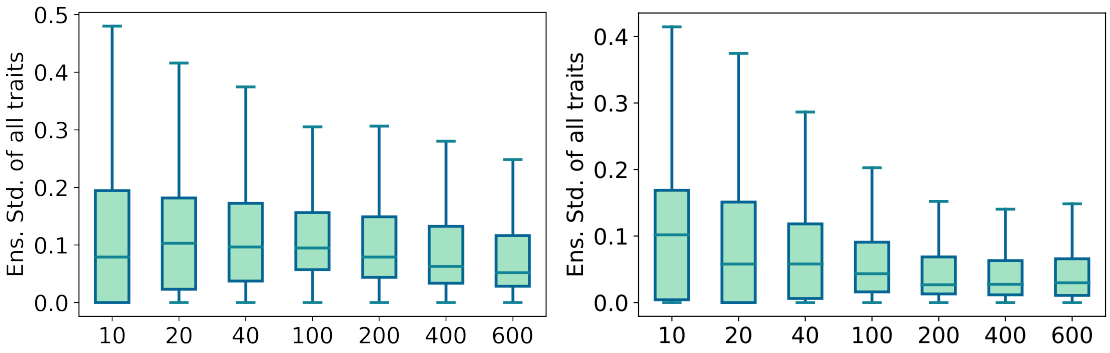

(a) Tree strategies

(b) Grass strategies

Figure 18: Box plots showing how the distribution of worldwide values of the ensemble standard deviation (std) of all 15 CWM plant trait parameters separately for tree and grass strategies for all considered diversity levels. Noting that all these parameter values are those "un-scaled" values in the range 0 to 1 so that they can be pooled into a single distribution.

3.5.3.6 Global distribution of biomass and productivity

The global biomass shows an increase in ensemble mean global biomass production with increasing diversity, from roughly 680 to 800 Gton carbon (Fig. 19 (a)). A considerable spread between ensemble members occurs at low diversity levels. There is a difference of around 1300 Gton carbon among two members with only 10 sampled strategies, which is almost double the amount of ensemble mean 700 Gton carbon. Global biomass production stabilizes and converges to about 800 Gton carbon with increasing diversity. The biomass spread is only about 100 Gton carbon at the high diversity levels. Such a large spread at low diversity is consistent with the large ensemble spread observed in the relative tree richness (Fig. 14). At low diversity levels, as global biomass is only dominated by a few strategies, once a few tree strategies survive, they quickly dominate and thereby contribute to large biomass. Fig. 19 (b) shows the annual mean global gross primary productivity (GPP). The ensemble mean GPP stabilizes at about 220 Gton carbon per year with increased diversity. A substantial decrease is depicted when diversity increases at low diversity levels. The ensemble spread reduces with increasing diversity.

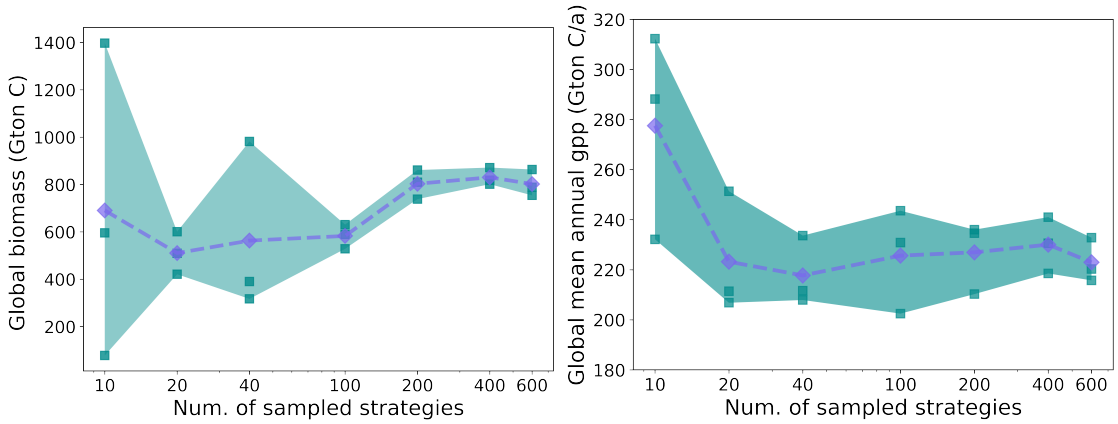

(a) (b)

Figure 19: (a) Global biomass. (b) Global annual mean gross primary productivity. Purple diamond dash-line shows the ensemble mean and cyan squares show each ensemble members.

3.5.4 Discussion

The extent to which variation in ecosystem function can influence climate systems is largely unexplored. Little is known about the relative magnitude or the impact on climate. In this section, I explore the role of plant functional diversity in shaping global climate and ecosystem functioning. In particular, I focus on how changes in dominant traits and the related ecosystem function can modify climate mainly in biogeophysical aspects under different diversity regimes.

3.5.4.1 High functional diversity supports a robust regional climate

From the spectrum of diversity simulations conducted in this section, the regional climate varies substantially at low diversity. Such a high sensitivity is consistent with the high sensitivity reported in previous modeling studies, of which the regional climate is reported to be sensitive to prescribed land surface characteristics. However, I find that terrestrial regional climate is becoming more robust with increasing diversity. Simply put, a robust global climate pattern emerges with high plant functional diversity. In addition, there seems to exist a boundary tightly associated with the environment that the global ecosystems can exploit. Increasing diversity behaves in a way that maximizes the degree of climate-vegetation interaction. These results deliver an important message: plant functional diversity is likely critical to supporting a robust regional and global climate. With increasing diversity, terrestrial climate converges towards a cooler and wetter world. Changes in diversity level can modify mean terrestrial precipitation by 30 mm/year and mean temperature by 0.45 K (see Section 3.5.3.1). Here, I discuss the possible reasons behind this speculation. Why does regional climate converge among ensemble members with increased diversity?

Climate converges with increasing diversity because more resource-optimized strategies survive

The strong difference in climate found among ensemble members at low diversity arises primarily because the initial set of growth strategies is largely undersampled. The hypothetical functional traits used for plant representation in the model are constructed from a 15-dimensional space. In the low diversity level simulations, this multi-dimensional trait space is barely explored by a few dozen sampled strategies. Since no strategy can survive in all possible environments, the total number of survival strategies is fairly small. This further implies that in some regions, no strategy survives, and in other regions, only one or a few strategies survive. With only a few strategies surviving globally, the

trait values realized by these few survivors diverge among ensemble members. This is shown by the large deviation observed in traits (see Fig. 18 and Fig. 17). Therefore, such large differences in their functional trait values contribute to different ecosystem functions. For instance, differences in the evapotranspiration modify the partition in the surface energy balance and so ultimately lead to different climate conditions across the ensemble members. In brief, the regional climates differ largely among low diversity ensemble members because the land surface properties are susceptible to the functional traits of the few survivors.

On the other hand, when more strategies are sampled, the trait space is better or more evenly explored. This implies that strategies with a wider range of functional capabilities can survive worldwid. One possibility for the observed convergence between ensemble members may be that more strategies that can better cope with the imposed environments are sampled with increased diversity. To illustrate more on this point, one could imagine that the trait parameters form a multi-dimensional trait space. Noting that, if a plant strategy successfully survive in a particular environment, they must have developed specific trait combinations to cope in that respective environment. The general environmental conditions behave like a "climate envelope" that wraps around a region in this trait space. The growth strategies located in this region are the optimal in a given environment. When the trait space that offers the best adaptive strategies is better sampled, more optimized species with marginal differences in their functional capability survive. These strategies start to dominate and may further modify the environment to their favor. This argument is plausible because the results obtained here, either the convergence in regional climate or the CWM-traits, are the outcome of the successful survivors. In contrast, the non-optimal strategies have no impact because they simply die out or contribute little to the system. In brief, as a high diversity world has more sampling strategies, the likelihood that resource-optimal (located in the climate envelope) strategies are sampled is high. Therefore, similar ecosystem functions (offered by these optimal strategies) lead to similar vegetation-climate interactions so that global climates are becoming identical with increasing diversity. Next, I discuss the possible reasons behind this convergence.

Convergence to the state of high water-cycling with increasing diversity

As mentioned earlier, similar vegetation-climate interactions appear with increasing diversity. Terrestrial climate is becoming wetter and cooler with increasing diversity (see Fig. 7) and climate, both global and regional-scale, is robust in a high diversity world (see Fig. 8). How does regional climate con-

verge among ensemble members with increased diversity? An increase in tree dominance (see Fig. 15) principally governs the convergence of climate towards the climate pattern in high diversity: trees differ from grasses in their structural traits. Trees are bigger and are larger in biomass than grasses. By the biomass-scaling theory considered in JeDi-BACH, bigger strategies (i.e, bigger plants have more biomass) occupy more "area" than the subordinates so that the dominance of trees progresses when more trees succeed. There are two possible explanations for the increase in tree dominance.

The first possibility is that the increase in dominance is simply due to the increased number of sampled strategies. The relative tree richness is only half of that for grasses (Fig. 13). This indicates that the chance of trees surviving across the world are less at a low diversity level simply because only a few tree strategies are sampled. With increased diversity, more different tree strategies have the potential to take over land area. Hence, more land surfaces can be taken over by at least one tree strategy. This is consistent with the reduced extent of white regions on land in Fig. 14 (where no tree survived in any ensemble member).

However, this possibility is insufficient to explain why tree dominance increases, but the relative tree richness remains fairly stable across diversity levels (Fig. 13 (a)). In the absence of climate change, a similar relative tree richness across diversity levels should result in a similar biomass ratio between trees and grasses so that the dominance of trees should remain the same across diversity levels. On the contrary, tree dominance progresses and climate becomes cooler and wetter with increasing diversity. I speculate that a certain mechanism favors tree growth than grasses when diversity increases.

The second possibility may be that trees outperform grasses via certain feedback. With increased diversity, an increase in tree dominance would then, in some way, favor more growth of trees rather than grasses. The predominant differences between trees and grasses are in their structural traits. Trees consist of woody tissues that allow them to grow taller and larger and penetrate deeper into soil than grasses. When trees and grasses tap into the soil at the same place, they compete for the available soil water, a mechanism implemented in JeDi-BACH. Deep roots can give an advantage to trees. Firstly, trees potentially have more soil water available at different soil layers with deeper roots. Therefore, trees can better access deep soil water than grasses. Trees thus experience minor water limitations and can perform relatively better than grasses. Secondly, once the dominance of trees surpasses grasses, trees start to dominate the removal of water from soils. Consequently, trees outcompete grasses by leaving grasses

with further water limitations. Lastly, trees utilizing soil water throughout dry and wet seasons may also play an important role.

In regions where water is the main limiting factor for plant growth, the distribution of water usage during dry and wet seasons is critical. Certainly, nutrient limitation plays a role, but it is not considered in JeDi-BACH. Because trees transpire more than grasses, trees can induce a shortening of the growing seasons of other strategies by pumping out soil water in a short period for their growth. Altogether, trees outcompete grasses by experiencing in general less water stress. The exact mechanism of the feedback relationship is not clear yet, but consistent results to this second possibility are observed (Fig. 9). Considering that changes in climate and ecosystem composition happen simultaneously and mutually influence each other, it is impossible to pinpoint either of the two possibilities discussed so far. It may also be the outcome of both possibilities. Although I have yet to identify the exact causality by which the convergence operates, the results discussed so far are consistent with the biodiversity and ecosystem functioning (BEF) relationship reported from the most up-to-date understanding of biodiversity (Cardinale et al., 2012) and is discussed in the section below.

3.5.4.2 Agreement with the observed biodiversity-ecosystem functioning relationship

The observed robustness of climate/ecosystem function associated with high functional diversity is in many aspects in agreement with the biodiversity-ecosystem functioning (BEF) relationship summarized by Cardinale et al. (2012). Several consensus statements on BEF are summarized therein.

> *"There is now unequivocal evidence that biodiversity loss reduces the efficiency by which ecological communities capture biologically essential resources, produce biomass, decompose and recycle biologically essential nutrients (consensus one, Cardinale et al. (2012).)"*

Terrestrial precipitation and evaporation increase with diversity and converge towards a distinct climate for a high diversity world (see Fig. 7 and Fig. 10). The water exchange between land and atmosphere varies substantially at low functional diversity and shows an asymptotic behavior towards high diversity levels. I speculate that an increase in diversity, followed by more resource-optimized strategies, pushes the system to a high water-cycling state. Global root depth is one of the critical factors controlling terrestrial hydrology. The root zone depth determines the amount of water cycling between soil, vegetation, and atmosphere, and back. With an increase in tree dominance, deeper roots (see Fig. 9) indicate more available soil moisture for plant growth, inducing more

evapotranspiration (ET). Meanwhile, an increase in above-ground trunks increases the surface roughness length, reduces surface wind speed, and thus has an opposing effect by reducing potential evapotranspiration. Nevertheless, there is a net increase in ET that leads to more precipitation and a reduction in temperature. More precipitation therefore replenishes the water storage in soils. These results coincide with the so-called soil moisture-precipitation feedback described by Seneviratne et al. (2010). With increased diversity, the total amount of water stored, accessed and recycled on land (in the root zone) increases along with the deepening of global root depth. Therefore, I suspect that terrestrial water exchange between soil water and the atmosphere is approaching a maximum with increased diversity so that no further improvement in moisture cycling is observed. Such a high water-cycling state can be depicted by the upper boundaries shown in Fig. 7 and Fig. 10. Such asymptotic behavior is consistent with the BEF relationship as ecosystem functions (i.e, ET, GPP, or biomass) generally increase with the number of sampled strategies and reach asymptotes at a certain point.

Combining the results discussed so far, it is found that plant functional diversity can shift the terrestrial climate from a dry and warm grassland world to a moist and cool forest world by enhancing water-turnover. From the environment's point of view, the main result is that high functional diversity will support a robust climate on both regional and global scales.

From an ecosystems' point of view, high functional diversity is widely associated with the resilience/stability of the system.

> *Biodiversity increases the stability of ecosystem functions through time. ... there is no theoretical reason to believe that biodiversity should enhance all forms of stability. However, theory and data both support that total resource capture and biomass production are more stable in more diverse communities (consensus two, Cardinale et al. (2012)).*

Also, the simulated global total biomass production shows an asymptotic behavior when approaching a high diversity world (Fig. 19). The observed increase in total biomass, the convergence of ecosystem function and climate, and the CWM traits with increasing diversity are largely consistent with the so-called redundancy hypothesis (Walker, 1992). At the asymptotic level, adding more strategies into an ecosystem does not contribute to more improvement in ecosystem function; it potentially provides "invisible" stability by having many redundant strategies. These redundant strategies work as insurances and replace strategies with a similar function in case they die out under disturbance. Despite that, addressing any kind of stability is not feasible concerning the simulations conducted in this study and, certainly, ecosystem resilience involves

many complex mechanisms. One can speculate that an ecosystem with high plant functional diversity possibly supports greater stability than a low diversity one in a coupled model simulation —- a hypothesis that is investigated later in Chapter 4.

3.5.5 Conclusions and Summary

In this study, I conduct a series of ensemble simulations with different levels of diversity using a new prototype of the plant diversity model JeDi-BACH with an interactive atmosphere. The analysis of the coupled simulations with a 'self-organizing' vegetation model JeDi-BACH allows, for the first time, to identify the importance of functional trait diversity for shaping global climate and ecosystem functions. The discussion revolves around the biogeophysical component of the climate system. I find that,

1 Plant functional diversity level is critical for supporting robust climate and ecosystem functioning. A high diversity world implies that the ecosystems are likely to exploit the maximal condition (resources) provided by the environment.

From the point of view of the environment, I find that regional climate converges with increasing diversity and global climate converges towards a high water-cycling state. From the point of view of the ecosystem, high functional diversity results in similar ecosystem functioning because there are simply more optimal growth strategies that can maximize resource efficiency. Essentially, I find that increasing plant functional diversity can modify the terrestrial climate from a dry and warm grassland world to a moist and cool forest world via maximizing the moisture cycling on land.
Based on these findings, it is suspected that the high regional climate sensitivity to land surface characteristics reported in previous modeling studies (Groner et al., 2018; Alton, 2011; Verheijen et al., 2013) stemmed from the poor representation of ecosystem complexity. JeDi-BACH, as a new prototype of a plant diversity model can, to a certain degree, circumvent such an issue because it offers a different modelling perspective to mimic more biosphere-like features (i.e, the selection of adaptive strategies are based on environmental condition and plant functional trade-off relationships).

2 The observed convergence in ecosystem functioning with increasing diversity (from model simulations) agrees with the biodiversity-ecosystem functioning (BEF) relationship obtained in field experiments. Such analogy to observations reinforces the topics that are so far largely unexplored — the link between climate and the diversity-resilience relationship.

Despite the fact that the exact mechanism behind the convergence of both climate and ecosystem functions with increasing diversity has not yet been identified, the presented model results are consistent with the BEF relationship found in ecological field experiments. With high functional diversity, the likelihood of having resource-optimized strategies (or species in real ecosystem) is high, so that the efficiency for an ecosystem to utilize resources increases with diversity. As demonstrated in the simulation results, global ecosystems tend to explore all resources provided by the environment so that terrestrial hydrological cycle enhances with increasing diversity. In other words, global ecosystems are, seemingly, pushing the vegetation-climate interaction towards a high water cycling state with increasing diversity that, as a result, leads to a wet and cool climate. Furthermore, if the turnover of resources is high, such an ecosystem is also likely more resilient as the exploration of resources is simply better. This is in line with the redundancy hypothesis — the observed asymptotic behavior hints at the potential resilience of the ecosystem that comes with increased biodiversity. Though examining the stability of ecosystems is beyond the scope of our current study, I surmise that this new prototype of the JeDi-BACH model is more suitable for capturing "ecosystem resilience" than the traditional PFT approach. In fact, JeDi-BACH mimics more biosphere-like features so that the ecosystem organizes on its own while mutually responding and modifying the environment.

3.6 Sensitivity to parameter changes

In the previous section, climate and ecosystem functions are found to be robust at a high diversity level. Based on this result, I proceed on assessing other aspects of JeDi-BACH. During the development of the model, I identified some ambiguity in four plant trait parameters: α, $\mathtt{fapar}$, κ_{rd}, and Q10. Their values cannot be fully justified in the model due to either of the following reasons: (i) the parameter is of technical nature and has no clearly measurable counterpart, (ii) the parameter is measurable but data are missing, (iii) the parameter is newly introduced by me and was not present in the original JeDi so that no estimate for this parameter exists. I conduct and analyze sensitivity experiments to assess the potential uncertainty arising from these parameters, in this section. These four parameters and their related plant functions are described as follows:

1 α is the soil wetness threshold, which determines, together with a temperature threshold, the begin and end of growing seasons (see eq. (14)). A plant growth strategy can enter a growing season only if the soil moisture is above this threshold. In JeDi-BACH, all plant growth strategies are controlled by the same α value.

2 $\mathtt{fapar}$ is the light limitation parameter, which I newly introduced in JeDi-BACH to prevent unrealistic growth of leaves (see Section 2.5.6). $\mathtt{fapar}$ operates like a brake, that slows down plant growth to avoid overinvestment when light interception by a strategy gets too high. For instance, a growth strategy reduces investing in growing new tissues when the total light interception at the canopies approaches 90%.

3 κ_{rd} is the conversion coefficient, used to convert root carbon into root depth (see eq. (30)). In the model, a plant strategy's soil water accessibility is determined by its root depth. This value was never justified in the previous model JeDi-DGVM.

4 In JeDi-BACH, the sensitivity of plant respiration to temperature is expressed in the form of an Arrhenius equation (see eq. 39). Q10 is the parameter used in the equation to estimate changes in maintenance respiration per 10 K in temperature (e.g., a Q10 value of 2 doubles maintenance respiration with an increase in temperature from 0°C to 10°C).

3.6.1 Experiment setup

To investigate the extent to which global climate and ecosystem function depend on the four parameters, for each parameter two sensitivity experiments were conducted in this chapter. Table 4 summarizes the experiment design with the considered parameters and their values. All model simulations are conducted at high diversity with 400 sampled strategies.

I conduct nine simulations, including one control (CTRL) simulation and eight sensitivity simulations. The aim is to compare the results of the sensitivity experiments with the CTRL simulation to obtain the order of magnitude in climate/ecosystem functioning change. The parameter values are modified substantially to observe a significant impact. These eight simulations were continued from the same spin-up simulation (see Section 3.4.1). Each simulation is conducted with only one parameter changed at a time. All sensitivity experiments are carried out in an AMIP-type setup. The simulations are forced by prescribed SSTs, SIC, greenhouse gasses, and aerosols for 1979 to 2014 following the CMIP6 AMIP protocol (Eyring et al., 2016). I use the last 15 simulation years (2000 to 2014) of all nine simulations for the analysis in this section.

Experiment	Parameters				Legend shown on figures
	α	$fapar$ (tree/grass)	κ_{rd} (tree/grass)	Q10	
CTRL	0.4	0.9/0.78	2250/550	2	CTRL
alpha_1	0.5	-	-	-	$\alpha = 0.5$
alpha_2	0.6	-	-	-	$\alpha = 0.6$
fapar_1	-	0.8/0.6	-	-	$fapar = 0.8$
fapar_2	-	0.85/0.7	-	-	$fapar = 0.85$
rd_1	-	-	1125/275	-	$rd = half$
rd_2	-	-	4500/1100	-	$rd = doubled$
q10_1	-	-	-	1.2	$q10 = 1.2$
q10_2	-	-	-	1.6	$q10 = 1.6$

Table 4: List of selected parameter values conducted in the respective simulation.

Note that, ideally, a separate coupled spin-up should be performed for each parameter change, and then compared with the control simulation. However, such a procedure is not feasible considering the computational resources needed. Instead, all sensitivity simulations are continued from one common spin-up simulation. This may not be a perfect setup because there is the possibility that some strategies that died in this spin-up could be able to survive in the sensitivity simulations, given the parameter changes. Nevertheless, the chosen experiment setup keeps the total computational cost in a feasible range.

3.6.2 Results

3.6.2.1 Sensitivity of global net primary productivity to changing parameters

I compare net primary productivity (NPP) among sensitivity simulations to estimate the variation of ecosystem response to the selected plant parameters. NPP is a measure of the net amount of carbon used for plant growth. Note that the experiment design allows us to understand whether the relative change in NPP (or terrestrial climate discussed in the following sections) has a similar magnitude as the relative change imposed to the parameters. Table 5 lists the comparison of parameter values and the global NPP difference between the sensitivity and CTRL simulations. Out of the four parameters, global NPP is most sensitive to the parameter `fapar`. The relative changes of the other three parameters are rather minor regarding the magnitudes of parameter changes. This implies that NPP, on the terrestrial scale, is fairly robust to α, κ_{rd}, and Q10.

On the zonal scale, I compare the difference of NPP to the CTRL simulation (ΔNPP) at each latitude for the eight sensitivity simulations (Fig. 20). To improve readability, the following discussion is described all based on the comparison of a sensitivity simulation to the CTRL simulation.

Both `alpha_1` and `alpha_2` simulations show a zonal reduction in annual NPP (Fig. 20 (a)). Both simulations have more mid-latitude reduction than in the tropics. In general, the `alpha_2` shows a greater NPP reduction than the `alpha_1` simulation, with a largest reduction of about 0.25 GtC at 50N. These results imply that raising the soil moisture threshold for plant growth leads to more reduction in mid- to high-latitudes (30-60N and 30-60S). This is likely because tropics (30S-30N) receive on average more precipitation than extra-tropics and tropics have less seasonality.

Changes in the `fapar` parameter lead to more NPP in the tropics than at mid-latitudes (Fig. 20b). Both simulations with a change in `fapar` show an increase in tropical NPP. In `fapar_1` and `fapar_2` simulations, NPP increases by about 0.13 GtC and 0.08 CtC per latitude between 20S-20N, respectively. A slight reduction in NPP is observed in high-latitudes in the `fapar_2` simulation. The differences between tropics and extra-tropics are likely because the growing season often lasts year-round in the often warm and wet tropics. Tropical ecosystems might overinvest into canopy growth when trying to intercept sunlight to the maximum, such that the carbon gain per unit of carbon invested into growth may not be economic/efficient. Smaller `fapar` values (meaning an earlier brake for slowing down plant growth) may reduce inefficient plant growth

and lead to an increase in NPP.

The parameter κ_{rd} demonstrates more uniform changes across latitudes in both simulations where it is changed (Fig. 20c). Simulation rd_1 yields around 0.1-0.2 GtC increase in NPP per degree of latitude across both tropics and mid-latitudes. In general, the rd_1 simulation yields greater absolute changes in NPP than rd_2. In the latter, we see reductions in NPP in most latitudes, and reductions are larger in the tropics, reaching on average roughly 0.09 GtC per latitude between 20S-20N. These results are consistent because the cost for growing a unit root per unit carbon is smaller with a smaller κ_{rd} value. Likewise, a larger κ_{rd} value implies that the cost for growing roots to the same root depth is larger and, leading to a world-wide NPP reduction.

Changing the Q10 value leads to different NPP variations between the tropical and mid-latitude regions (Fig. 20d). Zonally, the magnitudes of increase in the tropics are much larger than in mid-latitudes. The tropics show 0.19 and 0.16 GtC increases per latitude in Q10_1 and Q10_2 simulations, respectively, while reductions of about 0.05 and 0.06 GtC/degree in the mid-latitudes. Smaller Q10 values imply that the cost for maintenance respiration is reduced so that a substantial NPP increase is observed. Also, warm regions, such as tropics and subtropics, show a larger reduction as the rate of increase by temperature is less steep with a smaller Q10 value.

	Difference in parameter value	Relative difference in parameter	Global annual NPP (GtC/year)	ΔNPP (GtC/year)	Relative ΔNPP (%)
CTRL	-	-	94.2	-	-
alpha_1	+0.1	+25%	91.6	-2.6	-2.76%
alpha_2	+0.2	+40%	84.5	-9.7	-10.30%
fapar_1	-0.1/-0.18	-11%/-23%	100.5	6.2	+6.58%
fapar_2	-0.05/-0.08	-5%/-10%	98.9	4.6	+4.88%
rd_1	-1125/-275	-50%	107	12.9	+13.69%
rd_2	+2250/+550	+100%	86.3	-7.8	-8.28%
q10_1	-0.8	-40%	103.5	9.2	+9.77%
q10_2	-0.4	-20%	106.4	12.1	+12.85%

Table 5: Size of parameter change in comparison to the resulting change in NPP found in the sensitivity simulations. Column 2 lists the difference in parameter values to the CTRL ones. The two values shown in the experiment `fapar` and `rd` indicate separately the values used for tree and grass. Column 3 lists the relative increase/decrease to the parameter value used in CTRL. Column 4 is global annual NPP (GtC/year). Column 5 shows the difference in global annual NPP to CTRL. Column 6 is the relative change to CTRL in percent. Note that the relative changes in parameter values (column 3) do not imply linearity in ecological processes in the model. The value itself does not directly scale the corresponding plant functions associated with the parameter. The relative changes shown in percent only provide a general comparison regarding the CTRL simulation.

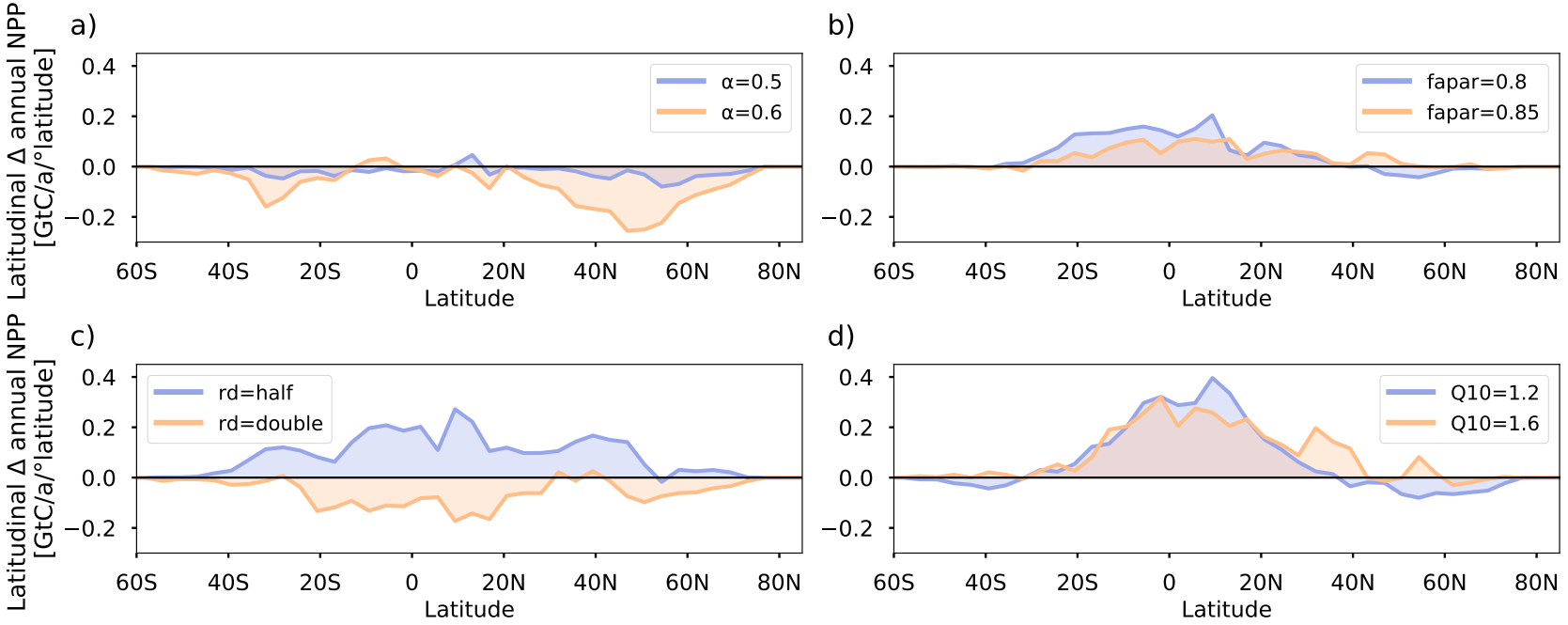

Figure 20: Difference of annual NPP latitudal sum to the CTRL simulation for four sensitivity parameters: a) the soil moisture threshold for growing season related parameter α , b) the light limitation parameter $\mathtt{fapar}$, c) the root depth related parameter $\kappa_{\mathtt{rd}}$, d) the temperature-dependence parameter Q10. The latitudinal sum is the integral of ΔNPP over the land surface area at each latitude.

3.6.2.2 Sensitivity of terrestrial climate to changing parameters

The terrestrial climate of the eight sensitivity and the CTRL simulation are analyzed to estimate the sensitivity of climate. Surprisingly, all eight sensitivity simulations give results nearly identical to those of the CTRL simulation (Fig. 21 (a) and (b)). This suggests that the large-scale atmospheric circulation generally remains the same despite the range of parameter changes tested.

To further evaluate regional differences, I assess differences in global terrestrial annual mean precipitation (mm/year) and 2-meter air temperature (K) between the eight simulations and the CTRL simulation (Fig. 22 and Fig. 23). The regional climate is statistically indistinguishable from the CTRL simulation in most terrestrial regions. This suggests that most regional climate is fairly robust to any parameter changes. However, the western Sahel regions demonstrate significant differences from the CTRL simulation.

In western Sahel region (5N to 18N; 15W to 18E), seven simulations (except q10_1) show an increase in temperature and only two simulations (alpha_2 and rd_2) show a significant reduction in precipitation. The western Sahel region is warmer and dryer in the sensitivity simulations than in the CTRL simulation. Out of the eight simulations, the rd_2 and alpha_2 simulations show the largest regional warming and drying in the western Sahel, where annual precipitation is reduced by between 150-500 mm and air temperature increased by about 1-1.5K. In comparison, the other six simulations have relatively minor changes in precipitation. To further analyze this behaviour, I also assess the differences in terrestrial annual mean evapotranspiration (ET) (mm/year) between the eight simulations and the CTRL simulation (Fig. 24). Similar to the precipitation pattern, the western Sahel regions show a significant reduction in ET. Significant changes in the central Sahara desert are detected in most simulations (except q10_2), but are excluded from the following discussion.

The drying and warming detected in the western Sahel region are likely associated with the reduction seen in ET. Western Sahel climate is dominated by the West African Monsoon. The southwesterly winds bring moisture from the Atlantic into the inner part of western Sahel. To further assess the changes at the regional scale, the difference in moisture transport of the alpha_2 simulation is chosen here for analysis to the CTRL simulation (Fig. 25). The differences in moisture transport near coastal regions in western Africa are small, implying that moisture transported from the Atlantic ocean via west African monsoon circulation are similar in both simulations along the coast. However, the difference in inland moisture transport points towards southwest, implying that the

moisture transport into the inner part of western Africa is weakened (see the size of arrows) in the alpha_2 simulation. The specific humidity also decreases (shown in red) in the alpha_2 simulation. These results are consistent with the reduction in precipitation and evapotranspiration shown in Fig. 22(b) and Fig. 24(b), suggesting that the weakening of moisture cycling in the western Sahel region is induced locally by the reduction in evapotranspiration.

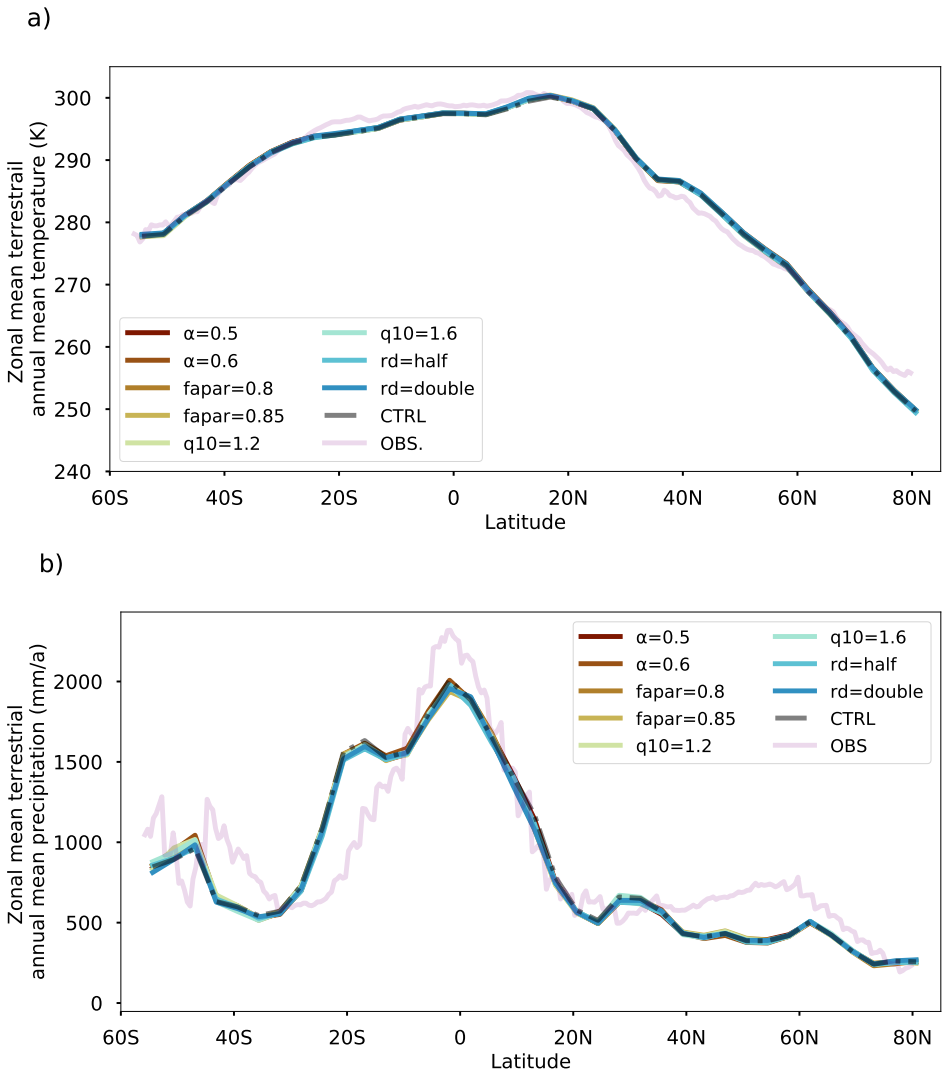

Figure 21: Comparison of the zonal mean climate over land: (a) annual mean 2-meter air temperature (K) (b) annual mean precipitation (mm/year). The satellite estimates (OBS) of precipitation and temperature are taken from the Global Precipitation Climatology Project (GPCPv2) (Adler et al., 2018) and CRU dataset (2000-2014) (Harris et al., 2014). The CTRL simulation is shown in a grey dashed-dotted line. Both satellites estimate are shown in purple. The legends for each sensitivity simulation are noted with their corresponding parameter values for readability (see Table 4 for related details).

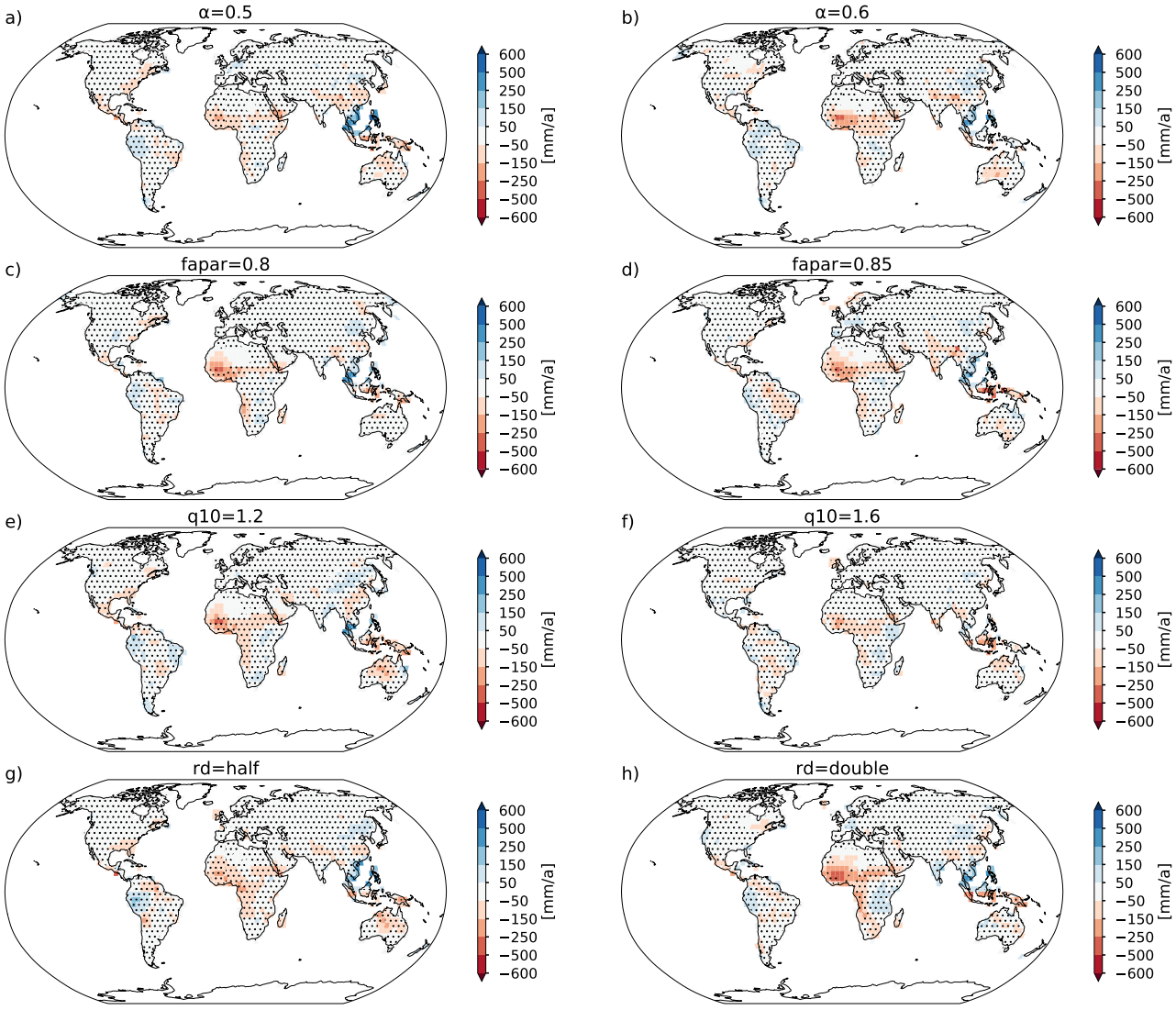

Figure 22: Difference of annual mean precipitation (mm/year) between each sensitivity simulation and CTRL simulation. Statistical significance is calculated according to a 5% level in a Mann-Whitney test. Note that regions marked with dots are statistically not distinguishable from the CTRL simulation.

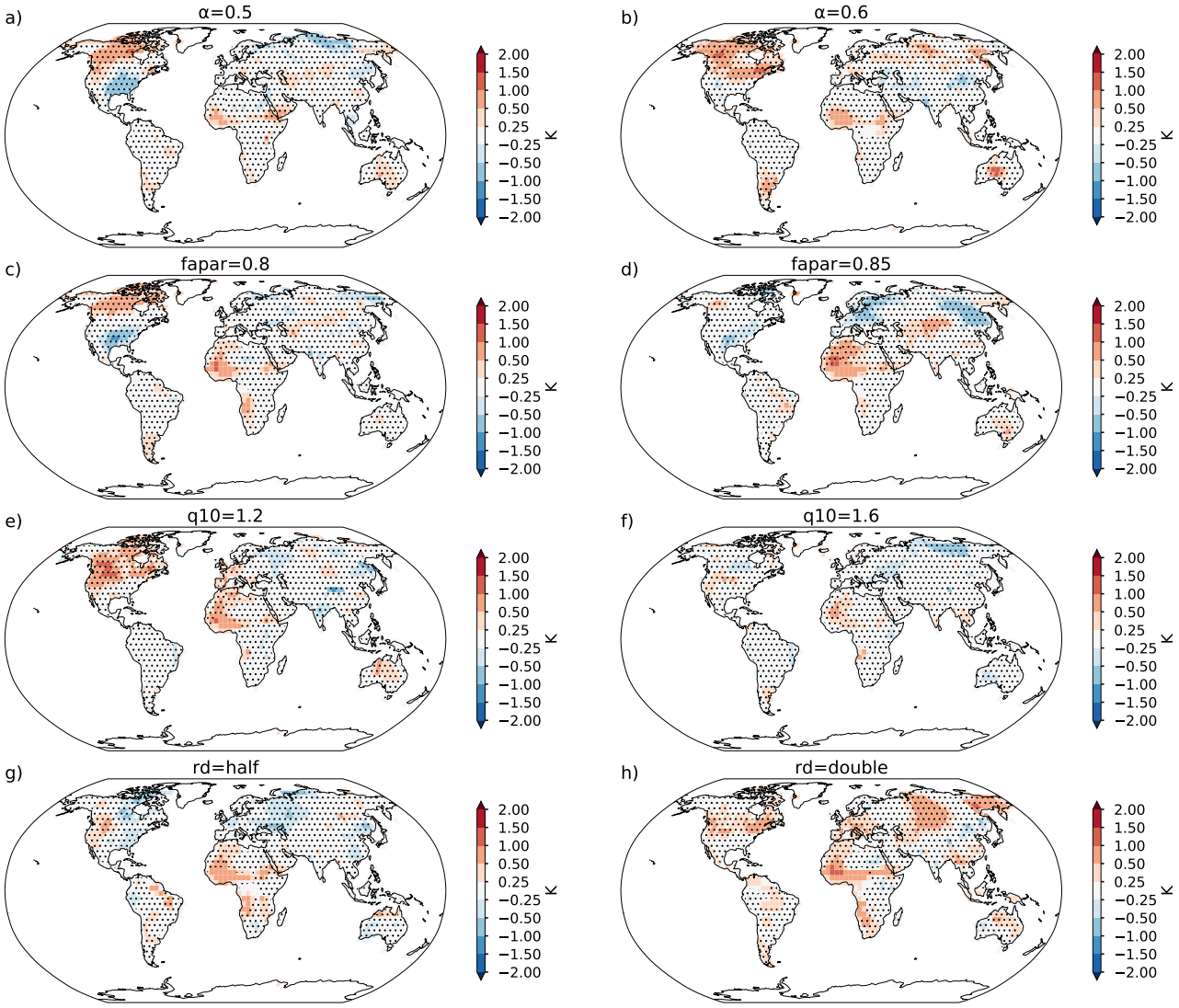

Figure 23: Difference of annual mean 2-meter air temperature (K) between each sensitivity simulation and CTRL simulation. Statistical significance is calculated according to a 5% level in a Mann-Whitney test. Note that regions marked with dots are statistically not distinguishable from the CTRL simulation.

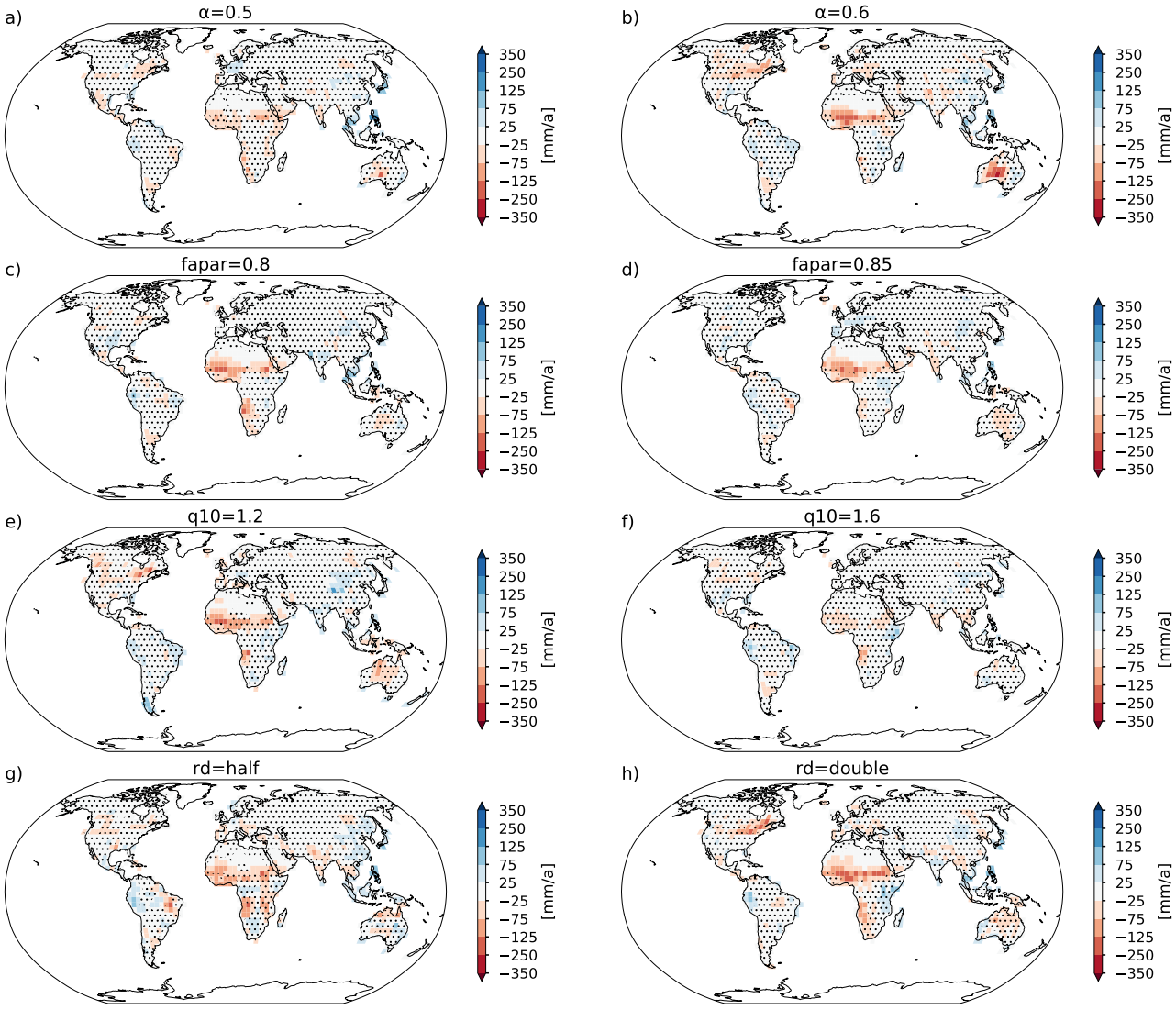

Figure 24: Difference of annual mean evapotranspiration (mm/year) between each sensitivity simulation and CTRL simulation. Statistical significance is calculated according to a 5% level in a Mann-Whitney test. Note that regions marked with dots are statistically not distinguishable from the CTRL simulation.

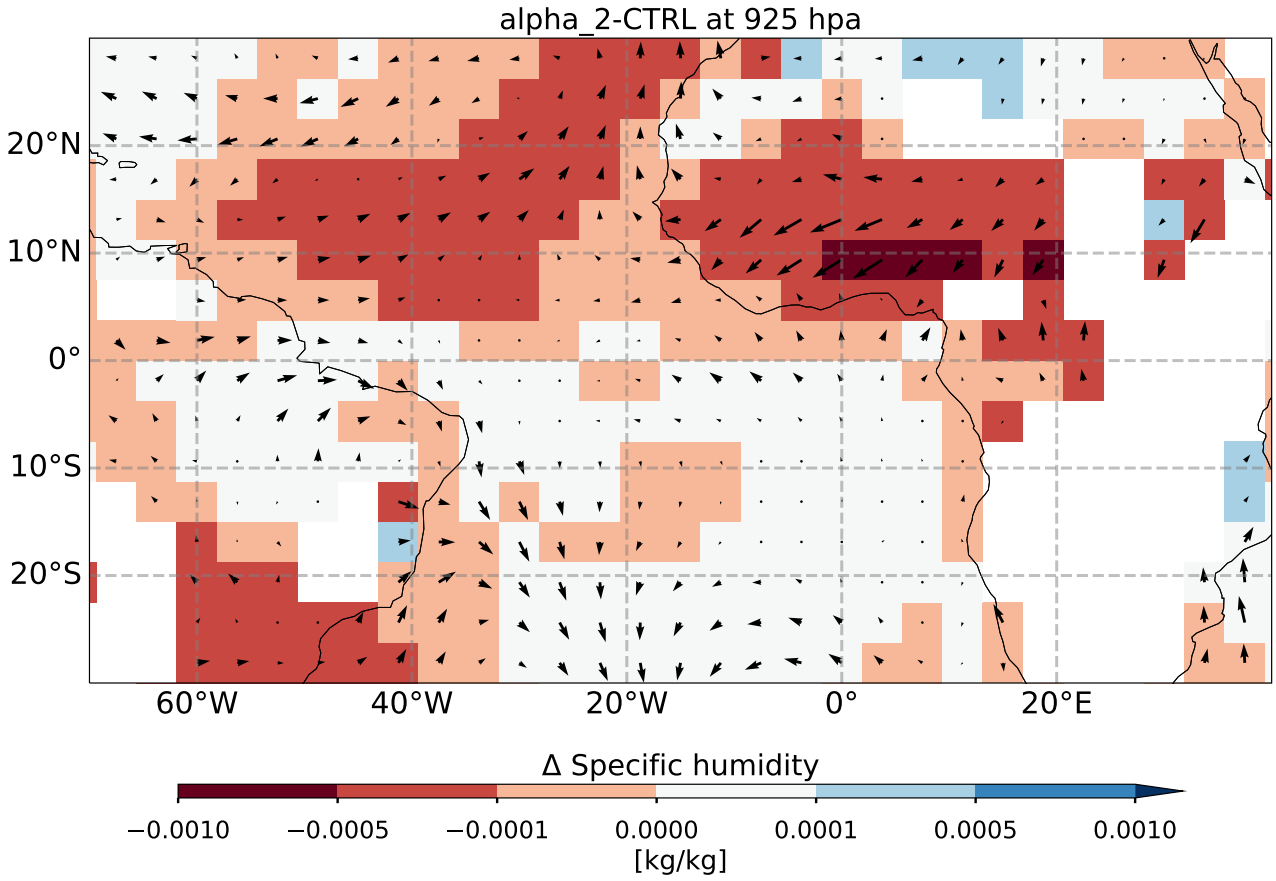

Figure 25: Difference of moisture transport at 935 hPa between the alpha_2 and CTRL simulation. The difference in the specific humidity (kg/kg) is shown in color. The terrain is shown in white (no data). The moisture transport is calculated as the product of wind field (m/m) and specific humidity at 935 hPa. The arrows imply the difference in moisture transport and the size indicates the magnitude.

3.6.2.3 Shuffling in ecosystem composition

In JeDi-BACH, the contribution (ecosystem functions) of individual plant growth strategies to the total fluxes (NPP, ET, etc.) in a given model grid-box is based on biomass-scaling theory proportional to their biomass (see Section 42). The "dominance" of a plant growth strategy in a grid-box is determined (ranked) by their total biomass (i.e., strategies with larger biomass dominate and occupy top rankings). A shuffle in the ranking happening during a simulation is an indication that the dominance of a strategy within an ecosystem changes. That is, the previously subordinate strategies (with lower rankings) outperform the previously dominant strategies (with higher rankings) and now occupy the upper rankings. Although the previous analysis revealed no significant changes in key variables, it may be that the parameter changes nevertheless has an effect on ecosystem structure.

In this section, I analyze whether and how the ecosystem composition changes between the CTRL simulation and the alpha_2 simulation as an example here. I assess how the ecosystem structure changes for the top 10 strategies in a grid cell located in tropical Congo (0°N; 15°E, see location in Fig. 26 (a)) and a grid cell situated at the western Sahel (13.125°N; 8°E, see location in Fig. 27 (a)). These two locations are chosen to investigate the possible causes behind the significant climate change detected in the previous section, in which the western Sahel ecosystem experiences significant regional climate change and the Congo ecosystem does not.

In the Congo ecosystem, strategy #364 is the most dominant strategy, which ranks 1st in this Congo grid-cell in the CTRL simulation (Fig. 26 (b)). The biomass ranked 2nd and the 3rd strategies are strategy #358 and #377, respectively. Despite being the most dominant strategy, strategy #364 is not necessarily the most productive one. In fact, the 3rd ranking strategy (strategy #337) has higher GPP than #364 in all 12 months.

The 10 top ranked strategies in alpha_2 simulation differ from those of the CTRL simulation. Two out of the ten strategies listed in the CTRL simulation have drastic ranking changes. Strategy #364 is no longer the most dominant strategy and even drops out of the top 10. Strategy #244, which was not a member the top 10 strategies in the CTRL simulation, makes it to the 7th rank. The most dominant strategy is replaced by strategy #337 (the 2nd strategy in CTRL). Strategy #66 outperforms two strategies and now ranks 8th. An advancement in ranking suggests that a strategy performs better than the others under the

new parameter values.

For ease of comparison, I present how productivity looks in alpha_2 using the ranking from CTRL (Fig. 26 (d)). The productivity appears to be more variable for some of those strategies in the alpha_2 simulation. For instance, strategy #30 becomes more "seasonal" instead of being "evergreen" in the CTRL simulation. Strategy #364 shows no data (shown as a white stripe) because this strategy is dead. This implies that strategy #364 can not survive with the new parameter value ($\alpha = 0.6$) in the alpha_2 simulation.

In the western Sahel ecosystem, the change in ecosystem composition between the CTRL and the alpha_2 simulations is different from the situation in tropical Congo (Fig. 27): First, dead strategies still occupy ranking in the top 10. This happens because, although being dead, they are still present with their biomass and thus occupy space. Strategy #207 is dead but is still the 8th (Fig. 27 (b)). Strategies #153, #40, #207, #31 are dead but are still present under the top 10 (Fig. 27 (c)). Second, the ranking of the dead strategies is shuffled in the alpha_2 simulation. Strategy #31 is ranked before strategy#40 and #207 in the CTRL simulation but is ranked behind the two strategies in the alpha_2 simulation (comparing Fig. 27 (b) and (c)). The replacement of dead strategies is important to the ecosystem functions and this is discussed in detail in the discussions later.

In JeDi-BACH, the contribution of plant strategies to grid-cell wide fluxes is proportional to their biomass. The shuffling of dominant strategies and the fact that the ecosystem has the ability to replace the dead strategies is the reason why almost everywhere climate changes are insignificant. The Congo ecosystem experiences shuffling in the composition, but the consequent impact on regional climate is insignificant. As different strategies have different ecosystem functions, how they respond to environmental changes or to the parameter changes determines their survival. As a result, how ecosystems shuffle their composition is key to the ecosystem functions.

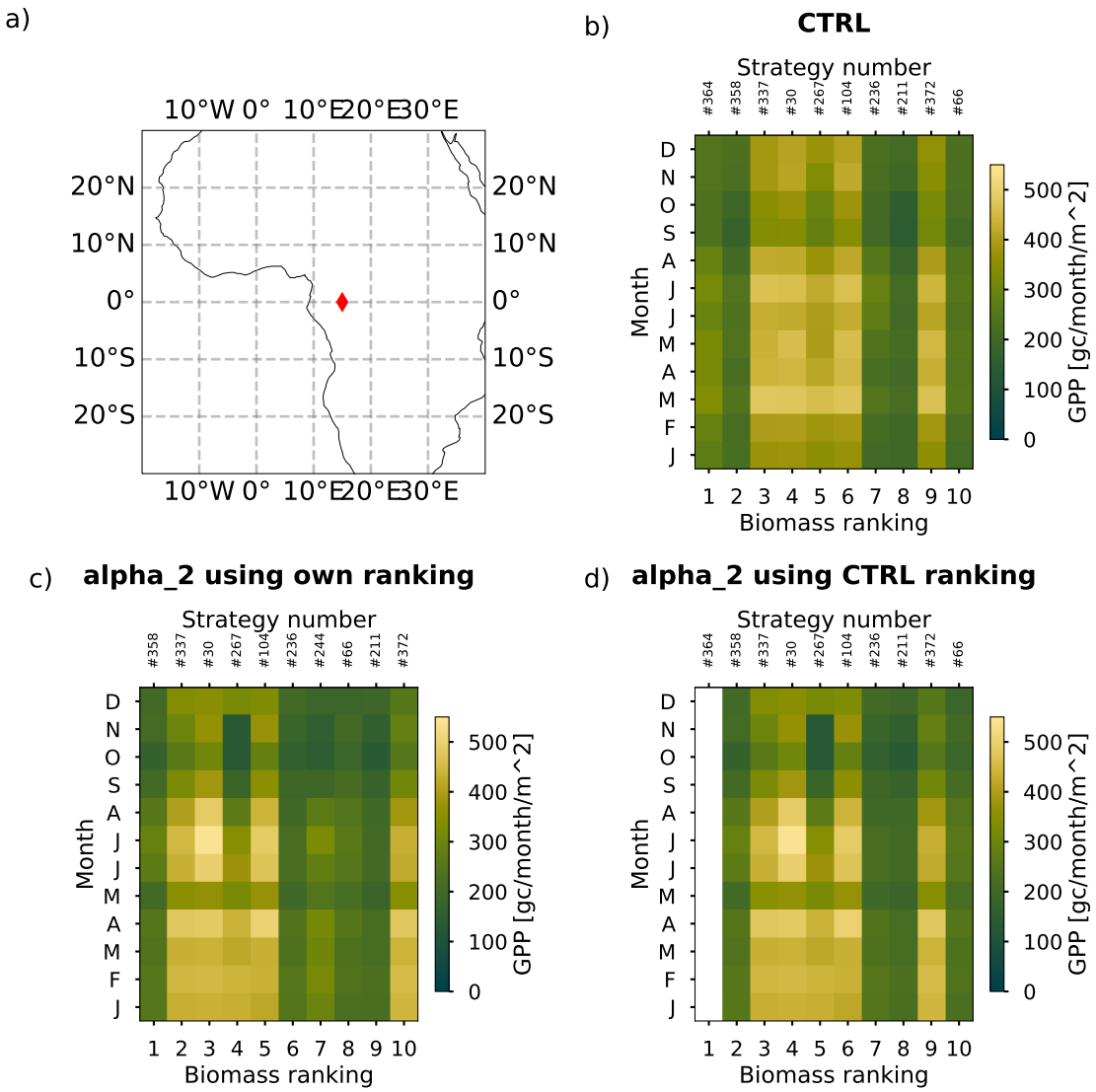

Figure 26: Comparison of biomass ranking in tropical Congo between CTRL and alpha_2 simulations. a) The location of the selected grid-cell (0°N; 15°E) is marked with a red diamond. The figures show the monthly GPP (gc/month/m^2) of the 10 top ranked strategies in the b) CTRL and c) alpha_2 simulations and d) the monthly GPP of the alpha_2 simulation using the same 10 strategies and ranking from the CTRL simulation. The x-axis shows the biomass ranking from 1 to 10. The y-axis indicates the time (month). The strategy labels corresponding to the rankings are shown on top. The colors indicate monthly GPP. For instance, strategy #364 is the most dominant strategy in the CTRL simulation, which ranks 1st in this Congo grid-cell.

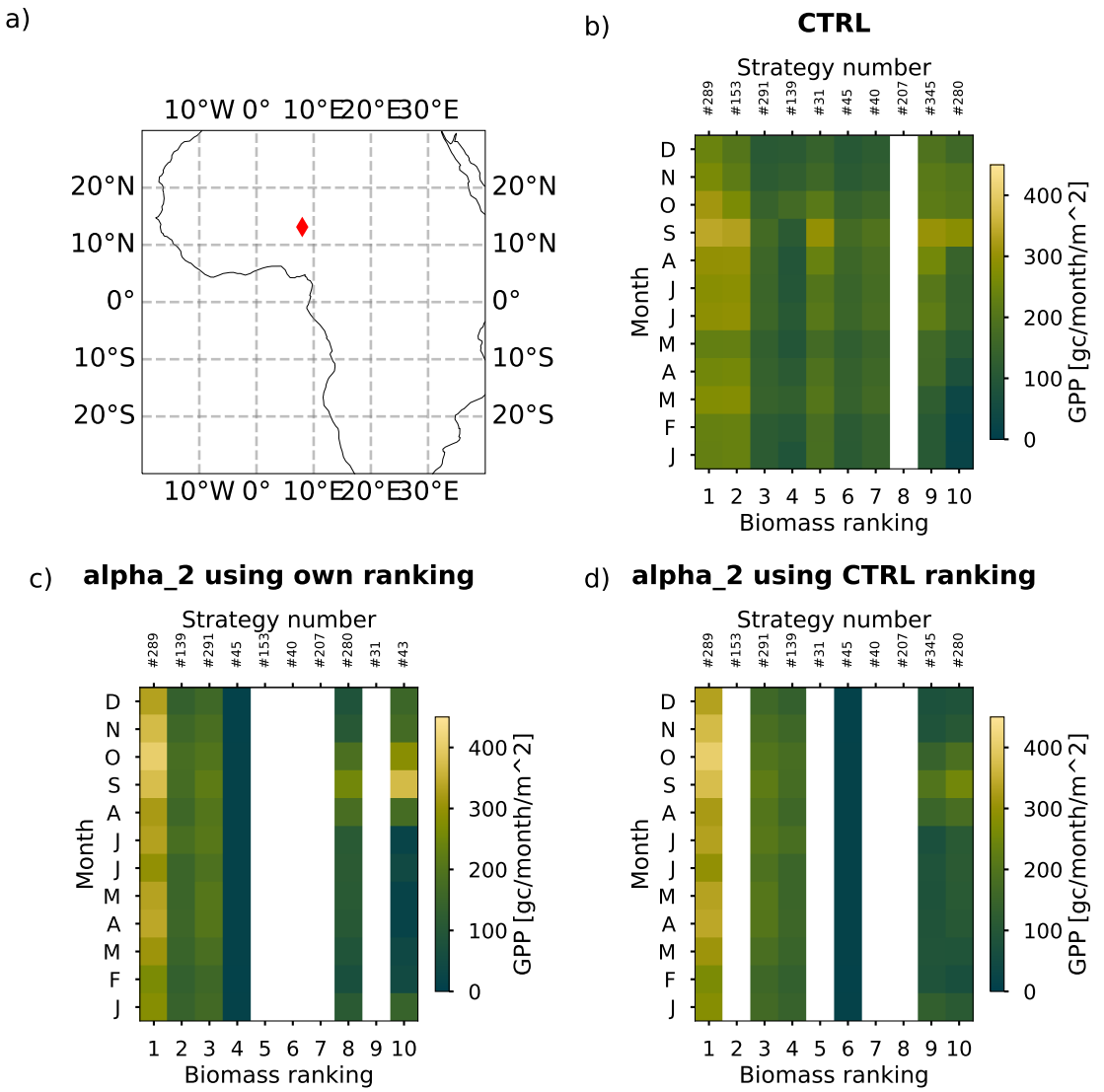

Figure 27: Comparison of biomass ranking in western Sahel between CTRL and alpha_2 simulations. a) The location of the selected grid-cell (13.125°N; 8°E) is marked with a red diamond. The figures show the monthly GPP (gc/month/m^2) of the10 top ranked strategies in the b) CTRL and c) alpha_2 simulations and d) the monthly GPP of the alpha_2 simulation using the same 10 strategies and ranking from the CTRL simulation. The x-axis shows the biomass ranking from 1 to 10. The y-axis indicates the time (month). The strategy labels corresponding to the rankings are shown on top. The colors indicate monthly GPP.

3.6.3 Discussion

In this section, I discuss how simulation results depend on the four parameters tested in my sensitivity analysis, and I assess how critical those parameters are to climate and ecosystem functioning. The parameter values were modified considerably to see whether model behaviour is sensitive to the modifications. If that is the case, these parameter values should be carefully chosen.

3.6.3.1 No proportionality between parameter changes and global NPP

To begin with, I find that the relative NPP change of the four parameters are rather small in comparison to the magnitudes of the parameter change on global scale (see Table 5). This implies that NPP is fairly robust on the global scale despite substantial parameter changes. However, the NPP change differs on the zonal scale. In the following, I discuss the causes for the zonal differences for each parameter.

The parameter α
In JeDi-BACH, the start/end of a growing season depends on the ambient temperature and the soil moisture (see Eq. (14)). The parameter α defines the minimum soil wetness for plants to grow. Thus one expects that a stricter threshold (meaning a higher α value) shortens growing seasons. In mid-latitude regions, the growing season is also thermally restricted. In both sensitivity experiments, the value of α is increased. Such high α values shortens the growing season further because plant strategies can only enter growing seasons when both temperature and soil moisture are larger than the given values, one of them being α. Thereby, at large threshold values, the growing season is so short that plants do not have enough time to develop leaves to assimilate carbon and may not be able to storage enough carbon for the cold seasons. This explains why in both simulations NPP is reduced. The reduction in NPP appears mainly in the extratropical region (30-60N and 30-60S), and more reduction is observed with increasing α as expected (Fig. 20 (a)).

However, on a global scale a threshold value of 0.5 (alpha_1) reduces global NPP by roughly 2% and a threshold value of 0.6 (alpha_2) reduces global NPP by 10% (as summarized in Table 5). These results suggest that the impact from a small change in α (from $\alpha = 0.4$ to $\alpha = 0.5$) is likely small, and a larger change ($\alpha > 0.5$) leads to a greater reduction in NPP.

Because the value of the relative soil wetness ranges between 0 (approaching wilting point) and 1 (approaching field capacity), it becomes unrealistic if α is

set too high. If α is too high, this means that only wet-climate adaptive strategies are simulated in the model. As a consequence, only wet regions in the world are colonized. While it is unrealistic to set $\alpha > 0.5$, the impact of varying α between 0.4-0.5 is small so that changes in α value can likely be disregarded.

Nevertheless, I argue that it is unrealistic to assign the same threshold value for all strategies in the model. In reality, different plants favor different types of soils and different soil wetness levels. Accordingly, α should be made as a random trait parameter in future model development.

The parameter `fapar`
The new `fapar` parameter serves to prevent overinvestment in plant growth. In JeDi-BACH, a reduction of the `fapar` value means that plant strategies slow down investing into new tissues earlier when light interception in leaf canopy approaches a state in which extra leaf growth gives no extra gain in productivity. Growing seasons in the tropics are mostly year-round if no dry seasons are present. Plants may overinvest to the point that carbon gain per unit new grown tissue is no longer optimal. Thereby, a reduction of the `fapar` value, as done in the sensitivity experiments, may particularly influence the tropics. An earlier slow down in investment can prevent wasting energy on maintaining useless tissues, and thereby plants receive more NPP. In line with the expectation, both sensitivity simulations show increased NPP mainly in the tropics (Fig. 20 (b)). At the global scale, the increase in NPP seems to stabilize roughly at around 5%. An increased reduction in `fapar` does not induce a proportional increase in NPP (see Table 5). These results suggest that a reduction in `fapar` may cause a 5% increase in global NPP.

The parameter Q10
Q10 describes the proportional change in maintenance respiration with a 10K increase in temperature. Due to this relationship (see eq. 39), a smaller Q10 value reduces the maintenance respiration (R_m) in warm regions and increases R_m in cold regions. Plants receive more NPP because less energy is used for R_m. Both sensitivity simulations show consistent behavior upon the applied reduction of Q10: an increase in tropics and a reduction in mid-latitudes (Fig. 20 (d)). However, the magnitude of changes in NPP is not linearly related to the change in Q10 values. The simulations Q10_1 and Q10_2 only show 9% and 12% increases in global NPP despite 20 and 40% decreases in Q10, respectively, with respect to CTRL (Table 5). This disproportionality implies that a reduction in Q10 causes the global ecosystems maximally a 10% difference in global NPP.

The parameter κ_{rd}
The conversion coefficient κ_{rd} is used to associate root carbon to root depth. The global root depth in the CTRL simulation is optimal because the environments have selected the best strategies after a long spin-up period. Therefore, modifying the κ_{rd} value yields a sudden decrease or increase in global root depth and correspondingly changes balance of the soil hydrology. Doubling the κ_{rd} value, which is the case of the rd_2 simulation, leads to a sudden deepening of global root depth. Consequently, such a substantial modification may largely influence the global ecosystems and climate. Contrary to expectation, there is no drastic global climate change observed in Fig. 21 (further details on global climate are discussed in the next section). This result suggests that most of the terrestrial climates are insensitive to changes in κ_{rd}.

However, one sees changes of NPP at the global scale, which may be the results of the expected changes in water stress (Fig. 20 (c)). One possible reason behind the global change is described as follows: As most regions show no significant change in precipitation (see Fig. 22 (g), (h)), the net water influx within the root zone, or more precisely – the total soil water available within the root zone, should be similar in all simulations. A sudden deepening of global root depth reduces the relative soil wetness as the same amount of soil water is distributed across a deeper root zone. This, in turn, leads to higher water stress and reduces global NPP. On the contrary, a shallower root depth (as in the case of the rd_1 simulation) increases the relative soil wetness. As a result, water stress is reduced and leads to an increase in global NPP. A consistent decrease in the zonal sum of NPP is observed in the rd_2 simulation, and an increase in NPP is observed in the rd_1 simulation. However, this is a rough speculation because it is based on the assumption that soil texture is uniform in the whole soil column. Changing the parameter κ_{rd} leads to different geographic responses as the global distribution of soil texture profile varies across the globe. Nevertheless, global NPP differs only roughly 10 to 13% despite substantial changes (a 50% increase/reduction) in κ_{rd} value. Such a small impact implies that global NPP, and likely other ecosystem functions, quickly adjust to new parameter values. This implies that the global ecosystems are likely doing something to adapt to the new parameters.

To briefly conclude, despite different degrees of NPP changes are observed at the zonal scale, the overall changes in global NPP are relatively small in comparison to the magnitude of parameter change. The magnitude of ecosystem response in NPP is not proportional to the relative change in parameter values. I suspect that such robustness seen in global NPP is likely due to the ecosystem resilience sustained by high plant diversity. Because of ecosystem resilience, the

ecosystems always find a new combination of optimal strategies that can provide a strategy with similar ecosystem functions against disturbances. To some extent, the sensitivity tests conducted in this section are similar to natural disturbances from an ecosystem's point of view. I suspect that as long as the plant diversity is high, the ecosystems will "self-organize" themselves and sort out once again the optimal combination of strategies that can provide ecosystem functions similar to before.

3.6.3.2 With high plant functional diversity, the global climate is robust to changing parameters

Many previous modeling studies have pointed out that regional climate is sensitive to changes in land surface characteristics (Groner et al., 2018; Winckler et al., 2019). If surface properties, such as albedo, roughness, or vegetation types, change, regional climate changes. Surprisingly, in my study, the large-scale climate is found to be quite robust to parameter changes, at least to the ones studied here. Regardless of the magnitudes of the parameter value changes, the zonal terrestrial precipitation and temperature of all the sensitivity simulations are almost identical to the CTRL simulation (Fig. 21 (a) and (b)). This finding is an indication that even if some of the plant parameters dealt with in JeDi-BACH are not entirely justified, it doesn't matter. The global climate is anyway rather insensitive. However, why can climate be insensitive to the tests conducted here? In terms of the magnitude of the changing parameters, global ecosystems experience a drastic change in their ecological processes and thus should lead to worldwide climate changes. Yet, model simulations demonstrate the opposite. The reason behind the robustness is likely related to ecosystem resilience given by high plant diversity. To elaborate on this point, I discuss the Congo ecosystem, a case that no significant climate change happened despite a shuffling in the ecosystem composition. Then I discuss the western Sahel regions, a case that statistically significant warming and drying are detected.

In the `alpha_2` simulation, where the threshold for entering a growing season is stricter ($\alpha = 0.6$), all plant growth strategies respond differently to this parameter change. Some strategies benefit from this new parameter value, and some do not. As not every strategy can perform better or as well as before ("before" means the situation in CTRL simulation), global ecosystems shuffle until a new equilibrium combination of (resource-optimal) strategies is achieved. In the Congo ecosystem, the shuffling of the 10 top strategies is rather small (compared to the western Sahel ecosystem). Only two out of the ten strategies experience drastic change in their rankings. One strategy is dead and one new strategy enters to the top 10. The others only shuffle between their raking.

In addition, no dead strategy occupies the top ranking. This implies that the Congo ecosystem manages to quickly replace the empty space released from the dead strategy by the subordinate strategy. I speculate that the ability of the Congo ecosystem to shuffle and re-organize its composition, namely ecosystem resilience, is strong so that there is no significant regional climate change.

The resilience of an ecosystem determines whether the ecosystem can recover after disturbances. In all experiments performed in this study, a change in parameter value is similar to a disturbance. For this reason, if some dominant strategies within an ecosystem fail to sustain themselves under the new parameter value, this ecosystem's ability to offer an alternative strategy (or a group of strategies) is critical to sustain ecosystem functions. Suppose this ecosystem cannot replace the dead dominant strategies with other strategies that provide similar plant functioning. In that case, the ecosystem functions will change, such as evapotranspiration, which will then lead to regional climate change.

In the western Sahel regions, both evapotranspiration (ET) (see Fig. 22(b)) and precipitation decrease in the $\mathtt{alpha}_2$ simulation. A reduction in ET implies that the local recycling of moisture is weakened. As depicted in Fig. 25 (see the size of the arrows), the reduction in ET is consistent with the region with a reduction in moisture transport: The regional moisture transport into the western Sahel region is less than in the CTRL simulation (bigger arrows). This moisture reduction is associated with a decrease in specific humidity (shown as red color in Fig. 25). In addition, this moisture reduction is not induced by changes of the West African monsoon: The water transport from the ocean remains roughly the same (small arrows near coastal western Africa). Therefore, the local reduction in moisture due to less ET weakens the moisture transport over the west Africa monsoon region. Such changes in local moisture recycling also induce temperature changes: with less ET, more of the heat flux in the surface energy balance is partitioned to the sensible heat flux, which then warms the surface. This is consistent with an increase in the surface temperature shown in Fig. 23. What then causes the local reduction in ET in the western Sahel?

In the western Sahel ecosystem, dead strategies can still occupy rankings in the top 10 (see Fig. 27 (c)). It may seem odd that a dead strategy can still occupy a ranking. The reason behind this is due to a memory considered in biomass-scaling in the model (see eq.43). This memory is introduced to simulate the natural removal of a dead plant: a decade of decaying time for a dead strategy to disappear from an ecosystem. A dead strategy slowly empties its space (dominance) for other strategies to replace it. For this reason, when strategies die out due to disturbances (e.g. extreme weather or a stricter growing condi-

tion in this case), the ecosystem needs time to replace the empty space with other surviving strategies slowly. Therefore, these dead strategies can still occupy a high biomass ranking for a while until a complete replacement. This is likely the case with strategy #153. Strategy #153 is the second dominant strategy in the CTRL simulation, but dies in the alpha_2 simulation. It is slowly replaced by the other surviving strategies so that its ranking descends. In this way, ecosystem functions may change due to the sudden death of the dominant strategies.

In addition, the ranking of the dead strategies shuffles in the alpha_2 simulation: comparing Fig. 27 (b) and (c), strategy #31 is ranked before strategy#40 and #207 in the CTRL simulation but is ranked behind the two strategies in alpha_2 simulation. This can happen either because of a switch in the ranking before either strategy dies or because of the difference in timing of death. The latter case may sound trivial. However, which strategies die and when do they die may be important to ecosystem resilience. For instance, if many dominant strategies die at the same time due to disturbances, the ecosystem will encounter a sudden reduction in transpiration. Such a case is likely to trigger a series of hydrological changes and induce local climate change. I suspect that the reduction in ET observed in the western Sahel region to some degree follows this hypothesis. Because many dominant strategies die due to the change in α, the dead strategies contribute to "no" transpiration. Therefore, the ecosystem functions (i.e., evapotranspiration) change, leading to regional climate change.

The replacement of the dead (and dominant) strategies reveals an important issue concerning the robustness of ecosystem function and climate: the history, the composition of the ecosystem, and the scales of change in the composition of ecosystem matter. Based on the results presented in this chapter, I suspect that when plant functional diversity in an ecosystem is high, ecosystem resilience is determined jointly by the ability of dominant strategies to respond to disturbance and how "insured" the ecosystem is to offer replacing strategies that can replace the previous ecosystem functioning. If the ecosystem can replace and provide a similar ecosystem functioning to the previous state, regional climate remains similar. If the ecosystem cannot sustain its ecosystem functioning, regional climate will change correspondingly. Such hypothesis has already been, to some extent, demonstrated by modeling studies (Winckler et al., 2019; Boysen et al., 2020). Global deforestation (meaning a complete wipeout of the dominant ecosystem) leads to both regional and remote climate changes. Nevertheless, to what extent a change in ecosystem functions can influence regional climate (destruction of ecosystem resilience) is beyond the scope of the

present study.

The connection between plant diversity and ecosystem resilience has drawn large attention in research communities (Cardinale et al., 2012; Díaz et al., 2016; Naeem and Li, 1997) and the global public. To this point, the simulation results discussed so far reveal the connection between diversity and resilience, and it is now possible to investigate this relationship using the new diversity model JeDi-BACH. In the next chapter, I investigate the impact of resilience and diversity in relation to climate.

3.6.3.3 Limitation on tuning

One last issue that emerges from the sensitivity analysis concerns the tuning of a model like JeDi-BACH. The goal of tuning a model is, hopefully, that, by adjusting some parameters in the model, the model results become closer to reality. Unfortunately, this is unlikely the case in JeDi-BACH. As mentioned at the end of the Section 3.6.1, the ideal way to tune and test the sensitivity of JeDi-BACH would be to always perform a complete new spin-up with the intended parameter value. However, I doubt that much can be concluded from simply modifying parameter values. The reason is that, as I repeatedly discuss in this section, the ecosystems will sort out another combination of optimal strategies for the new prescribed parameter value.

In the classic PFT-based ESMs, the ecological processes of a PFT are directly related to its trait parameters (which are often described by a static look-up table), so that tuning the trait parameter values can likely fit model results better to observations. However, the situation is different in the JeDi-modelling approach. It is impossible to establish an entire causal relationship between a parameter of ecological process(-es), the ecosystem functions, and its impact on the environment. That is because the composition and ecosystem functions are no longer prescribed by a few static plant types. JeDi-BACH simulates plant ecosystems that are in some way "self-organizing." The selection of survivors involves many levels of complexity so that no significant change in ecosystem functioning may occur despite a change in parameter values. A dominant strategy may die and be replaced by other subordinates in the system. It is impossible to manipulate the model parameter such that the ecosystem behaves in a particular way to favor one strategy over the others. Ecosystem resilience will likely attenuate any tuning in parameter values.

3.7 Summary of sensitivity studies

This section aimed at exploring the sensitivity of climate and ecosystem functions to changes in the not-so-well known values of four plant trait parameters of JeDi-BACH in a setup with an interactive atmosphere. As the terrestrial climate is sensitive to changes in land surface properties, it is crucial to know whether these four parameters are critical to model results. For this purpose, I conduct a series of sensitivity simulations where eight different parameter values were tested. I focus the analysis on the relative magnitude of global NPP changes and terrestrial climate changes in response to the various parameter values. I find that:

1 Ecosystem resilience is critical for sustaining robust ecosystem functions and regional climate.

As ecosystem resilience is associated with the actual plant diversity (the total number of survived strategies) in JeDi-BACH, the robustness of simulation results found here is most likely due to the fact that a high diversity level was simulated. In the $\mathtt{alpha}]_2$ sensitivity simulation, the Congo ecosystem manages to adapt to the new parameter so that no significant regional climate change is detected, whereas the western Sahel ecosystem fails to shuffle and replace the dead strategies and thus leads to reduction in local moisture cycling and the regional climate becomes drier and warmer.

In JeDi-BACH, the contribution of a strategy is proportional to its biomass. Strategies outperform others when they can optimize their growth better than others. Based on this kind of "self-organizing" feature, I find that the shuffling in the composition of the dominant growth strategies is critical for sustaining local ecosystem functioning. In particular, if an ecosystem encounters disturbances, the ability of offering strategies to replace the dead dominant strategies is critical. Based on these findings, I hypothesize that a low diversity world and a high diversity world shall respond differently to disturbance given to their different ability to recover. A high diversity world is likely more resilient to disturbances. I investigate the importance of biodiversity-resilience relationship for shaping climate in Chapter 4.

2 High diversity ecosystems behave differently concerning tuning as compared to PFT-based models.

Tuning a classic PFT-based model can be done by tweaking parameter values to fit model results to observations. However, tuning a system that is able to adjust on its own is likely useless, as in the case of JeDi-BACH. In this study, I find that climate is insensitive to any of the four chosen trait parameters regardless of the magnitudes of the parameter value changes. Such a model behaviour indicates that even if some of the plant parameters in JeDi-BACH are not entirely justified, it does not matter as long as the parameter values fall within a plausible range. High diversity ecosystems always self-organize to find another combination of optimal strategies for the new prescribed parameter value. Ecosystem resilience, to a considerable extent, diminish any "disturbance" in the system. In this regard, I conclude that tuning the model JeDi-BACH, by varying parameter values, is vain.

4

BIODIVERSITY-RESILIENCE RELATIONSHIP IN AN ABRUPT WARMING SCENARIO

4.1 Introduction

In ecology, biodiversity and stability have been a subject of significant debate. The definition of biodiversity varies across different studies, with contradicting definitions of "diversity" causing confusion and debate amongst ecologists (Huston, 1997). In recent years, ecologists have shifted their focus from "diversity" to a more precise field of "functional trait diversity." Functional trait diversity has been repeatedly claimed to be associated with ecosystem resilience (Mccann, 2000; Isbell et al., 2011b; Cadotte, Carscadden, and Mirotchnick, 2011; Isbell et al., 2015). Plant functional traits are defined as any morphological, physiological, phenological feature of an individual plant. Species with different functional traits offer different functional features so that the existence of a variety of species increases the number of functions within an ecosystem. Though there is a positive correlation between biodiversity and ecosystem functions, ecosystem functioning reaches an asymptotic level at a certain point despite the addition of further species to the pool (Cardinale et al., 2012). This asymptotic behavior is commonly associated with the so-called redundancy theory (Walker, 1992). In an ecosystem with functionally redundant species, those that share similar functions but with marginal differences, can likely buffer damages caused by the loss of individual species so that the ecosystem displays high resilience following disturbance. These redundant species serve as insurance in the system. This hypothesis has been repeatedly supported and evidenced by a large body of research and has been put forward to explain ecological resilience and stability (Biggs et al., 2020; Wang et al., 2019; Cardinale et al., 2012; Cardinale et al., 2006; Díaz et al., 2013; Díaz et al., 2016; Westoby and Wright, 2006; Isbell et al., 2015; Naeem and Li, 1997; Naeem, 1998).

In light of rapid loss in global biodiversity, one question emerges: how does loss in diversity impact ecosystem function and global climate? According to a study based on five decades of observations, central Amazon rainforest trees (with high species diversity) have an increasing mortality rate due to extreme events such as droughts, heat, storms, and extreme rainy years (Aleixo et al., 2019). Intuitively, climate change is predicted to cause higher tree mortality rates. Based on the biodiversity-resilience theory, one may ask: will a high diversity ecosystem be more resilient to climate change than a low diversity ecosystem?

To assess the impact of biodiversity loss on ecosystem functioning at a global scale, a modeling study is the most comprehensive, flexible, and, perhaps most importantly, the most cost-effective approach. However, the Earth System Modeling (or Dynamic Global Vegetation Modeling) communities have struggled to assess the role of plant diversity at a global scale in recent years. The essential issue is that the plant parametrization scheme commonly used in the models (the so-called PFT-approach) is not sufficient to perform biodiversity-related studies (Alton, 2011; Wullschleger et al., 2014; Kattge et al., 2007). Neither functional trait diversity nor adaptation is adequately treated in these models. More precisely, these models cannot capture the full potential of the flexibility, adaptability, or plasticity of an ecosystem. One shortcoming of missing these aspects is that these models may overestimate or underestimate the impact of biodiversity on climate or ecosystem functions when making future projections.

In the previous chapters, I introduce the new plant trait diversity model JeDi-BACH. The advantage of this model is that the ecosystem can re-organize its combination of plant strategies so that the ecosystems adapt to environmental change. I use JeDi-BACH coupled with the atmospheric model ICON-A to investigate the role of plant functional diversity in shaping global climate and ecosystem functioning. I identify that 1) a world with a high diversity level supports a more robust global climate and ecosystem functioning than a low diversity world and that 2) ecosystem resilience is critical for a robust sustenance of ecosystem functioning and for a stable regional climate. These findings reinforce the association between biodiversity and resilience, in line with the ecological theories on biodiversity. Based on these findings, this chapter aims to address how ecosystems with different diversity levels respond to a substantial disturbance on a global scale. Previous modeling studies lack a plant diversity component in their models, so these studies are often inadequate for considering ecosystem adaptation (Verheijen et al., 2013). The new plant diversity model JeDi-BACH therefore provides the first exploratory look into the relation between diversity and resilience. More precisely it tests the

hypothesis of whether a high diversity system is, as commonly assumed, associated with strong resilience and how resilience is realized in the system.

4.2 Experiment setup

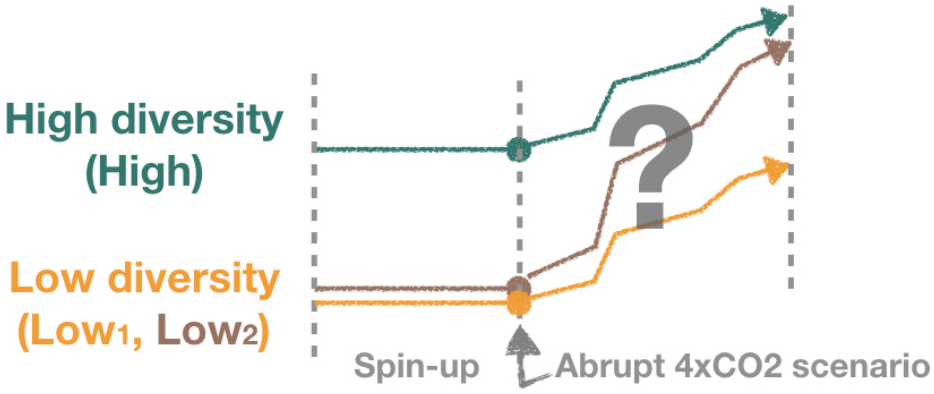

Figure 28: Diagram of $4xCO_2$ experiments

To test the aforementioned hypothesis about the diversity-resilience relationship, I conduct three experiments in the abrupt 4xCO2 warming scenario using JeDi-BACH. Hereafter, the term "disturbance" is used to refer to the sudden warming and increase in airborne CO_2 concentration. The term "disturbance" does not mean a short period of an extreme event. The "disturbance" imposed in my experiment setups (roughly an 8K increase in terrestrial temperature) causes a permanent change in the climate. Thereby, the "resilience" dealt with in this study only refers to "recovery": the degree of a system to recover a certain ecosystem process to the state before the disturbance.

Table 6 summarizes the simulations: the experiment High implies a high diversity world consisting of 400 sampled strategies. The other two experiments Low_1 and Low_2 are low diversity worlds consisting of 40 sampled strategies. An ensembles of two low diversity simulations is conducted to avoid bias at a low diversity level. Such a setup is chosen based on the outcome of Chapter 2: that climate and ecosystem functioning at a low diversity level are likely to differ more than at a high diversity level (see Fig. 7). As illustrated in Fig. 28, all these three experiments are conducted by first performing a spin-up. In this way, the biomass carbon pools and global climate are in equilibrium before the abrupt 4xCO2 scenario is applied. All simulations are conducted in an AMIP-type setup. The abrupt 4xCO2 scenario is realized in this setup by several simultaneous abrupt changes: the sea surface temperatures and the sea ice content are prescribed by the last 50-year (1990-2049) ICON model results from the experiment 4xCO2 of the CMIP6 common DECK experiments (Eyring et al., 2016) as well as the forcing of the greenhouse gasses, aerosols, and ozone concentrations. Additionally, no new strategy is allowed to appear after the abrupt

4xCO2 scenario, meaning that evolution is not considered. Therefore, global ecosystems in all three experiments need to deal with the abrupt warming with the existing set of strategies from their spin-up. In the following subsections, I investigate how ecosystems with different levels of diversity respond to the resulting sudden 5K global warming.

Experiment	Number of sampled strategies
High	400
Low_1	40
Low_2	40

Table 6: List of 4xCO_2 experiments at different diversity level.

4.3 Results

4.3.1 Response of terrestrial climate and ecosystem functioning

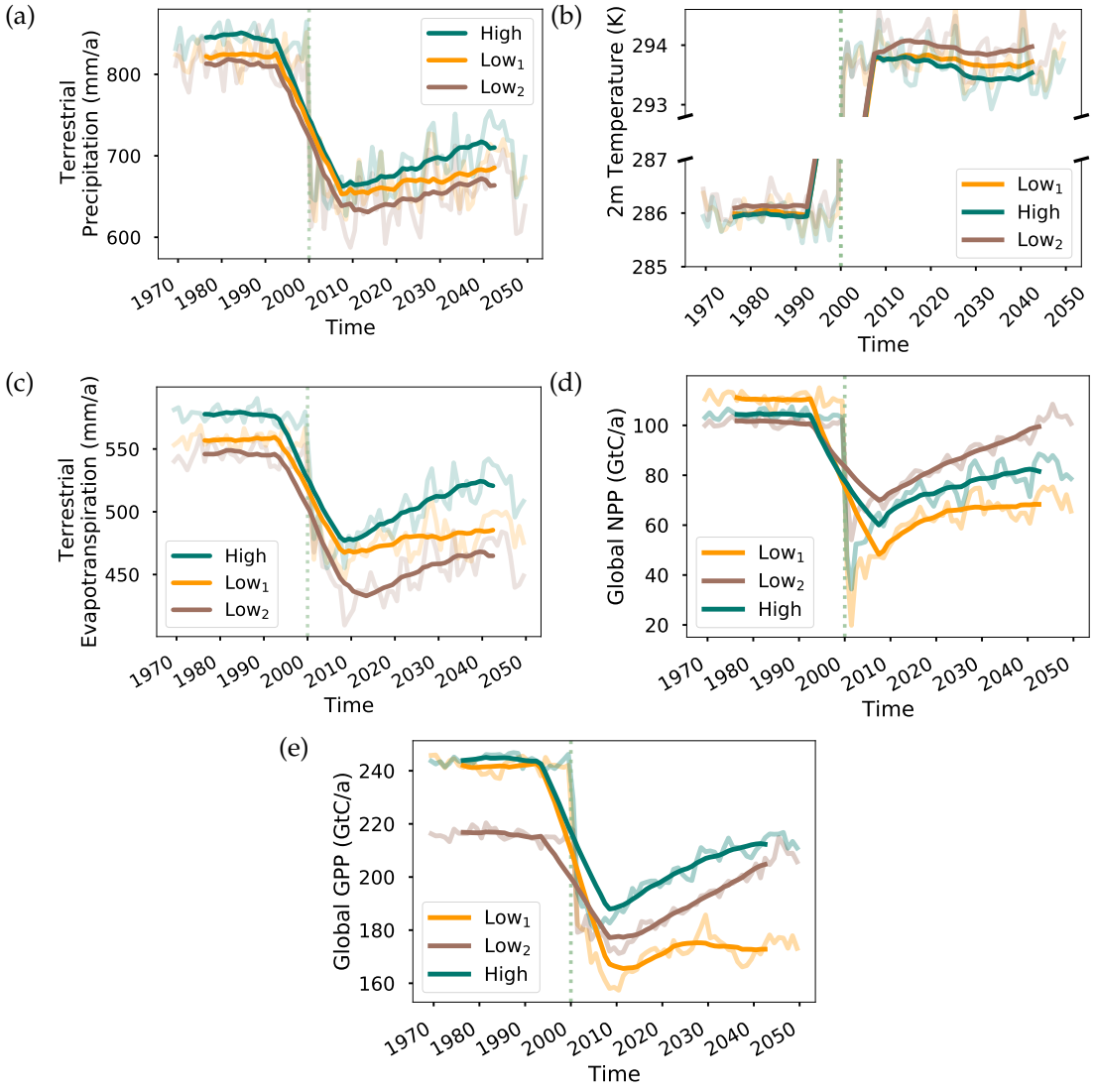

Figure 29: The development of terrestrial climate variables and ecosystem processes: (a) terrestrial mean precipitation (mm/a), (b) annual 2 meter air temperature, (c) evapotranspiration (mm/a), (d) net primary productivity (GtC/a), (e) gross primary productivity (GtC/a). The 15-year running means are shown in solid lines. The green/orange/brown lines respectively represent the experiment $\mathrm{High}/\mathrm{Low}_1/\mathrm{Low}_2$. The annual means of the respective simulations are shown in the lighter color lines.

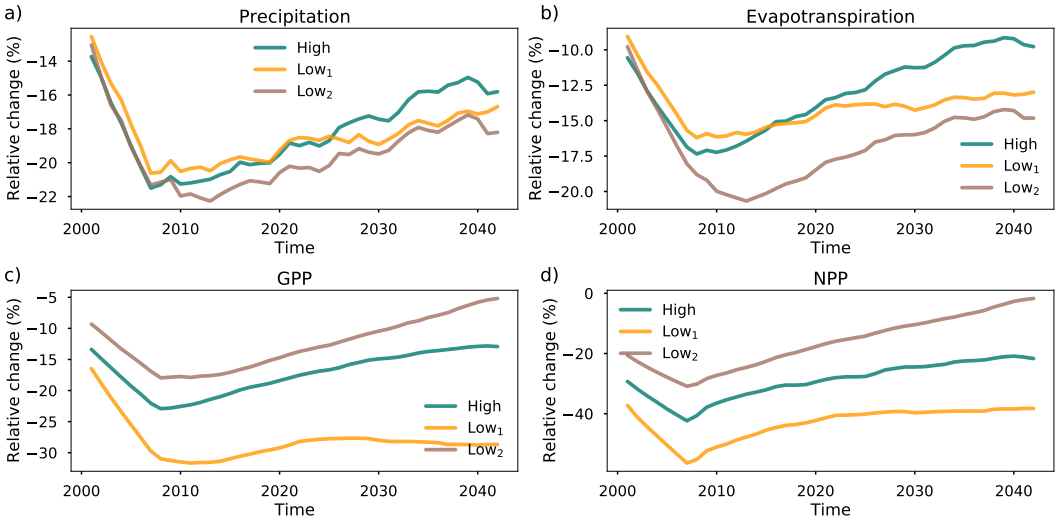

Figure 30: The relative change of (a) terrestrial mean precipitation, (b) evapotranspiration, (c) gross primary productivity, (d) net primary productivity in respect to the average over 1970-1999.

In general, all three experiments show a similar two-phases response to the abrupt disturbance (Fig. 29). For ease of discussion, I classify the two-phases response: first, a "shock phase" follows immediately after the disturbance. Second, an "adaptation phase" follows after the shock phase. During the shock phase, global climate and ecosystems undergo substantial change following the abrupt disturbance. Strategies that are not able to maintain themselves die out such that several ecosystems get substantially disrupted. The shock phase ends when the system reaches a minimum in the hydrological fluxes (precipitation and evapotranspiration; Fig. 29 (a) and (c)) and the in productivity (GPP and NPP; Fig. 29 (d) and (e)) and a maximum in terrestrial mean temperature. Afterwards, the adaptation phase starts. During the adaptation phase, ecosystems restore ecosystem functioning. The two phases in the three simulations are fairly similar in their overall timing, but their degree of change varies across the experiments. The shock phases of the experiments High and Low_1 occur roughly during the 2000s, and the adaptation phases start roughly from 2008 onward. The transition from the shock to adaptation phase in the experiment Low_2 occurs roughly five years later than it does in the other two simulations.

To compare across these different diversity levels, the recovery of a system is measured by comparing the current ecosystem functioning relative to the state before disturbance. The relative change of an ecosystem process or a climate

variable (χ) is calculated as

$$R(\chi) = \frac{\chi_{after} - \chi_{before}}{\chi_{before}},$$

where χ_{before} is the average of χ over the period 1970-1999, the 30-year mean before the disturbance. To smooth out inter-annual variability, χ_{after} is the 15-year running mean of variable χ. $R(\chi) < 0$ indicates a reduction in χ relative to the period before disturbance and $R(\chi) > 0$ implies a relative improvement. $R(\chi) = 0$ indicates that the system offers the same level of ecosystem functioning as before.

Terrestrial precipitation

All three simulations show a similar degree of reduction in terrestrial precipitation (P) during the 2000s (Fig. 29 (a)). But their degree of recovery in precipitation during the adaptation phase is different. The absolute reductions in precipitation are similar during the shock phase for all experiments. Terrestrial precipitation of the experiment $High/Low_1/Low_2$ decreases from roughly 849/822/818 mm/year to around 655/637/624 mm/year during the shock phase. Afterwards, the experiment High has the largest absolute increase in P during the adaptation phase. The precipitation of the experiment $High/Low_1/Low_2$ recovers to roughly 718/696/667 mm/year during the last 15 years of the adaptation phase.

The relative recovery of terrestrial precipitation reveals different degrees of changes among the three simulations (Fig. 30(a)). During the shock phase, the experiment Low_2 has the largest reduction in P. The experiments Low_1 and High have a similar degree of reduction in precipitation. During the adaptation phase, High shows the strongest recovery in P. The recovery in the experiment High quickly surpasses Low_1 at around 2025.

Terrestrial evapotranspiration

Terrestrial evapotranspiration (ET) is critical to regional climate as it controls the local water cycling. During the shock phase, the experiments High and Low_1 have similar degree of absolute reduction in ET and the experiment Low_2 experiences the largest reduction in ET (Fig. 29 (c)). Terrestrial ET of the experiment $High/Low_1/Low_2$ decreases from around 570/555/543 mm/year to the lowest value at around 465/459/433 mm/year during the shock phase and afterward recovers to roughly 512/488/457 mm/year in the last decade.

Among the three simulations, the experiment High has the strongest recovery in ET (Fig. 30 (b)), where ET recovers from roughly -16.8% to -8.4% within 40 years. Although the experiment Low_1 has the lowest reduction among the three, ET recovers only slightly from the lowest value -15.4% to -11.6% within 40 years during the adaptation phase. The experiment Low_2 experiences the largest reduction in ET and the recovery in Low_2 increases from -19.8% to -13.7% during the adaptation phase.

Terrestrial temperature

The response of the terrestrial temperature in all three simulations shows an abrupt increase immediately after 2000 followed by a slight reduction after 2010 (Fig. 29 (b)). The terrestrial temperature of the experiment High is always cooler than the other two low diversity simulations. The temperature in the high diversity world is cooler by about 0.07K than Low_1 and 0.16K cooler than Low_2 before the disturbance and becomes cooler respectively by 0.15 and 0.44K, respectively in the final 15 years of simulation (2035-2049). During the shock phases, the temperature differences between the experiment High and the other two are small. However, strong recovery in ET in the experiment High (Fig. 29 (c)) has led to a cooler climate towards the end of the adaptation phase so that the temperature difference between the High and the other two experiments is larger.

Global productivity

The response of the global productivity behaves differently to the hydrological fluxes (ET and P). The experiment Low_2 experiences the least reduction and the most vigorous recovery in both net primary productivity (NPP) and gross primary productivity (GPP) among the three (Fig. 29 (d) and (e)). GPP is reduced from about 215 to 180 GtC per year during the shock phase and recovers to 210 GtC per year during the adaptation phase. Likewise, the relative change in NPP and GPP recover to almost 0 and -5% respectively towards the end of the adaptation phase (Fig. 30 (c) and (d)), implying that global productivity recovers to almost the same level as before.

On the other hand, GPP in the experiment Low_1 decreases from roughly 240 to 160 GtC per year during the shock phase and recovers slightly, converging to 175 GtC per year afterwards. The relative change of GPP and NPP of the experiment Low_1 remains at around -28% and -40% after 2020. This implies that the global ecosystems in Low_1 are not as adaptive and productive to the new climate as compared to Low_2. The reduction of productivity in the experi-

ment High is relatively worse than Low_2 but better than Low_1. GPP and NPP reduce by roughly 20% and 30% during the shock phase and then both recover by around 10% (from -20% to -10% for GPP and from -30% to -20% for NPP) during the adaptation phase.

To summarize, none of the diversity worlds shows the best recovery in all ecosystem processes and climate aspects. However, the high diversity world is likely to have a more robust recovery in most aspects compared to the other two low diversity worlds. In particular, the high diversity world shows strong resilience in hydrological processes. Despite this, the experiment High and Low_1 experience similar levels of reduction in P and ET and an increase in temperature during the shock phase. The strong recovery of ET leads to a cooler climate in the experiment High than Low_1. However, low diversity does not necessarily mean worse resilience in all aspects. Although the experiment Low_2 has the most considerable reduction in hydrological processes (namely the degree of climate change is the largest in Low_2), the resilience in productivity is the strongest among the three experiments.

4.3.2 Regional response in tropical South America

To further investigate how the low and high diversity systems respond and resist disturbance at the local scale, the regional climate and ecosystems in tropical South America are analyzed as case-studies.

4.3.2.1 Precipitation regime

To assess the degree of climate change in each diversity world, the characteristics of annual precipitation are analyzed based on Konapala et al. (2020). Before the disturbance (first row in Fig. 31), the pattern of the precipitation regimes is fairly similar among the three experiments. This suggests that the ecosystems in tropical South America got adapted to similar precipitation characteristics among all diversity worlds. After the disturbance (second row in Fig. 31), the regime patterns of the three simulations differ considerably. The seasonal variation increases in regions from the northeastern coast towards regions inland, roughly parallel along the coasts. Regions on the northeastern coast of South America change either from H_pH_{ae} to H_pL_{ae} or H_pM_{ae} to M_pL_{ae}. The precipitation seasonality in these regions increases and the overall precipitation reduces substantially. The experiment $High$ has the smallest (area-wise) regime-changes among the three. The coastal region with H_pL_{ae} and M_pL_{ae} in the experiment Low_1 occupies more inland area than the experiment $High$. The experiment Low_2 has the largest regime change among the three. In particular, the region with H_pL_{ae} further expands to the central part of tropical South America. These results suggest that the high diversity world has much less regional climate change than the low diversity worlds, particularly in inland regions. The coastal climates are likely less dependent on the level of diversity because the meteorological conditions are strongly influenced by the oceanic conditions.

What is the cause behind the regime difference between the experiment Low_1 and Low_2? Why can ecosystems in the experiment Low_1 sustain a similar climate to the high diversity world but lose productivity? Why can ecosystems in the experiment Low_2 thrive even better despite substantial climate changes? To further assess these questions, two regional ecosystems at locations in the southern part of the Amazon are analyzed in more detail to investigate the mechanisms behind the change in the precipitation regimes.

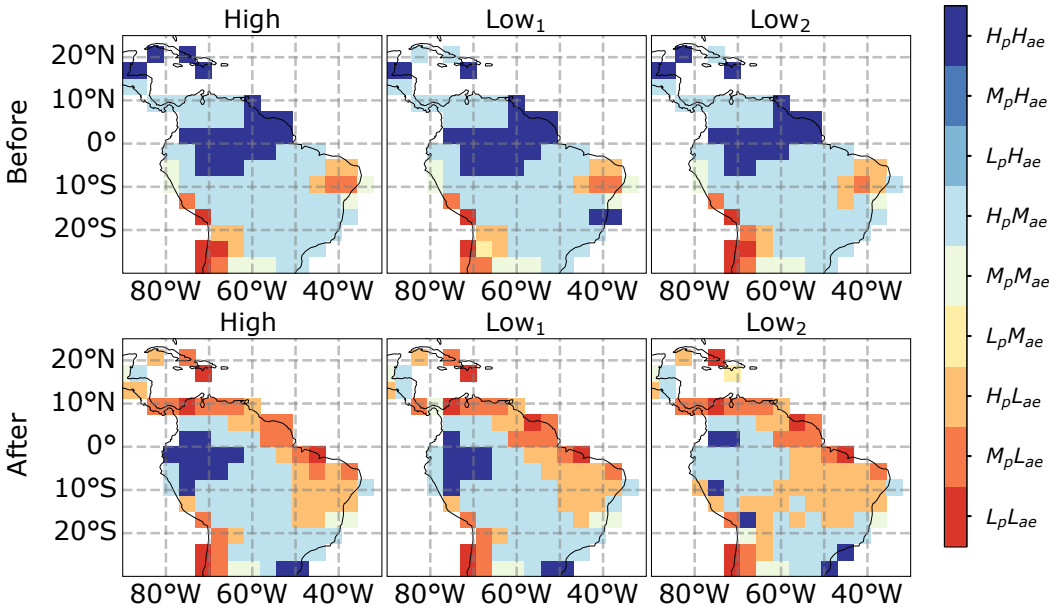

Figure 31: Comparison of the precipitation regime in tropical South America for two periods, before and after disturbance. The apportionment entropy (AE) is used to estimate the strength of seasonal variation of precipitation (see method in Konapala et al. (2020)). Lower AE values indicate higher seasonal variation, and higher AE values imply lower seasonal variation. Two aspects of precipitation, the annual precipitation and the seasonal variation (as defined by AE), are used together to characterize the precipitation regime. The terrestrial regions are classified into nine regimes based on the precipitation percentile thresholds (the 30th and the 70th percentiles). Values less than the 30th percentile are classified as low (L); values between the 30th and the 70th percentiles are moderate (M) and values greater than the 70th percentile are high (H). Upper row: mean precipitation regime before disturbance (1969-1999). For instance, a region with high annual precipitation and low seasonality is classified as H_pH_{ae}. H_p represents high precipitation. H_{ae} indicates high AE value and implies low seasonal variation. Likewise, a region with low annual precipitation and high seasonality is classified as L_pL_{ae}. Lower row: the last 15-year mean precipitation regime after disturbance (2035-2049). Panels present from left to right: the experiment High, Low_1, and Low_2.

4.3.2.2 Survival ratio

To estimate the response of ecosystems after abrupt disturbance, the survival ratio in tropical South America is analyzed. The central tropical South America loses about 30-50 % of its strategies in the low diversity worlds and roughly 20-30 % in the high diversity world (Fig. 32). These results suggest that extinction risks are much lower in ecosystems with high diversity then with low diversity.

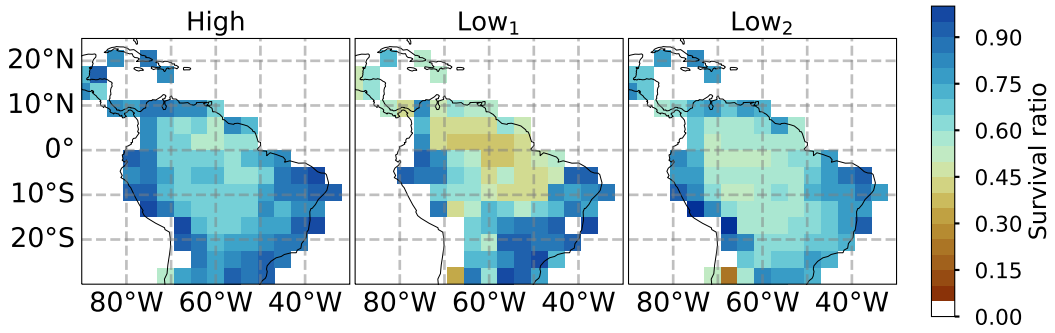

Figure 32: The survival ratio in tropical South America. White color implies total extinction. The survival ratio is calculated as the total number of surviving strategies in 2049 over the total number in 1999. Values close to 1 imply that most of the strategies in an ecosystem survive the disturbance. In contrast, values close to 0 indicate that most strategies that are alive before the disturbance die out towards the end of the simulation.

The ecosystems close to the Andes largely die out in all simulations. In particular, the experiment Low_1 shows a complete extinction near the Andes (shown as white color in Fig. 32), where none of the strategies survives the disturbance. Similarly, the experiment Low_2 also displays extinction in a few ecosystems near the Andes, whereas the experiment High still has a small portion of the ecosystems that survive.

The low survival ratio in the low diversity ecosystems is likely related to the regional precipitation regime change. Plant strategies die if they fail to sustain themselves when regional climate changes. The regions with a low survival ratio approximately correspond to the regions that experience changes in their precipitation regime (see comparison between Fig.31 and Fig. 32). Among the three simulations, the experiment High shows the highest survival ratio and has the smallest area with precipitation regime change. The link between the degree of regime change and the level of diversity may imply that the high diversity ecosystem can, to a certain degree, resist regional climate change.

4.3.2.3 Development of climate and ecosystems in a coastal and an inland region

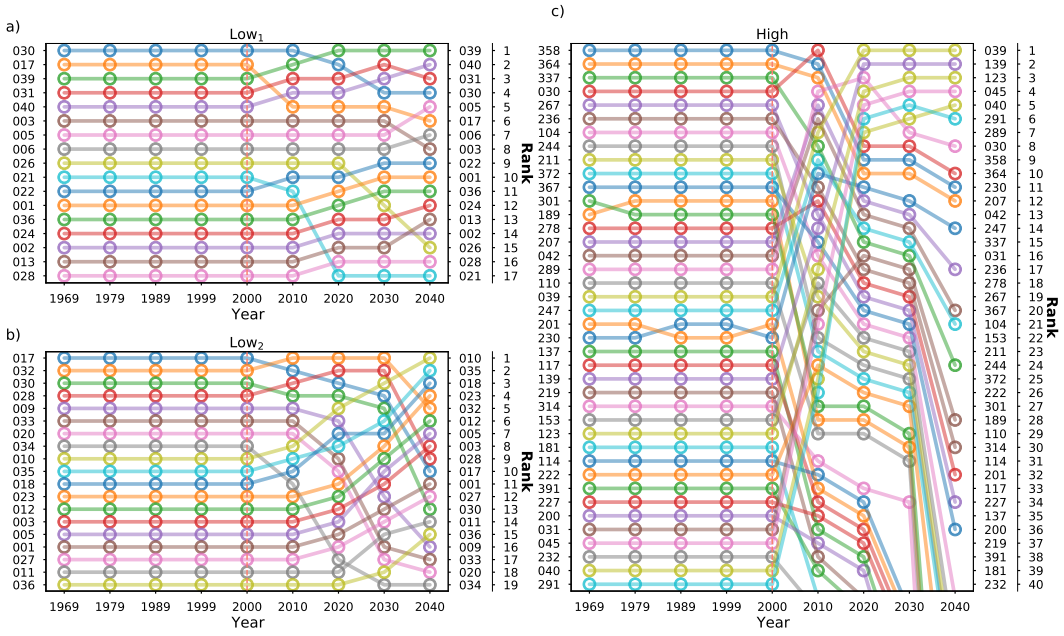

Figure 33: Development of ecosystem composition of the top ranking strategies in experiment a) Low_1, b) Low_2, and c) High at an inland ecosystem (located at 13.125S, 63.75W). The numbers listed on the left-axis represent the strategies in the respective experiment. The ranking (implying their dominance) descends from the top to the bottom of the figure. The space shown in the experiment High represents the strategies not listed in the top 40 before 2000.

As mentioned in section 4.3.2.1, the coastal regions are less dependent on the level of diversity because the environmental conditions are strongly pinned to oceanic condition, whereas inland ecosystems may modify regional climate. Two regional ecosystems, one inland and one coastal ecosystem, located in the southern Amazon are analyzed here to investigate how the regional climate and ecosystem processes are related to the ecosystems.

In JeDi-BACH, the ranking of the strategies in an ecosystem is based on their biomass (see Chapter 2.4 for details). Basically, strategies with larger biomass have greater dominance and therefore occupy the upper rankings. Fig. 33 shows the evolution of dominant strategies throughout the whole experiment period. There is barely any shuffling in the ranking before the disturbance. From 2000 on, individual strategies start to die out following the disturbance so one sees that the rankings in the ecosystems start to shuffle.

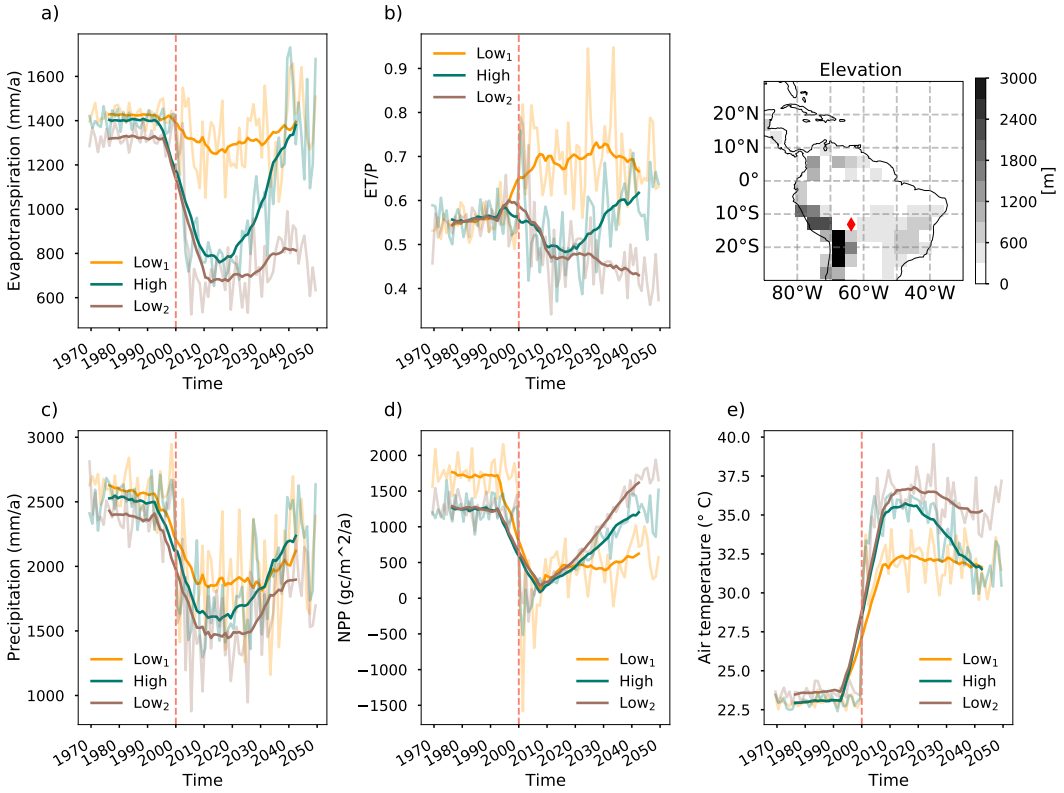

Figure 34: The response of ecosystem processes and climate variables at an inland ecosystem located at 13.125S; 63.75W (marked by a red diamond on the map). a) the annual evapotranspiration (mm/a), b) the mean annual ET-ratio relates evapotranspiration (ET) to precipitation rates, c) the annual mean precipitation (mm/a), d) the net primary productivity (gc/a), e) annual mean temperature (°C).

Among the three ecosystems, the ecosystem in the experiment Low_1 shows only minor shuffling in the top ranking strategies after disturbance (Fig. 33(a)). The top 5 dominant strategies from before 2000 (#030, #017, #039, #031 and #040) are reshuffled among themselves such that the top 5 strategies in 2040 remain almost the same. This stability in strategies implies that the ecosystem did not undergo serious adaptation despite sudden warming. The ecosystem survives and continues to live almost unchanged under the new scenario. This rather unchanged state of the ecosystem implies that the recovery of ecosystem functioning is likely weak or even missing if the dominant strategies can keep up their ecosystem processes after the disturbance. In contrast, the shuffling of the dominant strategies is more active and vigorous in the experiments High and Low_2. The experiment High experiences the strongest shuffling in its ecosystem composition. Such a strong shuffling in the ranking of the top dominant strategies implies that the ecosystem is re-organizing in its ecosystem composition.

This kind of adaptation is critical for the continued functioning of ecosystems under disturbances. In other words, having the ability to re-organize the composition allows the ecosystem to find a new combination of dominant strategies that may be able to cope with the new environment better than before. It should be noted that an ecosystem being capable of shuffling implies that it is not only passively adapting to the new environment, conversely this ecosystem is also influencing the environment.

Coinciding with the weak shuffling, the experiment Low_1 has relatively weak recovery (a weak recovery can be observed as an "L-shape" recovery in the plots, such as in Fig. 34 (d)) in most of the ecosystem processes and climate variables. NPP reduces from 1800 to nearly 200 $\frac{gc}{m^2 a}$ during the shock phase and only recovers to approximately 500 $\frac{gc}{m^2 a}$ in the last decade (Fig. 34 (d)). Since it is the composition of the top dominant strategies that primarily contributes to ecosystem functioning, minimal shuffling in an ecosystem implies that ecosystem functioning is controlled after the shock by the same dominant strategies. Although most of the ecosystem processes in Low_1 show only weak recovery, the ecosystem in Low_1, by chance, assures a good level of ET that is pretty comparable to the level before. Such robust water recycling via ET leads to a relatively small reduction in precipitation and only about 7°C increase in temperature as compared to the other two simulations. Accordingly, this ecosystem manages to sustain the precipitation with moderate seasonality ($H_p M_{ae}$, see Fig. 31.

In the case of an active re-organization, as observed in the experiment Low_2, the ecosystem shuffles to recover productivity. Despite strong climate change (roughly a 13°C increase in the air temperature and almost a 50 % reduction in ET), there is a strongly recovery in NPP after the disturbance and even exceeds the previous level. Such strong recovery in NPP in Low_2 can be observed as a "V-shape" recovery (Fig. 34 (d)). These results suggest that the ecosystem in the experiment Low_2 re-organizes and obtains a new ecosystem composition with higher productivity (than before the disturbance) despite a hot and highly seasonal precipitation regime ($H_p L_{ae}$, see Fig. 31).

Lastly, the experiment High experiences a strong recovery in all ecosystem processes and climate variables. The strong shuffling during the adaptation phase, as observed in Fig. 33 (c), leads to strong recovery in the water recycling process and NPP. In addition, in a secondary effect, the recovery of ET also leads to a decrease in temperature during the adaptation phase (from about 36°C to 32°C).

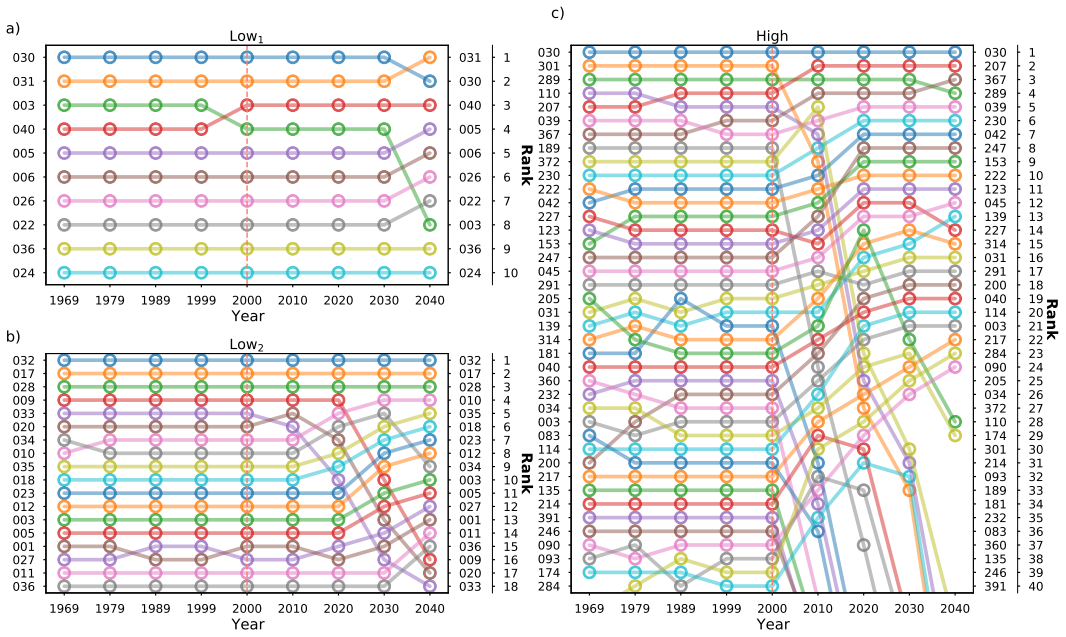

Figure 35: Development of the ecosystem composition of the top ranking strategies in experiment a) Low_1, b) Low_2, and c) High at an inland ecosystem located at 13.125S, 41.25W (marked by a red diamond on the map). The numbers listed on the left-axis represent the strategies in the respective experiment. The ranking (implying their dominance) descends from the top to the bottom of the figure. The space shown in the experiment High represents the strategies not listed in the top 40 before 2000.

Unlike the inland ecosystems, the coastal ecosystems (located at 13.125°S; 41.25°W) have somewhat similar responses among the three experiments. The shuffling in coastal ecosystem is minor compared to the inland ecosystem. Most top-ranking strategies survive and remain the dominant strategies despite disturbance (Fig. 35). This suggests that the ecosystems did not need to shuffle their ecosystem to adapt. The same combination of strategies still offers a similar degree of water and carbon turnover despite a few degrees of warming. The ecosystem processes and climate variables among the three ecosystems show no obvious breakdown-and-recovery response in any of the ecosystems and processes (Fig. 36). Their climate and ecosystem functioning responses are generally similar in timing and the degree of changes (see the end points in all three simulations). The coastal climate experiences less "shock" (~ 3.5K increase in temperature vs. 10K) as compared to the inland climate. This is because that the coastal climate is strongly influenced by the ocean, coastal ecosystems cannot modify environmental conditions. Therefore, one sees that there is more shuffling inland than at coastal sites.

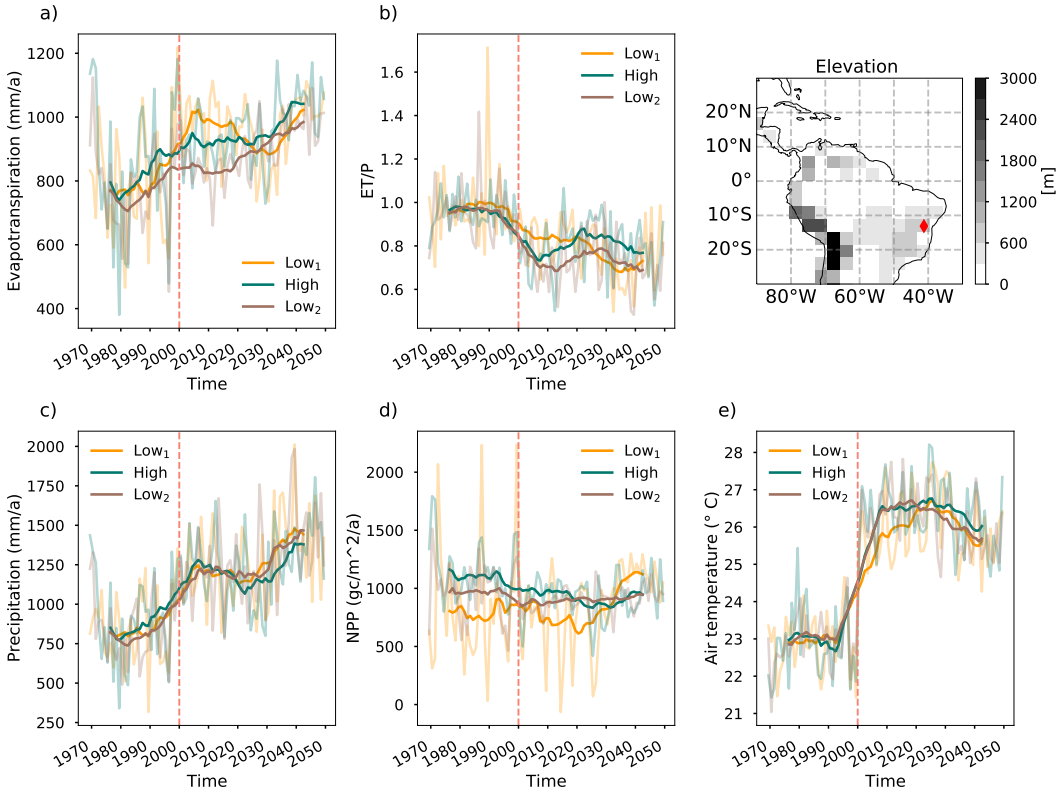

Figure 36: The response of ecosystem processes and climate variables located at a coastal ecosystem (located at 13.125S; 41.25W). a) the annual evapotranspiration (mm/a), b) the mean annual ET-ratio relates evapotranspiration (ET) to precipitation rates, c) the annual mean precipitation (mm/a), d) the net primary productivity (gc/a), e) annual mean temperature (°C).

4.4 Discussion

Regarding the biodiversity-resilience relationship, high functional diversity system is commonly associated with strong resilience. In the following, I discuss whether such a hypothesis is consistent with the results using JeDi-BACH and how ecosystem resilience is related to regional climate.

Inland climate and ecosystems are more sensitive to the level of diversity.

Compared to inland ecosystems, in coastal regions the responses of ecosystem processes and the climate are less sensitive to the diversity level of the ecosystems (Fig. 34 and Fig. 36). For instance, the air temperature only increases by about 3°C in coastal ecosystems, whereas the temperature increment increases by more than 10 °C inland after the disturbance. Such contrast between a coastal and an inland ecosystem can be attributed to different meteorological characteristics; essentially, how different moisture sources influence the regions. The climate near the coastal regions is dominated by the land-sea breeze system, whereas for the inland climate, water recycling via evapotranspiration is important. Therefore, in inland regions, the ability to sustain a good level of evapotranspiration is critical to the change in precipitation regime. For instance, the experiments High and Low_1 show no change in precipitation regime according to the hydrological classification of Konapala et al. (2020) (see Fig. 31) in the inland ecosystem (at 13.125°S; 63.75°W), being both classified as high precipitation with moderate seasonality (H_pM_{ae}). In contrast, the regime changes from high precipitation with moderate seasonality (H_pM_{ae}) to high precipitation with large seasonality (H_pL_{ae}) in Low_2. Therefore, the level of diversity is especially critical to inland climate and ecosystem processes.

To further elaborate on this point, one can see that the final states of climate and ecosystem processes differ largely among the three simulations at the inland site. The air temperatures inland can differ up to 4K in the last decade among the three simulations. Evapotranspiration differs up to about 600 mm/year, which is of similar magnitude as the evapotraspiration of the lowest ecosystem itself (800 mm/year for Low_2). On the contrary, the ecosystems in a coastal region shows no apparent difference in climate and ecosystem processes in its response to disturbance across different diversity levels. Such a difference between diversity levels among coastal and inland sites imply that the potential for ecosystems to buffer regional climate change varies substantially not only among different ecosystems but also at different locations. The difference in their resilience can lead to more substantial difference inland as different ecosystems take different advantage of this potential.

A high diversity system is more likely to offer strong resilience, whereas the risk for a low diversity system to fail is likely but not necessarily high.

To begin with, it is essential to understand what "resilience" means in this study. In a real-world scenario, a thriving ecosystem tends to increase the efficiency for capturing biologically essential resources so that it is insured against periods of unfavourable environmental conditions. Intuitively, the resilience of a system refers to the ability of a system to resist disturbance and recover after disturbance. Simply put, when a system can restore a disrupted process entirely to the same as before, this system has a strong resilience, and weak it it cannot. However, the term "resilience" is vague and possibly provides a wrong impression in this study. The "disturbance" treated in this study is not a temporary extreme event but a scenario that will certainly modify global climate permanently after disturbance. Therefore, despite the ecosystems' ability to buffer part of climate change they will not stop climate change and the climate can never recover to its previous state. For instance, a global average of 5K warming due to prescribed boundary conditions (SSTs) can never be reverted. Thereby, the "resilience" discussed here refers to the degree to which an ecosystem can recover a specific ecosystem process with respect to to the level before the abrupt disturbance. Looking more closely, the resilience of an ecosystem is determined by its adaptability in the form of shuffling its ecosystem composition (see Fig. 33), i.e. an ecosystem re-organizes its composition during the adaptation phase to cope with the new environmental conditions during recovery. It is important to note that adaptation does not mean that the ecosystem only passively responds to disturbance; this ecosystem also modifies the ambient climate. This implies that there might be a secondary effect to the system coming from adaptation (e.g., a milder climate change).

From the simulation results, both global climate and ecosystems experience a substantial shock phase among all simulations regardless of their plant diversity level though the adaptation does not appear in all ecosystems. Out of the three experiments, ecosystems with high diversity are more capable of restoring ecosystem processes than the low diversity ones. The strong recovery shown in ecosystem processes and climate appears both at the global and regional scale (see V-shape recovery in Fig. 34 and Fig. 30). This suggests that a high diversity world's risk of encountering a complete disruption in ecosystem processes is likely small. However, an ecosystem with low diversity does not necessarily imply a weak resilience after disturbance. For instance, although the experiment Low_2 barely recovers the hydrological fluxes, strong recovery in NPP still occurred (see Fig. 30 (c), (d), and Fig. 34(d)). These results are consistent with the general theory of the biodiversity-resilience relationship:

> *"Biodiversity increases the stability of ecosystem functions through time. ... there is no theoretical reason to believe that biodiversity should enhance all forms of stability (Consensus two, Cardinale et al. (2012).)"*

What determines ecosystems' degree of recovery? An ecosystem's ability to recover depends not just on the number of plant strategies. It also depends on the "insurance" of the system. It depends on the particular characteristics of the dominant strategies and the kind of strategies waiting in the reservoir that can potentially replace and outperform the previous dominant strategies once disturbances empty the niche. The resilience of a system is critically dependent on:

1. whether the dominant strategies are capable of resisting disturbance OR
2. whether the ecosystem has the adaptability to re-organize and obtain a new combination of strategies that can provide similar ecosystem functioning as before.

The first situation describes the case of experiment Low_1. There, the global ecosystems experience smaller increase in temperature during the shock phase (see Fig. 29 (b) and Fig. 34 (e)) because those strategies that survive the disturbance are always the dominant strategies. There are not enough subordinate strategies (in the sense of competitors) being able to outcompete the dominant strategies (see Fig. 33 (a)). By chance, these dominant strategies happen to be capable of sustaining a similar level of ET to that seen previously, so that Low_1 experiences the mildest change in climate during the shock phase. However, those dominant strategies are not as productive as before in the new climate, so the ecosystem can only partly recover NPP.

The second situation describes the experiments High and Low_2. The global ecosystems in High re-organize and obtain new combinations of strategies with strong carbon fluxes and hydrological fluxes (see Fig. 30). This is simply because ecosystems with high diversity have more potential (due to more sampled strategies) to contain strategies that favor a warm (after shock) climate. In addition, the adaptability of a high diversity system is likely to contribute to feedback on climate. Due to the high potential for shuffling, the ecosystem will select those strategies with good productivity and those with good accessibility to soil water. When more strategies that are capable of assuring good accessibility to soil water dominate the ecosystem, they contribute to strong evapotranspiration. Robust water recycling then cools the climate. This hypothesis is consistent with the cooling observed in the adaptation phase in Fig. 29(b)

and Fig. 34(e).

However, despite that the ecosystem in the experiment Low_2 also undergoes some degree of shuffling (see Fig. 34(b)), and that the new dominant strategies obtain good productivity, the new ecosystem could not recover evapotranspiration during the shuffling. Obviously, by chance the set of subordinate strategies contains some with a high water use efficiency such that NPP after shock becomes even larger than in the experiment High.

From these discussions, it is becoming clear that the level of functional diversity in some sense determines the coverage of their "insurance." High functional diversity is likely to have a higher potential to adapt. High potential implies that more ecosystem processes are "insured", or protected. But it should be noted that an ecosystem with low diversity does not necessarily mean a weak recovery. On the one hand, it is possible that the system does not need to recover if the dominant strategies can resist disturbances. This system is at least "safe" with respect to the shock considered here. On the other hand, a low diversity system can still recover ecosystem processes as long as this system, by chance, has strategies that can cope with the new environmental conditions. Nevertheless, a low diversity system's risk of failing is generally higher than for a high diversity system.

In the long run, ecosystems with high plant diversity are likely to persist.

One argument for such speculation originates from one of the consensuses on biodiversity and ecosystem functioning relationship summarized as:

> *The impact of biodiversity on any single ecosystem process is nonlinear and saturating, such that change accelerates as biodiversity loss increases. ... implying that initial losses of biodiversity in diverse ecosystems have relatively small impacts on ecosystem functions, but increasing losses lead to accelerating rates of change. (consensus three, Cardinale et al. (2012))*

The experiment results presented in this study, to some degree, support this relationship. In the results, most tropical South American ecosystems in the high diversity world manage to keep 70-80 percent of their number of strategies survived despite the sudden disturbance. In contrast, more than half of the ecosystems die out in low diversity worlds (Fig. 32). The sudden warming leads to considerable disruption in many ecosystem processes in the low diversity worlds. The losses in biodiversity lead to irreversible damage to their ecosystem adaptability. The abrupt warming imposed on the low diversity world possibly

wipes out an extensive amount of strategies so that the low diversity ecosystems do not have enough strategies to recover the ecosystem processes fully.

On the contrary, ecosystems with high functional diversity offer strong recovery in many ecosystem processes as many strategies wait in the reservoir. I speculate that a high diversity system can lower the risk of a massive die out in the system by mitigating regional climate. For instance, the high diversity system manages to cool the local climate via a strong recovery in evapotranspiration (see a 4 °C reduction during the adaptation phase in Fig. 34(e)). Such a cooling effect may be critical to strategies on the edge of dying from abrupt warming. The individual strategies and the ecosystem thrives on keeping the environment at a not-so-deadly level. I speculate that ecosystems with high functional diversity are likely to persist in the long run as there are still plenty of subordinate strategies waiting in the pool. Low diversity ecosystem may face extinction once various extreme events continue to occur and wipe out more and more strategies.

4.5 Conclusions and summary

This chapter explores how different plant diversity levels respond to a sudden warming scenario. As high functional diversity is commonly associated with high ecosystem resilience, I investigate whether such generality is also captured in the plant diversity model JeDi-BACH. In particular, the experiments are conducted in a coupled setup with the atmospheric model to see how important plant functional diversity is for shaping climate on the global scale. Based on the analysis of the three diversity experiments, I find that:

1 A high diversity system is more likely to show strong resilience[1] against disturbance due to high adaptability, whereas a low diversity system is likely to be more vulnerable to disturbance.

What I find in this study is that high diversity systems are associated with strong resilience in most ecosystem processes. This outcome is consistent with the empirical generality about the biodiversity-resilience relationship that high biodiversity is associated with high resilience or stability (Cardinale et al., 2012). However, strong resilience does not imply that high diversity should enhance all forms of stability and always have stronger resilience than a low diversity system. Instead, a low diversity system can, by chance, display strong recovery in a few ecosystem processes. A low diversity system can still adapt via shuffling (as in the case of experiment Low$_2$) and a low diversity system can still, by chance, simply survive through the disturbance with only one or a few robust strategies (as in the case of experiment Low$_1$). Nevertheless, a low diversity system is likely to be more vulnerable to disturbance and more susceptible to irrecoverable disruption once all strategies are wiped out from the system.

2 A high diversity system may, to some extent, be able to resist regional climate change.

One novelty of the present study stems from the features of the new plant functional diversity model JeDi-BACH, where ecosystems are modeled in a way that ecosystems can self-organize. Such a shuffling process in the ecosystem composition allows ecosystems to not only constantly adapt to, but also influence the environment. This feature of JeDi-BACH allows, for the first time,

1 The definition of resilience is defined in the sense of relative recovery as explained in Section 4.2

to investigate the roles of plant trait diversity in shaping climate and ecosystem functioning on a global scale. However, due to the limited number of simulations conducted in this study, it is not possible to draw statistical conclusions about the relationship between plant diversity and climate change. Nevertheless, the results across the three simulations hint at potential links to the resistance to regional climate change. First, the contrasting results on the inland and the coastal ecosystem imply that the level of diversity is critical to the regional climate in inland ecosystems. In particular, whether an ecosystem is capable of restoring the evapotranspiration can mediate local temperature by several degrees (e.g., the inland ecosystem is able to cool the climate by 4 °C in the experiment High, see Fig. 34(e)). Second, the terrestrial climate in a high diversity world remains always cooler and wetter than in other low diversity worlds despite the same warming scenario (boundary conditions). I speculate that a high diversity world is more capable of maximizing water turnover than the low diversity world. Therefore, the chance is likely higher for a high diversity world to resist drought or changes in precipitation regime (e.g., as clearly demonstrated in Fig. 31).

3 The adaptability of an ecosystem, through ecosystem shuffling, is critical to the recovery of ecosystem functioning.

From the experiments conducted in this study, I identify how resilience is associated with the level of diversity. As high diversity ecosystems have many different strategies, the possibility of finding an optimal combination of strategies that can keep water (or carbon) turnover high is likely to be high. Therefore, a high diversity system is typically strongly resilient so that strong recoveries (V-shape or U-shape recovery) in many ecosystem processes are likely to be achieved. Similarly, because low diversity systems have fewer strategies than high diversity ones, the likelihood for finding an optimal combination of strategies to strongly recover in all ecosystem processes is more unlikely, and therefore, a weak recovery (an L-shape recovery) is more likely to happen.

5

SUMMARY AND DISCUSSION

At the beginning of this dissertation, I identified the current challenges in investigating the importance of plant functional diversity on global climate and ecosystems for modeling studies. The classic plant functional type (PFT) approach commonly embedded in the Earth System Models is insufficient to explore the full potential of ecosystem complexity. I began by creating the new diversity model JeDi-BACH based on the so-called JeDi-approach (JeDi) (Kleidon and Mooney, 2000) into an Earth System Model to tackle these issues. With this new model, I could investigate the impact of plant functional diversity on climate in a coupled setup with the atmosphere model ICON-A. Later on, I explored the different aspects of plant functional diversity under various scenarios using JeDi-BACH in a coupled setup. In the following, I summarize the outcomes from these chapters and place them within a general scientific context at the end.

5.1 The new plant functional diversity model JeDi-BACH

In Chapter 2, I described the implementation of a new prototype of the JeDi modeling approach into the land component model JSBACH of the ICON-ESM based on the previous model JeDi-DGVM (Pavlick et al., 2013; Kleidon and Mooney, 2000) and constructed the new plant functional trade-off model called JeDi-BACH. I replaced the traditional PFT-approach used in JSBACH with several functional trade-off relationships. The goal was to create an ecosystem that acts more vividly and ecologically so that an ecosystem can adapt to the environment. The backbone of JeDi is to mimic how environments filter out species. The mechanism behind the selection for adaptive plant strategies is through several plant functional trade-off relationships related to the environmental conditions, plants' biochemical properties, the leaf economic spectrum relationship, and plant allometry. Having all these relationships established, JeDi first randomly generates many different plant growth strategies and potentially allows them to grow everywhere on land. Then, the environmental conditions filter out the survivors from different climates. In this way, terrestrial ecosystems

are represented by a richer set of growth strategies tailored to the respective environments by mechanistic trade-off selections via environmental filtering without many static empirical decisions underlying a PFT-approach.

Furthermore, while transferring the JeDi concept into JSBACH, I implemented several new features into JeDi-BACH to improve some plant functional aspects of the original plant functional trade-off relationships introduced by Kleidon and Mooney (2000); Pavlick et al. (2013). First, I adjusted several calculations that are decisive to the plant's growing season length to depend more on the environmental conditions (see Box1 in Chapter 2). Second, I replaced the function of fine roots in the original JeDi-approach by a new relationship that takes the soil wetness, the surface air humidity, and the root-shoot ratio into account (see Box2 in Chapter 2). In this way, I fixed the issue in the original formulation that produces "superspecies" that can easily outcompete other plants in securing soil water without much costs. Third, I added code to represent a structural difference between tree-like and grass-like strategies that were not considered in previous JeDi-series models (Chapter 2.2.4). Last, I coupled the model JeDi-BACH to the atmospheric model ICON-A. With this model setup, I assessed in subsequent parts of the study how different plant diversity levels affect climate and ecosystem functioning via vegetation-climate interactions.

5.2 Assessment of JeDi-BACH and the effect of biodiversity in shaping a robust climate

In Chapter 3, I assessed two different aspects of plant functional diversity using JeDi-BACH in a coupled setup with the atmospheric model ICON-A. First, I investigated the relationship between plant functional diversity in shaping global climate-vegetation systems (Chapter 3.5). Afterward, I investigated the robustness of simulation results obtained with JeDi-BACH concerning plant trait parameters (Chapter 3.6). In the first part, I focused on how different levels of diversity influence global climate and ecosystem functioning. In doing so, I found the following answers to my research questions:

> [1a] **What is the role of plant functional diversity in shaping the global climate-vegetation systems?**
> I found that global and regional climate and ecosystem functioning converge with increasing diversity towards well defined states. Global and regional climate and ecosystem processes become almost identical between high diversity worlds. This implies that in a world with high functional diversity climate and ecosystem functioning are likely to be more robust than in a low diversity world.

> In addition, I found that with increasing diversity the global climate is shifting towards a high water-cycling state . There seems to be a "plant diversity-climate feedback" that shifts both global and regional climate towards a cooler and wetter state with increasing diversity. This indicates that global ecosystems tend to exploit maximally environmental conditions (resources) as diversity increases. This new finding would not have been possible without such a model like JeDi-BACH whrere biodiversity has been represented explicitly. Accordingly, such a "biodiversity-climate feedback" has never been reported in previous PFT-based modeling studies focusing on vegetation-climate interactions.
>
> In this regard, I speculate that the high sensitivity to land-surface characteristics reported in PFT-based modeling studies likely stems from the poor representation of ecosystem complexity in the PFT-approach (Groner et al., 2018; Betts et al., 2004; Cox et al., 2004; Huntingford et al., 2008). Simply put, the PFT-approach cannot explore the full range of interactions between climate and resources.

The observed convergence of ecosystem functioning with diversity (see Fig. 7) agrees with the biodiversity-ecosystem functioning relationship obtained in field experiments (Cardinale et al., 2012). These simulation outcomes set the groundwork for the topic of the diversity-resilience relationship that I went on to investigate. Based on the outcomes from [1a], I further assessed the robustness of JeDi-BACH in a high diversity world. I investigated how sensitive the model results are to some trait-related parameters (see table 4 for the chosen parameters). I chose four parameters whose values were not properly justified during the development of JeDi-BACH. I performed a series of sensitivity simulations, modifying only one parameter value in each simulation. I then compared the results to a control simulation to investigate how much each parameter value changed the simulation results. I asked the question:

> [1b] **How does global climate depend on the treatment of certain plant trait representations?**
>
> Surprisingly, I found that global climate is robust to changes in all four of the chosen parameters; barely any terrestrial regions show significant climate change in the model simulations. Although global productivity shows slightly different changes among the model simulations, the relative changes in productivity are generally small compared to the magnitude of the parameter changes. The reason

> behind this robustness turned out to be that high diversity ecosystems have strong adaptability. In comparing the ecosystem composition of one Congo and one western Sahel ecosystem, I found that the ecosystem's ability to replace the top dominant strategies that die from disturbance quickly is critical to ecosystem functioning. No considerable disruption to the ecosystem process is observed in the Congo ecosystem (Fig. 26) because the ecosystem manages to replace the dead strategy quickly. In contrast, substantial disruption to the ecosystem process occurs in the western Sahel ecosystem because many dead strategies remain dominant and contribute nothing to the ecosystem process (shown as white space in Fig. 27). Ecosystem resilience, or adaptability, is critical for sustaining robust ecosystem functions and regional climate. This is attained in a high diversity system.

I conclude that although the four parameters tested in this study were not fully justified in JeDi-BACH, they do not significantly impact global climate. This means that the highly functionally diverse world simulated in JeDi-BACH responds differently to model tuning than a PFT-based model. If ecosystems can adapt, they are likely more resilient to disturbance. I speculate that the high sensitivity in global climate to vegetation characteristics found in previous PFT-based studies may partly be because the PFT-approach vastly underestimates and simplifies ecosystem complexity. The PFT-approach cannot explore the full potential of diversity-climate interactions as much as JeDi-BACH allows.

To this point, I have demonstrated that diversity levels are obviously critical to ecosystem stability. High diversity ecosystems tend to enhance the water-cycling, which pushes the global climate into a wetter and cooler state. High diversity ecosystems turned out to be strongly resilient against parameter changes (similar to disturbances). All these findings support the strong link between plant functional diversity and ecosystem resilience that aligns with general biological theory on biodiversity: a more diverse community is likely more adept at capturing resources and has more stable biomass production (Cardinale et al., 2012). I proceeded to investigate how ecosystems with different diversity respond to an abrupt warming scenario and how diversity is related to resilience in ecosystems.

5.3 Resilience of different diversity systems under an abrupt warming scenario

In Chapter 4, I investigated how different ecosystems with different diversity may respond to a sudden warming scenario. The redundancy hypothesis (Walker, 1992) suggests that ecosystems that consist of many functionally redundant species can likely buffer damages caused by the loss of individual species. Ecosystems can resist disturbances as they might be able to find a replacement species to restore against the damage. Based on this theory, a high diversity system is likely to demonstrate strong resilience to disturbance, and a low diversity system may be at a higher risk of irreversible disruption. I conducted three simulations with one high and two low diversity worlds to test this. I posed the question:

> [2] **How does a different level of plant diversity influence ecosystem resilience to drastic climate change?**
>
> In line with general expectations on the role of biodiversity, I found that a high diversity system is more likely to show strong resilience against disturbance and to recover several ecosystem processes due to its high adaptability. However, I found that a low diversity system can in certain cases, by chance, also resist disturbance. A low diversity system may happen to be "prepared" to resist a particular disturbance and be "insured" by replacement strategies to adapt to this particular disturbance although not necessarily to another kind of disturbance. Accordingly, a low diversity system's risk of failing is likely, but not necessarily, high.
>
> A high diversity world is more capable of keeping the water cycle in a high-turnover state than a low diversity world and thereby exploit environmental conditions more effectively. As a consequence, having strong adaptability can, to some extent, resist regional climate change so that a high diversity world has a greater chance at withstanding drought or changes in the precipitation regime.

I also found two other important aspects associated with the diversity-resilience relationship. First, I found that the adaptability of an ecosystem, through ecosystem shuffling, is critical to the recovery of ecosystem functioning. The adaptability in an ecosystem is realized by shuffling its composition. How an ecosystem re-organizes its composition to find a new resource-optimal set of strategies with similar ecosystem functions (e.g., evapotranspiration) is critical to the stability of the regional climate. Second, I found that different ecosystems have different adaptability at different locations. Because the land-sea breeze system

near the coast strongly imprints the meteorological conditions, the influence of different diversity levels on coastal climate is small. In contrast, the levels of plant diversity and their adaptability can considerably influence regional climate inland. These two findings are evident in the response of an inland Amazon ecosystem after disturbance. The high diversity ecosystem inland can recover evapotranspiration after the shock phase and cools the regional warming by almost 4K (see Fig. 34(e)).

5.4 Conclusions on the importance of plant trait diversity on climate from simulations using JeDi-BACH

One of the grand challenges in the modeling community for plant ecology and climate science is to understand how vegetation and climate interact and to predict changes in ecosystems following climate shifts while they are constantly growing, dying, reproducing, and interacting with each other. To answer this question, scientists select and parameterize some climate-relevant plant processes essential to their study interests in Earth System Models (ESMs), also known as climate models. Many studies using ESMs have investigated the importance of vegetation on global energy, water, and momentum with the atmosphere via biogeochemical and biogeophysical processes regarding several key processes (see e.g., Brovkin et al. (2009); Bonan (2008); Claussen, Brovkin, and Ganopolski (2001)). However, barely any study has tried to investigate the role of diversity on climate because the sub-scale processes in ecosystems were largely ignored. This gap originates from the PFT-approach. Due to computational limitations, climate models have since the 1980s used simplified representations of global vegetation and considered and simulated only the key processes relevant to climate. Parametrization is a straightforward, simple, and intuitive way to obtain general estimates of global vegetation processes. However, the PFT-approach has its limit. The field ecology community has pointed out that there is greater variation within a PFT than between PFTs for many plant traits (Pappas, Fatichi, and Burlando, 2014; Kattge et al., 2020). Building complex ecological relations on top of the PFT-approach is getting more complicated, and it is easy to lose track of what happens in a natural ecosystem (i.e, Verheijen et al. (2013) tried to implement trait variation into PFTs but they missed realistic traits and trade-off relationships in their modeling approach).

With more global field observations on plant traits available in recent years (Kattge et al., 2020), ecological modeling communities have started to shift the modeling focus to a more complex functional trait-based approach for sim-

ulating ecosystem diversity (Pavlick et al., 2013; Scheiter, Langan, and Higgins, 2013; Sakschewski et al., 2016). In contrast, although the advancement in computational resources in the past few decades has allowed for more complex processes to be resolved in every aspect of the climate system, simulations still need to be computationally feasible. As a result, ESMs still rely on the PFT-approach. The potential risks are that climate models may under-/overestimate the impact of plant diversity when producing future projections (Fisher and Koven, 2020). The approach largely ignores that ecosystem adaptability may contribute to climate and ecosystem stability. Similarly, in offline trait-based vegetation models vegetation only passively responds to climate. Offline models are at risk of missing the potential impacts of global vegetation on climate because vegetation-climate interactions are ignored. This can lead to an inaccurate prediction on the response of global vegetation. For instance, many studies have shown that offline vegetation models overestimate the frequency and severity of drought when predicting future climate change (Swann, 2018; Berg and Sheffield, 2018; Greve, Roderick, and Seneviratne, 2016). Obviously, the gaps for both offline and coupled modeling types can lead to great uncertainty when predicting how global vegetation and climate interact. At the current speed of biodiversity loss, it is pressing to investigate the role of plant functional diversity on global climate and ecosystems. In this dissertation, I responded to this need by constructing a new plant diversity model based on a new modeling concept that revolves around plant functional traits and trade-off relationships. JeDi-BACH is the first plant functional trait diversity model that can couple with an atmospheric model. This new tool was developed to study several topics on plant functional trait diversity and its impact on global climate and ecosystems. In the following, I place my findings within a general scientific context and discuss the potential shortcomings of my study at the end.

As I concluded from my study of the role of diversity on shaping robust global climate (Chapter 3.5.1), there is a plant functional diversity-climate feedback in the climate system that can modify global and regional climate and ecosystem functioning substantially. I found that vegetation-climate interactions move towards a high water-cycling state with increasing diversity. Because there are more resource-optimal strategies to survive in a high diversity world, regional and global climate become more robust. This is because that a high diversity ecosystem tends to exploit all resources provided by the environmental conditions. These outcomes from my modeling study are in line with the biodiversity-ecosystem functioning relationship found in field measurements (Cardinale et al., 2012). This consistency brings us to an important aspect of a high diversity ecosystem: the redundancy theory (Walker, 1992). A high diversity system contains many redundant strategies and this redundancy

is key to ecosystem stability, such that a highly diverse system is likely to be strongly resilient. Consistently with what the theory hypothesizes, I found that the ecosystem's adaptability for recovering ecosystem processes is decisive to how changes in terrestrial ecosystems can impact climate in my model simulations. Here, I give an example of how a high diversity system shows strong resilience in model simulations.

To begin with, evapotranspiration is known to be critical to the regional water cycling process and regional climate. Based on observational estimates, terrestrial evapotranspiration returns about 60% of land precipitation, (Oki and Kanae, 2006) and transpiration contributes about 80–90% of terrestrial evapotranspiration (Jasechko et al., 2013). As I found in Chapter 4, high diversity ecosystems display strong resilience in evapotranspiration after the substantial disruption following abrupt warming. The inland high diversity Amazon ecosystem manages to recover its evapotranspiration and thereby mediate regional temperature by 4K, whereas the low diversity ecosystems show a reduction of only 1K or less. Because the high diversity world shows strong resilience in evapotranspiration, it experiences the smallest changes (area-wise) in the precipitation regime in tropical South America than the two low diversity worlds.

Evidently, ecosystems with different diversity can result in different regional climate changes following disturbance depending on how well they recover evapotranspiration. Because ecosystems with high diversity are likely to recover evapotranspiration, I found that they can resist regional climate change to a certain degree. Moreover, I found that a high diversity system has a higher survival ratio than a low diversity one. Based on this result, I speculate that a high diversity system can to a certain degree "protect" itself against extinction by keeping the environmental conditions in a favorable range as a secondary effect.

After gaining a general understanding of plant functional diversity, I proceeded to ask the questions: what is the mechanism behind ecosystem resilience? How do ecosystems achieve resilience? In Chapter 4, I found that ecosystem adaptation is realized in JeDi-BACH in the form of ecosystem shuffling. Because JeDi-BACH simulates global ecosystems in a way that they self-organize in response to environmental conditions, plant strategies will constantly compete to gain dominance, so that the ecosystem as a whole will adapt to environmental changes. In this regard, I found that the adaptability of an ecosystem is determined by how well it is "insured" by its backup strategies. Intuitively, one might assume that a high diversity system should be more resilient than a low diversity one. The modeling results in Chapter 4 show consistently strong re-

silience in many ecosystem processes and climate variables in the high diversity system. However, I found that a low diversity system is likely, **but not necessarily**, only weakly resilient. An ecosystem's resilience is determined by whether an ecosystem, at the time of disturbance, is prepared with strategies that are either robust enough to resist the particular disturbance or is equipped with subordinate strategies that can replace the dead dominant strategies. Hence, by change, also a low diversity system can resist a disturbance or adapt to it.

Therefore, my modeling results reinforce the general importance of biodiversity: there is a general tendency for biodiversity to increase the stability of ecosystem functions, but it does not mean that biodiversity enhances all forms of stability (Cardinale et al., 2012). Nevertheless, I found that a few ecosystems in the Andes are wiped out in the low diversity simulations (see Fig. 32). Based on this result, I speculate that the risk of a low-diversity system to fail (in maintaining ecosystem functioning and resisting regional climate change) is likely higher than in a high diversity one, and that a low diversity system is at a higher risk of extinction if various kinds of disturbance occur (e.g., wildfire, windstorm, drought, and etc).

I would like to emphasize one thing before drawing conclusions for a high diversity system: although a high diversity system is likely strongly resilient, this does not imply that the system remains unchanged at all times in all aspects. In contrast, a high diversity system may go through a phase of reshuffling to find a new combination of strategies so that ecosystem functioning or regional climate may change due to reorganization associated with a phase of low productivity. Precisely because a high diversity system has the potential to shuffle, the ecosystem keeps shuffling its composition until the best combination is reached, so it can exploit the resources better. Such behavior is evident as a "V-shape" recovery in ecosystem functioning in Fig. 34. Though I cannot give statistical evidence on how resilient a high diversity system is to climate change, I have discussed and demonstrated that different diversity systems influence regional climate or ecosystem stability differently.

I close my study with some qualitative evidence gathered from each Chapter. As I demonstrated in my investigation of parameter sensitivity in view of plant diversity (Chapter 3.5.1), the ensemble spread of terrestrial and regional climate differences is considerably larger for low diversity systems than for high diversity ones. This is because that the overlaps in the value of the community-weighted mean functional traits (a measure of the average surviving plant traits in an ecosystem) among the three low diversity systems are small. This leads to different vegetation-climate interactions across different low diversity sys-

tems. In the sensitivity study to the four selected trait parameters (Chapter 3.6), global climates show no significant change to any of the trait parameters almost everywhere. This is because the high diversity ecosystems are able to compensate for all the parameter changes (which act like disturbances). As long as the ecosystem's adaptability can shuffle and replace the dominant strategies quickly, there will be no significant climate change. For instance, the considered Congo ecosystem shows strong adaptation, such that regional climate remains the same as before. In contrast, the western Sahel ecosystem cannot replace the lost, formerly dominant strategies, which leads to a strong reduction in evapotransiration, such that the regional climate becomes dryer and hotter than before. In Chapter 4, I found for the low diversity systems large differences at the end of the simulations in both the regional and terrestrial climate across differently diverse ecosystems following disturbance.

In contrast, the high diversity world always maintains a cooler and wetter climate compared to the low diversity worlds. At the regional scale, high diversity ecosystems in tropical South America manage to prevent more regions from changing towards a dryer and more seasonal regime as compared to the low diversity ecosystems. In particular, the vegetation-climate interactions in inland ecosystems are more influenced by ecosystem diversity, whereas coastal ecosystems show no clear differences. It follows that different ecosystems exploit the resources provided by the environmental conditions differently in different locations. I hypothesize that low diversity ecosystems might be more unpredictable in response to disturbance. Though it is beyond the scope of my dissertation, this finding supports the necessity to preserve biodiversity because high plant diversity seems to stabilize the system. With this in mind, a complete wipeout of high biodiversity ecosystems will undoubtedly do more harm than good. Diversity reduction in ecosystems does not allow them to maintain resilience. At the current unprecedented deforestation rate across major rainforests in the tropics (Silva Junior et al., 2021; Ritchie and Roser, 2021), permanent disruption to ecosystem processes such as the hydrological cycle may result and even if deforestation would be stopped immediately ecosystems may not recover with their full biodiversity potential within the next decades, let alone the next hundred or even thousand years.

5.5 Final remarks

A few issues should be raised concerning the particular modeling concept underlying this dissertation. In particular, how would the modeling approach influence the outcomes of my study?

5.5.1 Biomass-scaling approach

One remark is related to the biomass-scaling theory (Grime, 1998). In JeDi-BACH, the characteristics at the ecosystem level are calculated following this theory: strategies with large biomass are given more weight in summing ecosystem-wide fluxes, meaning that their dominance is proportional to their total biomass relative to the total biomass in the ecosystem. In view of the concept of ecological succession, changes in their dominance should be a slow process. Therefore, I implemented a memory factor with a value of ten years to simulate this behavior in the model. This factor essentially smooths out the change in strategies' cover fraction.

Is the biomass-scaling approach a reasonable way to "up-scale" ecosystem properties from individual plant strategies in the model?

To start with, I explain why this question arises here. In the original JeDi model, grasses are not explicitly simulated. The structural differences between trees and grasses have a distinct impact on climate by their differences in albedo, transpiration, biomass carbon, productivity, etc. Therefore, I implemented tree-like and grass-like strategies into JeDi-BACH. Intuitively, trees seem to benefit from the biomass scaling theory because of their large woody pools. In the following, I list the concepts that are captured by this theory in the model.

First, by biomass scaling strategies with large biomass physically occupy a larger space and take over more surface area so that their general contribution to ecosystem fluxes is larger than that of small biomass strategies. Second, biomass-scaling indirectly reflects competition in the system: by giving larger biomass strategies larger weights, they become the dominant strategies in the system, and thus they dominate the characteristics of the ecosystem. For instance, trees tend to have deep roots because they are physically more powerful than grasses in penetrating deeper soil layers. In such a way, they can dominate the extraction of soil water in their favor. Third, biomass-scaling captures to some degree ecological succession. During the model spin-up phase, every plant strategy is given an equal chance to colonize a "bare land". Grasses take advantage because they respond fast and grow fast to become the primary

dominant strategies in the early stage of succession. On the contrary, trees are slow-growth strategies that are rather expensive to keep alive. Therefore, there are likely only a few small trees at the beginning. After several decades of development, when more trees successfully survive, tree strategies finally outcompete grasses in the later stage of succession.

One might criticize this in the same way as Trinder, Brooker, and Robinson (2013): "Biomass has become the 'industry standard' for measuring competition, but we suggest that biomass cannot provide unambiguous insights into plant competition because it is the product of too great a range of factors and processes." However, I reach a different conclusion: despite being simple, the biomass-scaling theory captures several ecological principles that are useful when studying global ecosystems at the scale of a few hundred kilometers, as in JeDi-BACH.

Nevertheless, as natural disturbances that are critical for tree-grass competition, such as fire, herbivores, nutrient limitation, and windstorms are not simulated in JeDi-BACH, one should pay attention when investigating the competition between trees and grass in ecosystems like savannas.

Could the "shock" phases observed in the response of the ecosystem be caused by the memory factor?

In Chapter 4, the high diversity ecosystem shows a "V-shape" recovery in its response to abrupt warming. The ecosystem first experiences a "shock" phase and then slowly recovers its ecosystem process. As I found in my study, if an ecosystem cannot replace the lost, formerly dominant, strategies soon enough, these lost strategies still "occupy" a certain cover fraction and contribute nothing to ecosystem functioning (such as zero evapotranspiration) and thereby influences the stability of regional climate. The removal of lost strategies is faster than the development of the new dominant strategies. The rate in the removal of dead strategies could be the reason for the "shock" phase. If there would be no memory lag in the removal of strategies in the model, the subordinate strategies could immediately occupy the space created by the dead strategies. In this case, an ecosystem might experience a milder 'shock' in the system. However, it is not reasonable that one strategy can immediately "expand" its physical space as soon as another strategy dies. An instant expansion of a strategy's cover fraction (see Chapter 2.5.8.1 for details) would mean a physical expansion from tens to hundreds square kilometer within one single model time step (30 minutes in my model simulations). I argue that a ten-year memory factor is within a reasonable range concerning what is known in ecological succession. However,

this is possibly an open question for all dynamic vegetation models.

5.5.2 Limitation on interpretation and tuning

I draw a final remark on dealing with a model like JeDi-BACH that the modeling essence works completely differently to the traditional PFT-approach. One should note the limitations of interpreting the simulations conducted using JeDi-BACH. Climate modeling studies typically perform simulations in the following way to investigate the impact of vegetation on climate: two model simulations are conducted. One is the control simulation, where everything remains unchanged, and the other is a simulation with modifications of interest to the study. One then draws conclusions on the consequences of these modifications by comparing the results between the two. For instance, to see how root depth can influence the global hydrological cycle, one conducts a simulation without changes in root depth and the other with modified root depth. Thereby, conclusions on how climate is dependent on changes in root depth can be drawn. It is rather straightforward to conduct such simulation experiments and to interpret results with such a strategy because a particular component in the model is often a prescribed parameter in the control simulation.

However, the situation is quite different in JeDi-BACH. JeDi-BACH simulates ecosystems that are "self-organizing". Plant strategies need to sustain themselves depending on their functional capability. The selection of survivors involves many levels of complexity. It is impossible to establish an exact causal relationship between the ecological process and the environmental changes because ecosystem composition and ecosystem functioning are no longer prescribed by static parameters. As what I concluded from Chapter 3.6, no significant outcome on ecosystem functioning may occur despite trait parameter changes because a growth strategy can die and be replaced by other subordinates in the system. Therefore, it is impossible to manipulate the ecosystem to behave in a particular way by favoring one strategy over the others. Ecosystem resilience attenuates the changes from the environment. One cannot disentangle the dynamics of ecological processes from environmental changes. Instead, one needs to view the coupled climate system and ecosystem functions as a whole. In this regard, tuning a model like JeDi-BACH simply via tweaking parameters is likely vain.

There are some potentials to improve and extend my study for the future, such as:

- Gaining more statistics for the diversity-resilience study in Chapter 4 with more ensemble simulations.
- Working towards a higher model resolution (than the configuration used in this dissertation) so that a more realistic climate simulation and global vegetation distribution can be achieved.
- Improving the modeling component on the leaf phenology by implementing proper plant allometry.

Last, although there are still conceptual uncertainties in the new model JeDi-BACH, I argue that the outcomes of my dissertation are robust. All the findings from each chapter provide qualitative insights into the importance of plant functional diversity on global climate and ecosystems. By coupling with an atmospheric model, JeDi-BACH offers great potential for investigating biodiversity-climate interaction. One potential application is to use it for non-analogue climates such as paleoclimate where no present-day vegetation existed.

Part I

APPENDIX

A

APPENDIX

A.1 Remarks on the background climate

It is essential to note the potential biases in the simulations of the new modelling pair of JeDi-BACH and ICON-A. The primary issue rests in the background climate simulated by ICON-A. Many ICON-A configurations have not yet been tuned by the modelling group regarding a coupled atmosphere and land simulation. A major drawback in using them is that the simulated climate in R2B3 resolution of ICON-A has large biases to the present-day observation inherited from the poor features reported in Jungclaus et al. (2022); Schneck et al. (2022, submitted).

Fig. 37 demonstrates this by showing the annual mean global precipitation of my control (CTRL) simulation conducted in Chapter 3.6 in comparison to satellite estimates (OBS). Fig. 37 c) presents the difference between the two and d) shows the quotient of the two. In the CTRL simulation, the regions with largest bias are Eurasia, sub-tropical tropical monsoon, and savanna regions. Eurasia receives about 200 to 500 mm/year less annual precipitation than OBS (roughly 20-50% of OBS). The present-day region of warm-summer humid continental Eurasia (classified as Dfb by Koeppen climate classification) has turned into a cold semi-arid climate (BSk in Koeppen regime) in the model. The southern sub-tropical African region receives 1.5-3 times higher precipitation (600-1000 mm/year) than the OBS. To provide an overview of the zonal distribution of precipitation, Fig. 38 shows the zonal mean global precipitation between CTRL and the OBS. From the zonal mean, CTRL simulation overestimates precipitation in the subtropic regions (10-30N and 10-30S) and underestimates precipitation in mid-to high-latitudes (30-60N and 30-60S).

As one of the primary factors, water broadly determines global vegetation distribution. Vegetation grows particularly well in regions that are rich in rain. Evaluating the modeled terrestrial ecosystem with observations is all in vain with such apparent precipitation biases in ICON-A. Therefore, the sensitivity simulations conducted in Chapter 3.6 certainly do not imply what parameter values are better than the others. It is only a feasibility test to demonstrate how

robust/sensitive the simulation results are. Namely, it provides an overview of the magnitude and the direction of how climate/ecosystem function may be influenced.

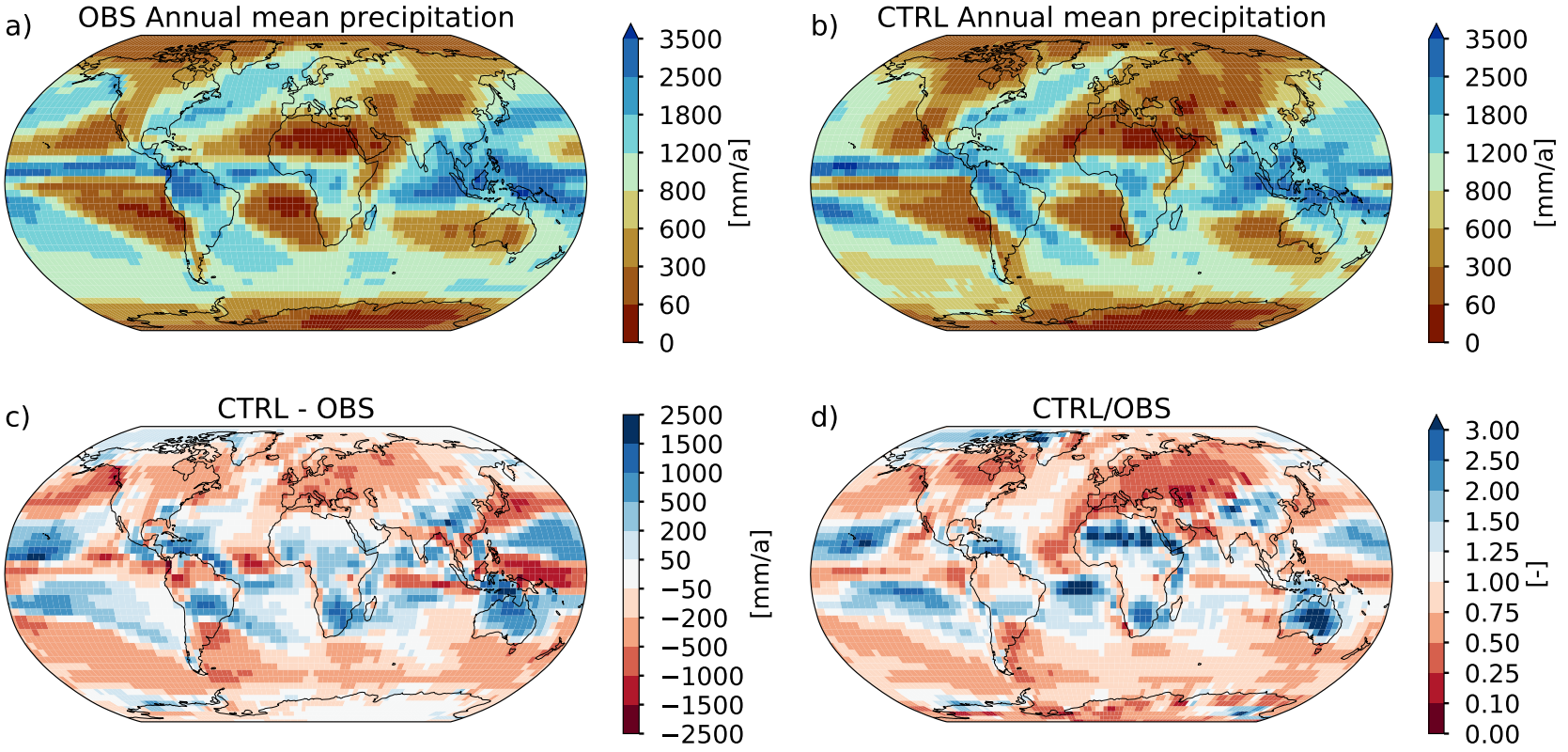

Figure 37: Comparison of ICON climate with the observation data (OBS). a) The OBS annual mean precipitation (mm/year) averaged between 2000-2014 taken from the satellites estimate Global Precipitation Climatology Project (GPCPv2) (Adler et al., 2018), b) the CTRL simulation, c) the difference between CTRL to OBS, d) the division between CTRL to OBS.

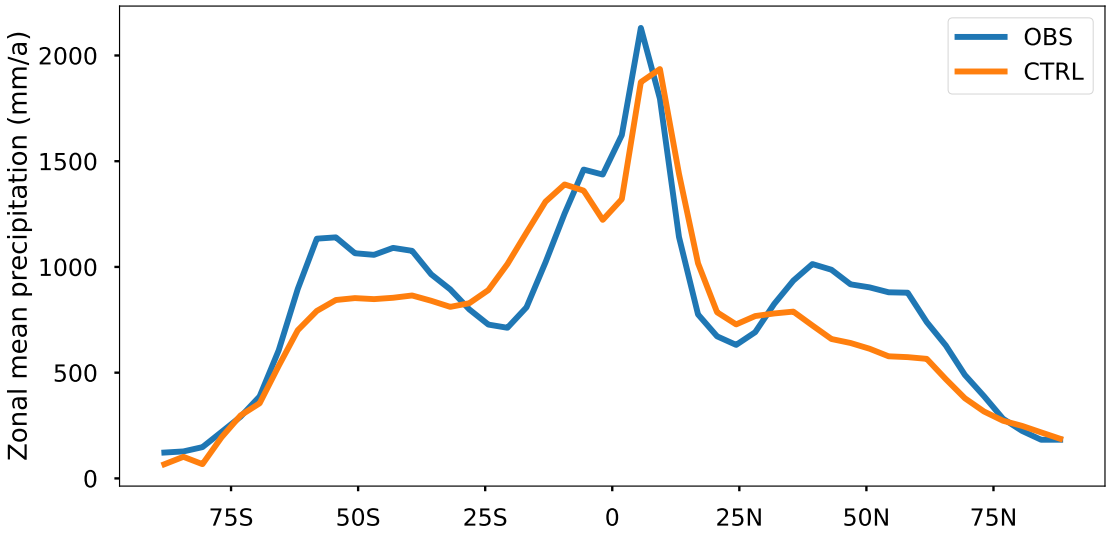

Figure 38: Comparison of zonal mean annual mean global precipitation (mm/year) between CTRL simulation (orange line) and satellite estimates (OBS, blue line). Precipitation is the average between 2000-2014 from the Global Precipitation Climatology Project (GPCPv2) (Adler et al., 2018).

Learning is the only thing the mind never exhausts,
never fears,
and never regrets.

— Leonardo Da Vinci

ACKNOWLEDGMENTS

I recall that the first task I got at the beginning of my study from Martin was "you need to marry – JeDi and JSBACH." I didn't know what was coming ahead of me at that time, so I started as an optimistic newbie. The moment I started to build the model JeDi-BACH into ICON-ESM, a naughty monster was born, and a long-lasting fight with this creature began. This seemingly undefeatable creature could only be tamed with endless struggles, screams, trial-and-error, and occasionally sprinkled with a bit of excitement. Little by little, breaking the creature into pieces and reshaping it into a new form, it finally came to the point that, I'd say, it's finally under control. This achievement was only possible because of my mentor, Christian Reick, who supported me with endless discussions, shared his invaluable knowledge about vegetation modeling with me, encouraged me, and dedicated himself to helping me through every doubt and trouble I had. Without the guidance from Martin Claussen and Axel Kleidon, I would have been lost in the modeling world without advancing my own research. Their questions and comments have pulled me out of a pure modeling spiral and placed me in a different perspective to shape my study.

In the past few years, I received countless help from many people. I could never finish my study without them. Thank you to Reiner Schnur for saving me over and over again from all the technical issues with JeDi-BACH and for being so patient with me all the time. Thank you to Antje Weitz, Cornelia Kampmann, and Michaela Born for patiently walking me through all bureaucracy, particularly towards the end of my study, one of the most stressful moments in the past few years. Life in this hopelessly long COVID situation plus Hamburg's grey skies would not have been the same without the calls for snacks, teatimes, beers, and lunches with the land-PhDs Zoe Rehder, Guilherme Mendoca, Hao-Wei Wey, Nora Specht, Josephine Wong, Meike Schickhoff, and Mateo Duque. Many thanks to Woon Mi Kim, Geet George, Arjun Kumar, David Nielsen, Xiangshan Tian, and many other Hamburgers for always getting me out of Geomatikum tower for fresh air. Complaining and making fun of our Ph.D. life

together certainly was a great way of rechanging my mind. A special thanks to my former roommates Zoe Rehder and Clara Henry for the exotic meals and the time we spent together. You believe in me more than I do. I cannot express how lucky I am to meet you in my life.

I could never survive this four-year-long battle without my family's endless cheering and love. Invaluable packages were sent across the globe just to deliver physical love to me from home. Thank you to my sisters Hsin-Yuan Hu and Hsin-Wen Hu, who love me and help me without hesitation. You always encourage me to pursue my dream. Thank you to Hsiu-Feng Hsu, my beloved mother, who always holds me with unconditional love, cares about me more than myself, and teaches me how to care for and love others. Finally, thank you to Wei-Chun Hu, my father, who silently sent me love and supported me more than anyone else would do. Papa, be proud; the pouring love you gave me has made me who I am today.

BIBLIOGRAPHY

Adler, Robert F et al. (2018). "The Global Precipitation Climatology Project (GPCP) monthly analysis (new version 2.3) and a review of 2017 global precipitation." In: *Atmosphere* 9.4, p. 138.

Aleixo, Izabela et al. (2019). "Amazonian rainforest tree mortality driven by climate and functional traits." In: *Nature Climate Change* 9.5, pp. 384–388.

Alton, Paul B. (2011). "How useful are plant functional types in global simulations of the carbon, water, and energy cycles?" In: *Journal of Geophysical Research: Biogeosciences* 116.1, pp. 1–13. ISSN: 01480227. DOI: 10.1029/2010JG001430.

Barthlott, Wilhelm, Wilhelm Lauer, and Anja Placke (1996). "Global distribution of species diversity in vascular plants: Towards a world map of phytodiversity (globale verteilung der artenvielfalt höherer pflanzen: Vorarbeiten zu einer weltkarte der phytodiversität)." In: *Erdkunde*, pp. 317–327.

Becking, Lourens Gerhard Marinus Baas (1934). *Geobiologie of inleiding tot de milieukunde*. 18-19. WP Van Stockum & Zoon.

Bellard, Céline et al. (2012). "Impacts of climate change on the future of biodiversity." In: *Ecology letters* 15.4, pp. 365–377.

Berg, Alexis and Justin Sheffield (2018). "Climate change and drought: the soil moisture perspective." In: *Current Climate Change Reports* 4.2, pp. 180–191.

Betts, RA et al. (2004). "The role of ecosystem-atmosphere interactions in simulated Amazonian precipitation decrease and forest dieback under global climate warming." In: *Theoretical and applied climatology* 78.1, pp. 157–175.

Biggs, Christopher R et al. (2020). "Does functional redundancy affect ecological stability and resilience? A review and meta-analysis." In: *Ecosphere* 11.7, e03184.

Bloom, Arnold J, F Stuart Chapin III, and Harold A Mooney (1985). "Resource limitation in plants-an economic analogy." In: *Annual review of Ecology and Systematics* 16.1, pp. 363–392.

Bonan, Gordon B (2008). "Forests and climate change: forcings, feedbacks, and the climate benefits of forests." In: *science* 320.5882, pp. 1444–1449.

Boysen, Lena R et al. (2020). "Global climate response to idealized deforestation in CMIP6 models." In: *Biogeosciences* 17.22, pp. 5615–5638.

Brovkin, Victor et al. (2003). "Stability analysis of the climate-vegetation system in the northern high latitudes." In: *Climatic change* 57.1, pp. 119–138.

Brovkin, Victor et al. (2009). "Global biogeophysical interactions between forest and climate." In: *Geophysical research letters* 36.7.

Brummitt, Neil, Ana Claudia Araújo, and Timothy Harris (2020). "Areas of plant diversity—What do we know?" In: *Plants, People, Planet* December 2019, pp. 1–12. ISSN: 2572-2611. DOI: 10.1002/ppp3.10110.

Cadotte, Marc W., Kelly Carscadden, and Nicholas Mirotchnick (2011). "Beyond species: Functional diversity and the maintenance of ecological processes and services." In: *Journal of Applied Ecology* 48.5, pp. 1079–1087. ISSN: 00218901. DOI: 10.1111/j.1365-2664.2011.02048.x.

Cardinale, B J et al. (2006). "Effects of biodiversity on the functioning of trophic groups and ecosystems." In: *Nature* 443, pp. 989–992.

Cardinale, Bradley J et al. (2012). "Biodiversity loss and its impact on humanity." In: *Nature* 486.7401, pp. 59–67.

Chave, Jerome et al. (2009). "Towards a worldwide wood economics spectrum." In: *Ecol. Lett.* 12.4, pp. 351–366. ISSN: 14610248. DOI: 10.1111/j.1461-0248.2009.01285.x.

Claussen, Martin, Victor Brovkin, and Andrey Ganopolski (2001). "Biogeophysical versus biogeochemical feedbacks of large-scale land cover change." In: *Geophysical research letters* 28.6, pp. 1011–1014.

Claussen, Martin et al. (2013). "Simulated climate–vegetation interaction in semi-arid regions affected by plant diversity." In: *Nature Geoscience* 6.11, pp. 954–958.

Collatz, Go J, M Ribas-Carbo, and JA Berry (1992). "Coupled photosynthesis-stomatal conductance model for leaves of C4 plants." In: *Functional Plant Biology* 19.5, pp. 519–538.

Cox, Peter M et al. (2004). "Amazonian forest dieback under climate-carbon cycle projections for the 21st century." In: *Theoretical and applied climatology* 78.1, pp. 137–156.

De Wit, Rutger and Thierry Bouvier (2006). "'Everything is everywhere, but, the environment selects'; what did Baas Becking and Beijerinck really say?" In: *Environmental microbiology* 8.4, pp. 755–758.

Díaz, Sandra et al. (2013). "Functional traits, the phylogeny of function, and ecosystem service vulnerability." In: *Ecology and evolution* 3.9, pp. 2958–2975.

Díaz, Sandra et al. (2016). "The global spectrum of plant form and function." In: *Nature* 529.7585, pp. 167–171. ISSN: 14764687. DOI: 10.1038/nature16489. URL: http://dx.doi.org/10.1038/nature16489.

Diaz, Sandra and Marcelo Cabido (2001). "Vive la différence: plant functional diversity matters to ecosystem processes." In: *Trends in ecology & evolution* 16.11, pp. 646–655.

Eyring, Veronika et al. (2016). "Overview of the Coupled Model Intercomparison Project Phase 6 (CMIP6) experimental design and organization." In: *Geoscientific Model Development* 9.5, pp. 1937–1958.

Farquhar, Graham D, S von von Caemmerer, and Joseph A Berry (1980). "A biochemical model of photosynthetic CO 2 assimilation in leaves of C 3 species." In: *Planta* 149.1, pp. 78–90.

Field, C and HA Mooney (1986). "photosynthesis–nitrogen relationship in wild plants." In: *On the economy of plant form and function: proceedings of the Sixth Maria Moors Cabot Symposium, Evolutionary Constraints on Primary Productivity, Adaptive Patterns of Energy Capture in Plants, Harvard Forest, August 1983*. Cambridge [Cambridgeshire]: Cambridge University Press, c1986.

Fisher, Joshua B et al. (2014). "Modeling the terrestrial biosphere." In: *Annual Review of Environment and Resources* 39, pp. 91–123.

Fisher, Rosie A and Charles D Koven (2020). "Perspectives on the future of land surface models and the challenges of representing complex terrestrial systems." In: *Journal of Advances in Modeling Earth Systems* 12.4, e2018MS001453.

Gates, W Lawrence et al. (1999). "An overview of the results of the Atmospheric Model Intercomparison Project (AMIP I)." In: *Bulletin of the American Meteorological Society* 80.1, pp. 29–56.

Giorgetta, Marco A et al. (2018). "ICON-A, the atmosphere component of the ICON earth system model: I. Model description." In: *Journal of Advances in Modeling Earth Systems* 10.7, pp. 1613–1637.

Greve, Peter, Micheal L Roderick, and Sonia I Seneviratne (2016). "Aridity under conditions of increased CO 2." In: 18.2015, p. 12666.

Grime, JP (1998). "Benefits of plant diversity to ecosystems: immediate, filter and founder effects." In: *Journal of Ecology* 86.6, pp. 902–910.

Groner, Vivienne P. et al. (2018). "Plant functional diversity affects climate-vegetation interaction." In: *Biogeosciences* 15.7, pp. 1947–1968. ISSN: 17264189. DOI: 10.5194/bg-15-1947-2018.

Hagemann, Stefan (2002). "An improved land surface parameter dataset for global and regional climate models." In.

Harris, IPDJ et al. (2014). "Updated high-resolution grids of monthly climatic observations–the CRU TS3. 10 Dataset." In: *International journal of climatology* 34.3, pp. 623–642.

Harris, Richard W (1992). "Root-shoot ratios." In: *Journal of Arboriculture* 18.1, pp. 39–42.

Harrison, Sandy P et al. (2021). "Eco-evolutionary optimality as a means to improve vegetation and land-surface models." In: *New Phytologist*.

Hollinger, D. Y. et al. (2010). "Albedo estimates for land surface models and support for a new paradigm based on foliage nitrogen concentration." In:

Glob. Chang. Biol. 16.2, pp. 696–710. ISSN: 13541013. DOI: 10.1111/j.1365-2486.2009.02028.x.

Hourdin, Frédéric et al. (2017). "The art and science of climate model tuning." In: *Bulletin of the American Meteorological Society* 98.3, pp. 589–602.

Huntingford, Chris et al. (2008). "Towards quantifying uncertainty in predictions of Amazon 'dieback'." In: *Philosophical Transactions of the Royal Society B: Biological Sciences* 363.1498, pp. 1857–1864.

Huston, Michael A (1997). "Hidden treatments in ecological experiments: re-evaluating the ecosystem function of biodiversity." In: *Oecologia* 110.4, pp. 449–460.

Isbell, Forest et al. (2011a). "High plant diversity is needed to maintain ecosystem services." In: *Nature* 477.7363, pp. 199–202.

Isbell, Forest et al. (2011b). "High plant diversity is needed to maintain ecosystem services." In: *Nature* 477.7363, pp. 199–202. ISSN: 00280836. DOI: 10.1038/nature10282. URL: http://dx.doi.org/10.1038/nature10282.

Isbell, Forest et al. (2015). "Biodiversity increases the resistance of ecosystem productivity to climate extremes." In: *Nature* 526.7574, pp. 574–577.

Jasechko, Scott et al. (2013). "Terrestrial water fluxes dominated by transpiration." In: *Nature* 496.7445, pp. 347–350.

Jungclaus, Johann H et al. (2022). "The ICON Earth System Model Version 1.0." In: *Journal of Advances in Modeling Earth Systems* 14.4, e2021MS002813.

Kabat, Pavel et al. (2004). *Vegetation, water, humans and the climate: A new perspective on an internactive system*. Springer Science & Business Media.

Kattge, J. et al. (2007). "TRY - a global database of plant traits." In: *New Phytologist* 174.2, pp. 367–380. ISSN: 0028646X. DOI: 10.1111/j.1469-8137.2007.02011.x. URL: http://doi.wiley.com/10.1111/j.1365-2486.2011.02451.x.

Kattge, Jens et al. (2009). "Quantifying photosynthetic capacity and its relationship to leaf nitrogen content for global-scale terrestrial biosphere models." In: *Global Change Biology* 15.4, pp. 976–991. ISSN: 13541013. DOI: 10.1111/j.1365-2486.2008.01744.x.

Kattge, Jens et al. (2020). "TRY plant trait database – enhanced coverage and open access." In: *Glob. Chang. Biol.* 26.1, pp. 119–188. ISSN: 13652486. DOI: 10.1111/gcb.14904.

Kleidon, A and H A Mooney (2000). "A global distribution of diversity inferred from climatic contraints: results from a process-based modelling study." In: *Global Change Biology* 6, pp. 507–523. ISSN: 13541013. DOI: 10.1046/j.1365-2486.2000.00332.x.

Kleidon, Axel et al. (2009). "Simulated geographic variations of plant species richness, evenness and abundance using climatic constraints on plant func-

tional diversity." In: *Environmental Research Letters* 4.1. ISSN: 17489326. DOI: 10.1088/1748-9326/4/1/014007.

Knorr, Wolfgang (1997). "Satellitengestützte Fernerkundung und Modellierung des globalen CO2-Austauschs der Landvegetation." PhD thesis. University of Hamburg Hamburg.

Konapala, Goutam et al. (2020). "Climate change will affect global water availability through compounding changes in seasonal precipitation and evaporation." In: *Nature communications* 11.1, pp. 1–10.

Laliberté, Etienne and Pierre Legendre (2010). "A distance-based framework for measuring functional diversity from multiple traits." In: *Ecology* 91.1, pp. 299–305.

Larcher, W. (1996). "Ökophysiologie der Pflanzen: Leben, Leistung und Strebewältigung der Pflanzen in ihrer Umwelt. 5., völlig neubearbeitete Auflage. – 394 S., 347 Abb., 78 Tab., Pp. DM 78,–. ISBN 3-8252-8074-8 (UTB)." In: *Flora* 191.

Lieth, Helmut (1974). "Purposes of a Phenology Book." In: *Phenology and Seasonality Modeling*. Ed. by Helmut Lieth. Berlin, Heidelberg: Springer Berlin Heidelberg, pp. 3–19. ISBN: 978-3-642-51863-8. DOI: 10.1007/978-3-642-51863-8_1. URL: https://doi.org/10.1007/978-3-642-51863-8_1.

Loreau, Michel et al. (2001). "Biodiversity and ecosystem functioning: current knowledge and future challenges." In: *science* 294.5543, pp. 804–808.

Malhi, Yadvinder et al. (2008). "Climate change, deforestation, and the fate of the Amazon." In: *science* 319.5860, pp. 169–172.

McElwain, Jennifer C (2018). "Paleobotany and global change: Important lessons for species to biomes from vegetation responses to past global change." In: *Annual review of plant biology* 69, pp. 761–787.

Mccann, Kevin Shear (2000). "The diversity–stability debate." In: 405.May.

Mottl, Ondřej et al. (2021). "Global acceleration in rates of vegetation change over the past 18,000 years." In: *Science* 372.6544, pp. 860–864.

Naeem, Shahid (1998). "Species redundancy and ecosystem reliability." In: *Conservation biology* 12.1, pp. 39–45.

Naeem, Shahid and Shibin Li (1997). "Biodiversity enhances ecosystem reliability." In: *Nature* 390.6659, pp. 507–509.

Newbold, Tim et al. (2015). "Global effects of land use on local terrestrial biodiversity." In: *Nature* 520.7545, pp. 45–50.

O'Malley, Maureen A. (2007). "The nineteenth century roots of 'everything is everywhere'." In: *Nat. Rev. Microbiol.* 5.8, pp. 647–651. ISSN: 17401526. DOI: 10.1038/nrmicro1711.

Oki, Taikan and Shinjiro Kanae (2006). "Global hydrological cycles and world water resources." In: *science* 313.5790, pp. 1068–1072.

Ollinger, S V et al. (2008). "Canopy nitrogen, carbon assimilation, and albedo in temperate and boreal forests: Functional relations and potential climate feedbacks." In: *Proc. Natl. Acad. Sci.* 105.49, pp. 19336–41. ISSN: 1091-6490. DOI: 10.1073/pnas.0810021105. URL: http://www.pnas.org/content/105/49/19336.full.

Pappas, Christoforos, Simone Fatichi, and Paolo Burlando (2014). "Terrestrial water and carbon fluxes across climatic gradients: does plant diversity matter?" In: *New Phytologist* 16.i, p. 3663. ISSN: 1469-8137. DOI: 10.1111/nph.13590.

Pavlick, R. et al. (2013). "The Jena Diversity-Dynamic Global Vegetation Model (JeDi-DGVM): a diverse approach to representing terrestrial biogeography and biogeochemistry based on plant functional trade-offs." In: *Biogeosciences* 10.6, pp. 4137–4177. ISSN: 1726-4189. DOI: 10.5194/bg-10-4137-2013. arXiv: arXiv:1011.1669v3. URL: http://www.biogeosciences-discuss.net/9/4627/2012/https://www.biogeosciences.net/10/4137/2013/.

Pfeiffer, Mirjam et al. (2020). "Climate change will cause non-analog vegetation states in Africa and commit vegetation to long-term change." In: *Biogeosciences* 17.22, pp. 5829–5847. ISSN: 17264189. DOI: 10.5194/bg-17-5829-2020.

Qi, Yulin et al. (2019). "Plant root-shoot biomass allocation over diverse biomes: A global synthesis." In: *Glob. Ecol. Conserv.* 18.18, e00606. ISSN: 23519894. DOI: 10.1016/j.gecco.2019.e00606. URL: https://doi.org/10.1016/j.gecco.2019.e00606.

Reich, Peter B. (2014). "The world-wide 'fast-slow' plant economics spectrum: A traits manifesto." In: *J. Ecol.* 102.2, pp. 275–301. ISSN: 00220477. DOI: 10.1111/1365-2745.12211.

Reich, Peter B, Michael B Walters, and David S Ellsworth (1997). "From tropics to tundra: global convergence in plant functioning." In: *Proceedings of the National Academy of Sciences* 94.25, pp. 13730–13734.

Reich, Peter B. et al. (2008). "Scaling of respiration to nitrogen in leaves, stems and roots of higher land plants." In: *Ecol. Lett.* 11.8, pp. 793–801. ISSN: 1461023X. DOI: 10.1111/j.1461-0248.2008.01185.x.

Reick, Christian H et al. (2021). "JSBACH 3-The land component of the MPI Earth System Model: documentation of version 3.2." In.

Reu, Björn et al. (2014). "Future no-analogue vegetation produced by no-analogue combinations of temperature and insolation." In: pp. 156–167. DOI: 10.1111/geb.12110.

Ritchie, Hannah and Max Roser (2021). "Forests and deforestation." In: *Our World in Data*.

Ryan, M. G. (1991). "A simple method for estimating gross carbon budgets for vegetation in forest ecosystems." In: *Tree Physiol.* 9.1-2, pp. 255–266. ISSN: 0829-318X. DOI: 10.1093/treephys/9.1-2.255.

Sakschewski, Boris et al. (2015). "Leaf and stem economics spectra drive diversity of functional plant traits in a dynamic global vegetation model." In: *Global Change Biology* 21.7, pp. 2711–2725. ISSN: 13652486. DOI: 10.1111/gcb.12870.

Sakschewski, Boris et al. (2016). "Resilience of Amazon forests emerges from plant trait diversity." In: *Nature Climate Change* 6.11, pp. 1032–1036. ISSN: 17586798. DOI: 10.1038/nclimate3109.

Scheiter, Simon, Liam Langan, and Steven I Higgins (2013). "Next-generation dynamic global vegetation models: learning from community ecology." In: *New Phytologist* 198.3, pp. 957–969.

Schneck, Rainer et al. (2022, submitted). "Assessment of JSBACH as land component of the Max Planck Institute for Meteorology Earth System Models." In.

Schulze, Ernst-Detlef et al. (2019). "Dynamic Global Vegetation Models." In: *Plant Ecology*. Springer, pp. 843–863.

Seneviratne, Sonia I et al. (2010). "Investigating soil moisture–climate interactions in a changing climate: A review." In: *Earth-Science Reviews* 99.3-4, pp. 125–161.

Seneviratne, Sonia I et al. (2013). "Impact of soil moisture-climate feedbacks on CMIP5 projections: First results from the GLACE-CMIP5 experiment." In: *Geophysical Research Letters* 40.19, pp. 5212–5217.

Shinozaki, Kichiro et al. (1964). "A quantitative analysis of plant form-the pipe model theory: I. Basic analyses." In: *Japanese Journal of ecology* 14.3, pp. 97–105.

Silva Junior, Celso HL et al. (2021). "The Brazilian Amazon deforestation rate in 2020 is the greatest of the decade." In: *Nature ecology & evolution* 5.2, pp. 144–145.

Soh, Wuu Kuang et al. (2017). "Palaeo leaf economics reveal a shift in ecosystem function associated with the end-Triassic mass extinction event." In: *Nature plants* 3.8, pp. 1–8.

Stein, Michael (1987). "Large sample properties of simulations using Latin hypercube sampling." In: *Technometrics* 29.2, pp. 143–151.

Swann, Abigail L.S. (2018). "Plants and Drought in a Changing Climate." In: *Curr. Clim. Chang. Reports* 4.2, pp. 192–201. ISSN: 21986061. DOI: 10.1007/s40641-018-0097-y.

Thornley, J. H.M. (1970). "Respiration, growth and maintenance in plants." In: *Nature* 227.5255, pp. 304–305. ISSN: 00280836. DOI: 10.1038/227304b0.

Thornley, JHM and MGR Cannell (2000). "Modelling the components of plant respiration: representation and realism." In: *Annals of Botany* 85.1, pp. 55–67.

Trenberth, Kevin E, John T Fasullo, and Jeffrey Kiehl (2009). "Earth's global energy budget." In: *Bulletin of the American Meteorological Society* 90.3, pp. 311–324.

Trinder, Clare J, Rob W Brooker, and David Robinson (2013). "Plant ecology's guilty little secret: understanding the dynamics of plant competition." In: *Functional Ecology* 27.4, pp. 918–929.

Verheijen, L. M. et al. (2013). "Impacts of trait variation through observed trait-climate relationships on performance of an Earth system model: A conceptual analysis." In: *Biogeosciences* 10.8, pp. 5497–5515. ISSN: 17264170. DOI: 10.5194/bg-10-5497-2013. URL: http://www.biogeosciences.net/10/5497/2013/.

Violle, Cyrille et al. (2007). "Let the concept of trait be functional!" In: *Oikos* 116.5, pp. 882–892. ISSN: 16000706. DOI: 10.1111/j.0030-1299.2007.15559.x.

Vitousek, Peter M and Robert W Howarth (1991). "Nitrogen limitation on land and in the sea: how can it occur?" In: *Biogeochemistry* 13.2, pp. 87–115.

Walker, Brian H (1992). "Biodiversity and ecological redundancy." In: *Conservation biology* 6.1, pp. 18–23.

Wang, Yongfan et al. (2019). "Global evidence of positive biodiversity effects on spatial ecosystem stability in natural grasslands." In: *Nature communications* 10.1, pp. 1–9.

Warszawski, Lila et al. (2013). "A multi-model analysis of risk of ecosystem shifts under climate change." In: *Environmental Research Letters* 8.4, p. 044018.

Westoby, Mark and Ian J Wright (2006). "Land-plant ecology on the basis of functional traits." In: *Trends in ecology & evolution* 21.5, pp. 261–268.

Williams, John W. and Stephen T. Jackson (2007). "Novel climates, no-analog communities, and ecological surprises." In: *Front. Ecol. Environ.* 5.9, pp. 475–482. ISSN: 15409309. DOI: 10.1890/070037.

Winckler, Johannes et al. (2019). "Nonlocal effects dominate the global mean surface temperature response to the biogeophysical effects of deforestation." In: *Geophysical Research Letters* 46.2, pp. 745–755.

Wright, Ian J et al. (2004). "The worldwide leaf economics spectrum." In: *Nature* 428.6985, pp. 821–827.

Wullschleger, Stan D. et al. (2014). "Plant functional types in Earth system models: Past experiences and future directions for application of dynamic vegetation models in high-latitude ecosystems." In: *Annals of Botany* 114.1, pp. 1–16. ISSN: 10958290. DOI: 10.1093/aob/mcu077.

Hinweis / Reference

Die gesamten Veröffentlichungen in der Publikationsreihe des MPI-M
„Berichte zur Erdsystemforschung / Reports on Earth System Science“,
ISSN 1614-1199

sind über die Internetseiten des Max-Planck-Instituts für Meteorologie erhältlich:
http://www.mpimet.mpg.de/wissenschaft/publikationen.html

All the publications in the series of the MPI -M
„Berichte zur Erdsystemforschung / Reports on Earth System Science“,
ISSN 1614-1199

are available on the website of the Max Planck Institute for Meteorology:
http://www.mpimet.mpg.de/wissenschaft/publikationen.html